

AD-A162 553

SPACE-FREQUENCY SAMPLING CRITERIA FOR ELECTROMAGNETIC
SCATTERING OF A FINITE OBJECT(U) OHIO STATE UNIV
COLUMBUS ELECTROSCIENCE LAB F Y FOR AUG 85

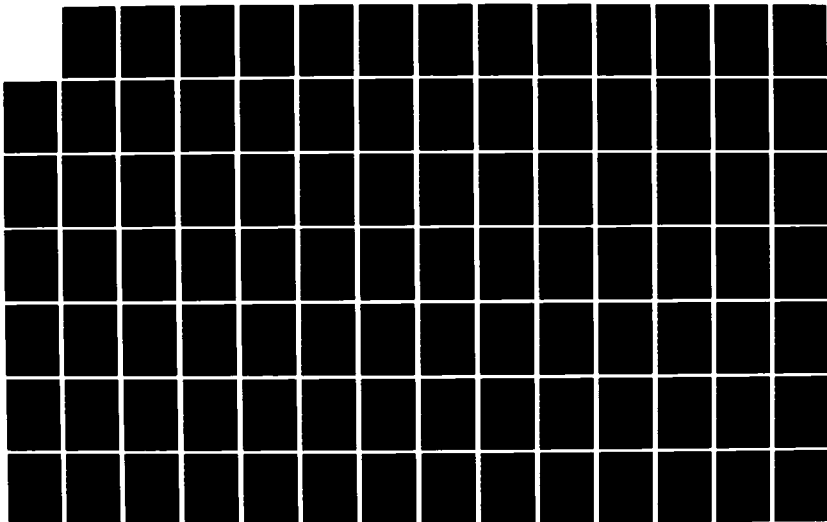
1/3

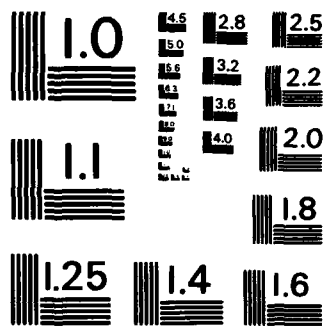
UNCLASSIFIED

ESL-714190-11 N00014-82-K-0037

F/G 20/14

NL





MICROCOPY RESOLUTION TEST CHART
NATIONAL BUREAU OF STANDARDS-1963-A



The Ohio State University

AD-A162 553

SPACE-FREQUENCY SAMPLING CRITERIA
FOR ELECTROMAGNETIC SCATTERING OF A FINITE OBJECT

By

Fredric Y. S. Fok

The Ohio State University

ElectroScience Laboratory

Department of Electrical Engineering
Columbus, Ohio 43212

DTIC
S D
DEC 11 1985
D

Technical Report No. 714190-11
Contract No. N00014-82-K-0037
August 1985

Department of the Navy
Office of Naval Research
800 North Quincy Street
Arlington, Virginia 22217

DISTRIBUTION STATEMENT A
Approved for public release
Distribution Unlimited

85 11 05 039

NOTICES

When Government drawings, specifications, or other data are used for any purpose other than in connection with a definitely related Government procurement operation, the United States Government thereby incurs no responsibility nor any obligation whatsoever, and the fact that the Government may have formulated, furnished, or in any way supplied the said drawings, specifications, or other data, is not to be regarded by implication or otherwise as in any manner licensing the holder or any other person or corporation, or conveying any rights or permission to manufacture, use, or sell any patented invention that may in any way be related thereto.

AD-A162553

50272-101

REPORT DOCUMENTATION PAGE		1. REPORT NO.	2.	3. Recipient's Accession No.	
4. Title and Subtitle		SPACE-FREQUENCY SAMPLING CRITERIA FOR ELECTROMAGNETIC SCATTERING OF A FINITE OBJECT		5. Report Date August 1985	
7. Author(s) Frederic Y.S. Fok		9. Performing Organization Name and Address Ohio State University ElectroScience Laboratory 1314 Kinnear Road Columbus, Ohio 43212		8. Performing Organization Rept. No. 714190-11	
12. Sponsoring Organization Name and Address Department of the Navy Office of Naval Research 800 North Quincy Street Arlington, Virginia 22217		15. Supplementary Notes		10. Project/Task/Work Unit No.	
16. Abstract (Limit: 200 words)		13. Type of Report & Period Covered Technical		11. Contract(C) or Grant(G) No. (C)N00014-82-K-0037 (G)	
<p>This investigation concerns the sampling criteria in the wave number space for generating the spatial impulse response of a finite target. The impulse response of a finite target is important for target identification and imaging. The other purpose of this report is in the management of large amounts of data for potential application in the presentation of scattered field data and construction of such images. For clarity, monostatic impulse responses of up to two dimensions are considered.</p> <p>A proper choice of canonical confinement for the target in space can greatly reduce the number of samples required to sufficiently characterize the target's spatial impulse response. One dimensional impulse responses generated using two basic types of confinement: 1) isotropic and 2) parallelepiped, are compared. The two approaches show competitive reconstructed results. Though a sampling lattice may be more efficient in the sense of a reduced number of measurement points, it may be less effective when digital processing is involved. Specifically, the time consuming interpolation step is required to put data presented in other types of sampling lattice into the cubic type.</p> <p>Two dimensional impulse responses reconstructed from cubic sampled data are compared with those using Mensa et al.'s method. Two dimensional impulse responses obtained also indicate good potentials for image reconstruction via the spatial impulse response.</p>		14.		12. Contract(C) or Grant(G) No. (C)N00014-82-K-0037 (G)	
17. Document Analysis		18. Availability Statement		21. No of Pages 192	
a. Descriptors		19. Security Class (This Report) Unclassified		22. Price	
b. Identifiers/Open-Ended Terms		20. Security Class (This Page) Unclassified			
c. COSATI Field/Group					

TABLE OF CONTENTS

	<u>Page</u>
LIST OF TABLES.....	iv
LIST OF ILLUSTRATIONS.....	v
CHAPTER	
I. INTRODUCTION.....	1
II. THEORY.....	5
III. PRACTICAL CONSIDERATIONS.....	28
IV. ONE DIMENSIONAL IMPULSE RESPONSES.....	36
V. TWO DIMENSIONAL IMPULSE RESPONSES.....	81
VI. CONCLUSIONS.....	105
VII. RECOMMENDATIONS.....	113
APPENDIXES	
A. THE DERIVATION OF EQUATION (2-13).....	117
B. PROGRAMS DEVELOPED.....	131
REFERENCES.....	191



Accession For	
NTIS CRA&I	<input checked="" type="checkbox"/>
DTIC TAB	<input type="checkbox"/>
Unannounced	<input type="checkbox"/>
Justification	
<i>McDonnell</i>	
By	
Distribution /	
Availability Codes	
Dist	Avail and/or Special
A-1	

LIST OF TABLES

<u>Table</u>		<u>Page</u>
4-1	Efficiency comparison on 3 objects using 3 types of containment cells.....	43
4-2	The number of sampling points for 3 types of sampling on 3 objects over various frequency ranges.....	44
5-1	An example: Time estimation.....	91

LIST OF ILLUSTRATIONS

<u>Figure</u>		<u>Page</u>
2-1	Block diagram depicting system analogy.....	6
2-2	Periodicity of the canonical unit: parallelogram (shaded) with its images (dotted lined) defined by \bar{v}_1 and \bar{v}_2	14
2-3	New \bar{v}_1 and \bar{v}_2 defining a similar periodicity as Figure 2-2 except for the extra guard band.....	15
2-4	New \bar{v}_1 and \bar{v}_2 defining a similar periodicity as Figure 2-2 except the images are rotated around the unit.....	16
2-5	A choice of periodicity for the parallelogrammatic containment unit.....	19
2-6	Sampling lattice defined by the choice of periodicity in Figure 2-5.....	20
2-7	A choice of periodicity for the circular containment cell.....	22
2-8	Sampling lattice defined by the choice of periodicity in Figure 2-7.....	23
3-1	Frequency information available.....	29
3-2	Frequency information available after assumption is made about the negative frequency samples.....	32
4-1	Cosine tapering weighting (Equation 4-2 with $N_1=16$).....	45
4-2	Impulse response of a 6" metallic sphere with frequency samples taken every 60 Mhz over the range of 0 to 12 Ghz..	46

LIST OF ILLUSTRATIONS (CONTINUED)

<u>Figure</u>	<u>Page</u>
4-3	Impulse response of a 6" metallic sphere with frequency samples taken every 125 Mhz over the range of 0 to 12 Ghz and interpolated using Equation (4-1)..... 47
4-3a	Error of Figure 4-3 from Figure 4-2..... 48 (Magnification=10X)
4-4	Similar description as Figure 4-3, except frequency samples are taken every 250 Mhz..... 49
4-4a	Error of Figure 4-4 from Figure 4-2..... 50 (Magnification=10X)
4-5	Similar description as Figure 4-3, except frequency samples are taken every 500 Mhz..... 51
4-5a	Error of Figure 4-5 from Figure 4-2..... 52 (No magnification)
4-6	Similar description as Figure 4-3, except frequency samples are taken every 750 Mhz..... 53
4-6a	Error of Figure 4-6 from Figure 4-2..... 54 (No magnification)
4-7	Impulse response of a 6" metallic sphere at 0° aspect angle with 1-D frequency response interpolated from 2-D isotropic lattice samples taken with a safety factor of 1 over the range of 0 to 12 Ghz using Equations (4-3) and (2-13)..... 55
4-7a	Error of Figure 4-7 from Figure 4-2..... 56
4-8	Similar description as Figure 4-7, except the aspect angle is .72°..... 57
4-8a	Error of Figure 4-8 from Figure 4-2..... 58
4-9	Similar description as Figure 4-7, except the aspect angle is 1.44°..... 59
4-9a	Error of Figure 4-9 from Figure 4-2..... 60
4-10	Similar description as Figure 4-7, except the aspect angle is 30°..... 61

LIST OF ILLUSTRATIONS (CONTINUED)

<u>Figure</u>	<u>Page</u>
4-10a	Error of Figure 4-10 from Figure 4-2..... 62
4-11	Impulse response of a 6" metallic sphere at 0° aspect angle with 1-D frequency response interpolated from 2-D cubic lattice samples taken with a safety factor of 1 over the range of 0 to 12 Ghz using Equations (4-3) and (2-11).. 63
4-11a	Error of Figure 4-11 from Figure 4-2..... 64
4-12	Similar description as Figure 4-11, except the aspect angle is 1.19°..... 65
4-12a	Error of Figure 4-12 from Figure 4-2..... 66
4-13	Similar description as Figure 4-11, except the aspect angle is 2.39°..... 67
4-13a	Error of Figure 4-13 from Figure 4-2..... 68
4-14	Similar description as Figure 4-11, except the aspect angle is 45°..... 69
4-14a	Error of Figure 4-14 from Figure 4-2..... 70
4-15	Impulse response of a 6" metallic sphere at 0° aspect angle with 1-D frequency response interpolated from 2-D isotropic lattice samples taken with a safety factor of 3 over the range of 0 to 12 Ghz using Equations (4-3) and (2-13)..... 71
4-15a	Error of Figure 4-15 from Figure 4-2..... 72 (Magnification=10X)
4-16	Similar description as Figure 4-15, except the aspect angle is 0.35°..... 73
4-16a	Error of Figure 4-16 from Figure 4-2..... 74 (Magnification=10X)
4-17	Similar description as Figure 4-15, except the aspect angle is 30°..... 75
4-17a	Error of Figure 4-17 from Figure 4-2..... 76 (Magnification=10X)

LIST OF ILLUSTRATIONS (CONTINUED)

<u>Figure</u>	<u>Page</u>
4-18	77
Dimensional perspective among the sphere, cube and sphere cap cylinder used in the example..... (Diameter of sphere = 6 inches)	
4-19	78
The number of samples specified by the different types of sampling lattices on a sphere cap cylinder described in Figure 4-18.....	
4-20	79
The number of samples specified by two types of sampling lattices on a 6" sphere.....	
4-21	80
The number of samples specified by two types of sampling lattices on the cube described in Figure 4-18.....	
5-1	92
2-D impulse response of a finite metallic circular cylinder with 6" in length and 3" in diameter. Frequency samples are taken at the cubic sampling lattice over the range of 2 to 5 Ghz and Fourier transformed discretely into the spatial domain. Data are taken over the half plane: $0 < \theta < \pi$	
5-1a	93
Contour plot of Figure 5-1.....	
5-2	94
2-D impulse response of a finite metallic circular cylinder with 6" in length and 3" in diameter. Frequency samples are taken over 6 rings: 2.5,3,3.5,4,4.5,5 Ghz and transformed into the spatial domain via Mensa et al.'s method. Data are taken over the half plane: $0 < \theta < \pi$	
5-2a	95
Contour plot of Figure 5-2.....	
5-3	96
Similar description as Figure 5-2 with 10 additional frequency rings: 5.5,6,6.5,7,7.5,8,8.5,9,9.5,10 Ghz.....	
5-3a	97
Contour plot of Figure 5-3.....	
5-4	98
Similar description as Figure 5-3, except the data are taken over the full 360° plane: $0 < \theta < 2\pi$	
5-4a	99
Contour plot of Figure 5-4.....	
5-5	100
The plot of the absolute value of the amplitude in Figure 5-4.....	
5-5a	101
Contour plot of Figure 5-5.....	

LIST OF ILLUSTRATIONS (CONTINUED)

<u>Figure</u>	<u>Page</u>	
5-6	2-D impulse response of a 6" metallic sphere with its centre situated at (3",0). Frequency samples are taken at the cubic sampling lattice over the range of 0 to 12 Ghz. The data are cosine tapering weighted before Fourier transformed discretely into the spatial doamin. Data are taken over the half plane: $\pi < \theta < 2\pi$	102
5-6a	Contour plot of Figure 5-6.....	103
5-7	Path length of a creeping wave on a metallic sphere.....	104
A-1	Hexagonal integration limit.....	118
B-1	Flow chart showing the relationship among the written programs.....	132

CHAPTER I
INTRODUCTION

Discrete data sampling at the Nyquist rate (or better) for the reconstruction of continuous waveforms is well known. However, the application of the sampling theorem [1,2] is often limited to one dimensional problems. This report will explore an application of the N dimensional sampling theorem to inverse scattering. More specifically, the application is on the reconstruction of the spatial impulse response of a finite object using different sampling criteria. The different aspects of the N dimensional sampling theorem are investigated to produce efficient sampling criteria in the wave number space such that the spatial impulse response of a finite object is sufficiently characterized. In addition, the impulse response concept is extended to create possibly an image of the object.

The impulse response [3,4] is important both in target identification and imaging. The impulse response concept, as most people understand, is a far field one dimensional time response concept. This time response waveform when applied in scattering can be plotted on a distance abscissa after the factor due to the speed of the wave is

accounted for. If one can obtain the frequency responses of a finite object for all aspect angles over the 4π solid angle, the inverse Fourier transform of the total frequency response into the spatial domain forms an image which is called the spatial impulse response.

i.e., the impulse response of a finite object at \bar{x} is

$$f(\bar{x}) \triangleq \frac{1}{(2\pi)^3} \int_{-\infty}^{\infty} F(\bar{k}) e^{j(\bar{k} \cdot \bar{x})} d\bar{k} \quad (1-1)$$

where $F(\bar{k})$ = the far field frequency response of a finite object at \bar{k} in the space-frequency domain

$$\bar{x} = (x_1, x_2, x_3)$$

$$\bar{k} = (k_1, k_2, k_3)$$

$$d\bar{k} = dk_1 dk_2 dk_3$$

The three dimensional function $f(\bar{x})$ for all \bar{x} 's in the x-space constitutes an image called the spatial impulse response.

The spatial impulse response can be divided into two types - the monostatic and the bistatic. The monostatic spatial impulse response uses monostatic frequency responses of all aspect angles. The bistatic spatial impulse response uses the bistatic frequency responses of all receiving aspect angles. The spatial, two dimensional, or one dimensional impulse responses discussed hereafter will all be referring to the monostatic case unless otherwise stated. The data used are also monostatic data. However, the theory to be discussed is also applicable to bistatic cases. Furthermore, only two dimensional frequency data are

used in the discussion, so this report will emphasize the two dimensional impulse response only.

In the introduction, the theme and purpose of this report are defined. A brief description on each of the following chapters is also included. In Chapter II, the impulse response, sampling theorem and their relationship are discussed. The basics of the one dimensional impulse response concept and the one dimensional sampling theorem are first reviewed. Using the idea of the settling time, one can relate the impulse response to the sampling theorem. Then the one dimensional impulse response concept is extended to the three dimensional space. Lewis and Bojarski's [5,6] work in the area is also briefly contrasted. A decision rule based on Petersen and Middleton's [7] definition of sampling efficiency is introduced so that one can decide on the more efficient sampling grid. There is also a discussion on Petersen and Middleton's N dimensional sampling theorem and its different forms which depend on the different types of sampling techniques. Then Mensa et al.'s [8] polar transformation and single frequency approach to two dimensional Fourier transform is rederived. Their approach presents a new perspective to the Nyquist sampling criteria.

Some practical aspects of the theory in Chapter II are considered in Chapter III. Even though the discussion is in one dimension, it is also applicable to two and three dimensional analyses. The real signal requirement on Fourier transform is rederived. This helps to clarify the problem of non-zero imaginary parts during data processing. Using the sampling theorem interpolation scheme, the frequency bandwidth's

relationship to target size and spatial resolution is considered. A common problem that may be easily overlooked in data processing is the periodicity of the Fourier series representation to solve the Fourier integral. This is also restated in the last part of Chapter III.

In order to build some confidence in the different forms of Petersen and Middleton's sampling criteria, results of interpolating one dimensional impulse responses are presented in Chapter IV. The interpolation scheme used is the same as in the sampling theorem, except the infinite summation is a finite summation. The interpolated results using one dimensional sampled data appear first in the chapter to preview the interpolation via two dimensional sampled data. Later, an example is chosen to compare the efficiency of different sampling grids. Two dimensional impulse responses computed using discrete two dimensional Fourier transform are compared with results using Mensa et al.'s approach to Fourier transformation in Chapter V. The potential of using the spatial impulse response for target imaging is explored in the last part of the report.

CHAPTER II

THEORY

Some of the basic concepts on impulse response and one dimensional sampling theorem are individually reviewed. Then the two concepts are combined and extended to three dimensional space. The different aspects of N dimensional sampling theorem are introduced. Finally, Mensa et al.'s approach to two dimensional Fourier transform and sampling is also discussed.

If an impulsive electric field is incident on a target, the normalized far zone time domain scattering will be the impulse response of the target at that particular aspect angle and polarization. The approach to be used herein to obtain the impulse response is similar to deconvolution. First, the scattered field (a complex function of frequency) is divided by the spectrum of the incident wave. This result is then inverse Fourier transformed to produce the desired impulse response.

Let $f(t)$ be the input signal in time
 $F(\omega)$ be the input frequency spectrum
 $h(t)$ be the impulse response of the target
 $H(\omega)$ be the frequency response of the target
 $c(t)$ be the output signal in time
 $C(\omega)$ be the output frequency spectrum

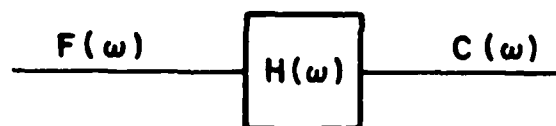


Figure 2-1. Block diagram depicting system analogy

By the convolution theorem of Fourier transform theory [2]

$$C(\omega) = F(\omega)H(\omega) \quad (2-1)$$

$$\Leftrightarrow H(\omega) = \frac{C(\omega)}{F(\omega)} \quad (2-2)$$

Fourier transformed,

$$h(t) = \frac{1}{2\pi} \int_{-\infty}^{\infty} \frac{C(\omega)}{F(\omega)} e^{j\omega t} d\omega \quad (2-3)$$

According to Kennaugh and Moffatt [3], the impulse response will decay exponentially for large values of $(t - \frac{r}{c})$

where t -time

r -distance between observation point and the origin

c -speed of light

Therefore, one can define a settling time when the impulse response has its amplitude embedded in the noise level. For all practical purposes, the settling time will be the end of the impulse response. Thus, the impulse response is a time limited signal. From the sampling theorem [1,2]: "A time limited signal can be reproduced from its discrete frequency values, if it is sampled over the complete frequency domain using the Nyquist rate." As a consequence, the impulse response may be reproduced by measuring its frequency spectrum at the Nyquist sampling rate (f_s). (i.e., $f_s < 1/2T$; where the signal is limited in time to $\pm T$)

Or, if

$$f(t) = 0 \quad |t| > T$$

then

$$F(\omega) = \sum_{n = -\infty}^{\infty} F\left(\frac{n\pi}{T}\right) \frac{\sin(\omega T - n\pi)}{\omega T - n\pi} \quad (2-4)$$

where the samples are taken at $\omega = n\pi/T$, but n is taken from $-\infty$ to ∞ .

Now, let's consider the concept of marching in time. An impulsive magnetic field incident upon a solid conducting body, sets up current \mathbf{J} on the surface. As a result, $\mathbf{J} = \hat{n} \times \mathbf{H}^T$ will start generating a scattering field in all directions. After the wave passes over the target, the current created decays exponentially. The scattered field behaves similarly. At one aspect angle, the time, where the onset of the scattered waveform is observed, corresponding to the time required for the wave to reach the initial scattering point on the target and return to the radar, is designated as the initial time T_i . The time (T_f) before the final exponential decay occurrence defines the end of the target.

Let x be the length of the object along the line of sight

at one aspect angle

Δt be the time difference between the initial time and

the final time at that aspect angle

c be the speed of light

$$\Delta t = T_f - T_i$$

then,

$$2x = c\Delta t$$

$$x = \frac{c(T_f - T_i)}{2} \quad (2-5)$$

Any physical object has finite dimensions. If it is located in a rectangular coordinate system (\bar{x} : x_1, x_2, x_3), then it can be said to have limited dimensions in the \bar{x} coordinates. Namely, the object is confined by:

$$x_1^a < x_1 < x_1^b$$

$$x_2^a < x_2 < x_2^b$$

$$x_3^a < x_3 < x_3^b$$

where $x_1^a, x_2^a, x_3^a, x_1^b, x_2^b, x_3^b$ are some real constants.

The confinement of an object in space is equivalent in saying its spatial impulse response is time limited, as the impulse response has a settling time for every aspect angle. Using the above argument, if the impulse response measurement is obtained at all aspect angles, then an image of the object may be generated from the data.

The approach taken here is a little different from Lewis-Bojarski's work [5,6]. They use physical optics approximation to arrive at the formulation for imaging. In another words, they do not use the information on the shadowed side. The object is illuminated in every direction. Information on the 4π solid angle is required, even though measurement on the complete solid frequency sphere is difficult to be implemented. With the help of the N dimensional sampling theorem, which is described later, the implementation becomes more practical. If one requires information over a finite frequency range, then the infinite number of samples over the 4π solid angle is converted to a finite number of samples. The N dimensional sampling theorem defines a sufficient sampling criterion to characterize space limited or wave number limited signal. Thus, the response at any point may be interpolated from the sampled data using the reconstruction scheme defined by the sampling theorem.

To employ the sampling theorem, the signal must be limited in time or frequency. In this case, the object is limited in three dimensions. The transformed space will be the wave number space. Ideally, the frequency response or the k-space response can be reproduced by sampling in the k-space discretely but over the infinite space. To obtain the spatial impulse response, a three dimensional inverse Fourier transform is performed on the k-space response.

While there is only one sampling theorem, there are different forms of the sampling that satisfy the sampling theorem. In one dimension, the different forms depend on how the time limited signal or the frequency limited signal is assumed to repeat itself. In three dimensions, the forms depend on how the target is placed in the reference plane (x_1, x_2, x_3), and how the target's images are repeated in the three dimensional space. Theoretically, there are infinitely different forms of the sampling, as there is an infinite number of different target shapes, sizes and orientations. One would prefer a general sampling scheme that is applicable to all, or at least most, objects with any orientation. This is where the canonical containment cell fits in. These canonical containment cells are usually of simple geometries so that a wide variety of targets can be confined by their boundaries. Examples of these simple geometries are sphere, parallelepiped, ellipsoid, finite cylinder. Thus the forms of the sampling depend on the choice of the canonical confinement units and how the unit's images are repeated in the three dimensional space.

Two simple canonical units to be treated in this report are the sphere and parallelepiped. A decision rule between these two types of units will be discussed. First, the concept of sampling efficiency will be defined. The following efficiency formula is a modified version of the original formula defined by Petersen and Middleton [7].

$$\eta_s = \frac{\text{CONSERVATIVE ESTIMATE OF THE VOLUME OF THE OBJECT}}{\text{VOLUME OF THE SMALLEST SPHERE ENCLOSING THE OBJECT}} \quad (2-6)$$

= Efficiency for isotropic sampling

$$\eta_p = \frac{\text{CONSERVATIVE ESTIMATE OF THE VOLUME OF THE OBJECT}}{\text{VOLUME OF THE SMALLEST PARALLELEPIPED ENCLOSING THE OBJECT}} \quad (2-7)$$

= Efficiency for parallelepipedic sampling

Rule:

$$\eta_s > \eta_p \quad \text{use spherical confinement} \quad (2-8)$$

$$\eta_s < \eta_p \quad \text{use parallelepiped confinement}$$

The N dimensional sampling theorem obtained by Petersen and Middleton [7] is: "A function $F(\bar{k})$ whose inverse Fourier transform $f(\bar{x})$ vanishes over all but a finite portion in x-space can be everywhere reproduced from its sampled values taken over a lattice of points

$\{l_1\bar{u}_1 + l_2\bar{u}_2 + \dots + l_n\bar{u}_n\}; l_1, l_2, \dots, l_n = 0, \pm 1, \pm 2, \dots$ provided that the vectors $\{\bar{u}_j\}$ are small enough to ensure non-overlapping of the x-space signal $f(\bar{x})$ with its images on a periodic lattice defined by the vectors $\{\bar{v}_i\}$, which $\bar{v}_i \cdot \bar{u}_j = 2\pi\delta_{ij}$."

Let's consider the non-overlapping condition in the N dimensional sampling theorem. The requirement is 'non-overlapping' of the object cell $f(\bar{x})$ with its images on a periodic lattice. Thus, the periodic lattice is not uniquely defined. Any one of Figure 2-2, 2-3, or 2-4 has a valid two dimensional periodicity. Their respective periodicity is defined by their respective $\{\bar{v}_1, \bar{v}_2\}$. This non-uniqueness provides flexibility on the choice of the confinement cell.

However, an efficient sampling lattice may be defined. Petersen and Middleton [7]: "An efficient sampling lattice is one which uses a minimum number of sampling points to achieve an exact reproduction of a space limited function." In another words, the closest packing of the object cell and its images without overlapping will be efficient. $\{\bar{v}_1, \bar{v}_2, \bar{v}_3\}$ will be changed if the images are rotated around the object cell; hence, the sampling lattice is still not fully defined (Figures 2-2 and 2-4). Nevertheless, any set of $\{\bar{v}_1, \bar{v}_2, \bar{v}_3\}$ defined by the above criterion will have the same efficiency, or the same number of sampling points.

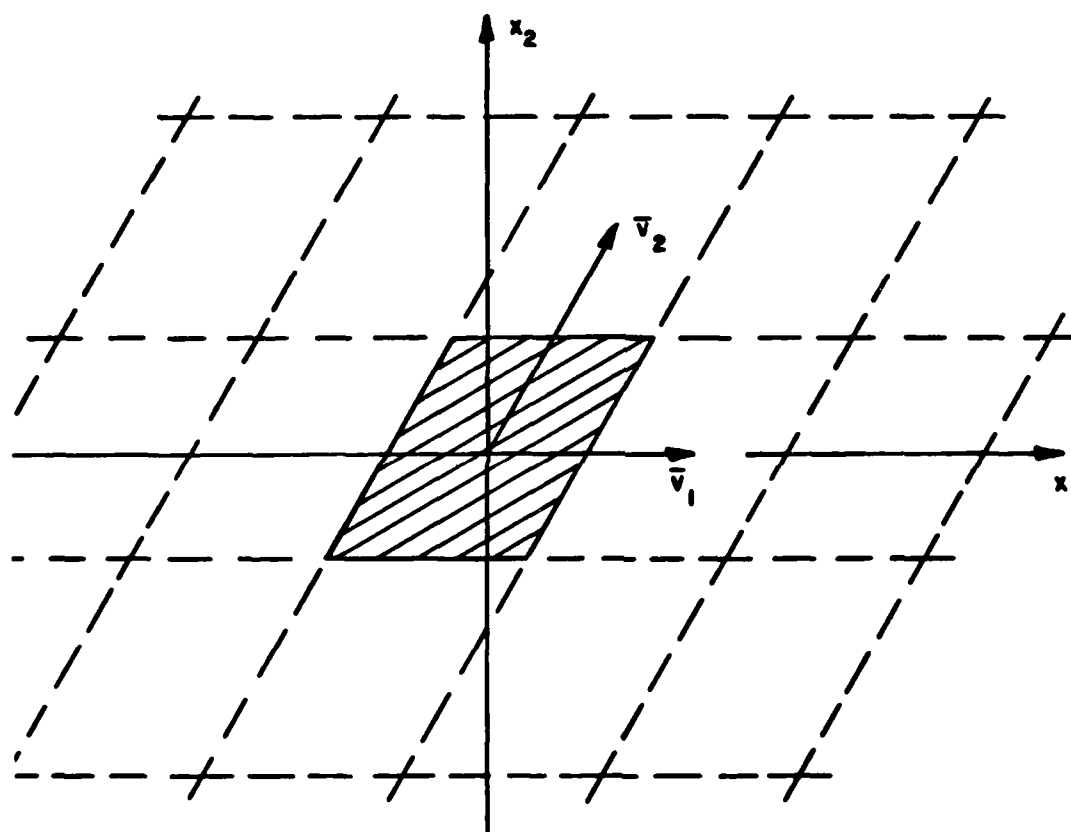


Figure 2-2. Periodicity of the canonical unit: parallelogram (shaded) with its images (dotted lined) defined by \bar{v}_1 and \bar{v}_2

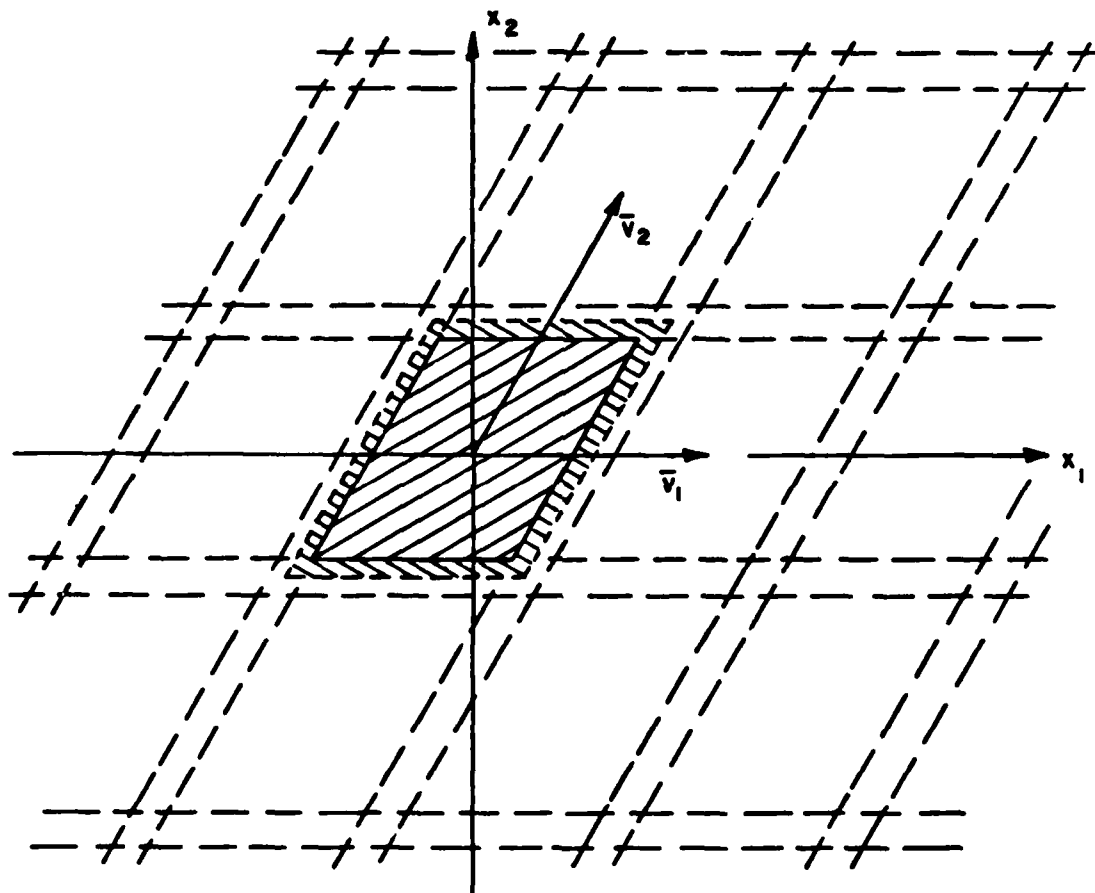


Figure 2-3. New \bar{v}_1 and \bar{v}_2 defining a similar periodicity as Figure 2-2 except for the extra guard band

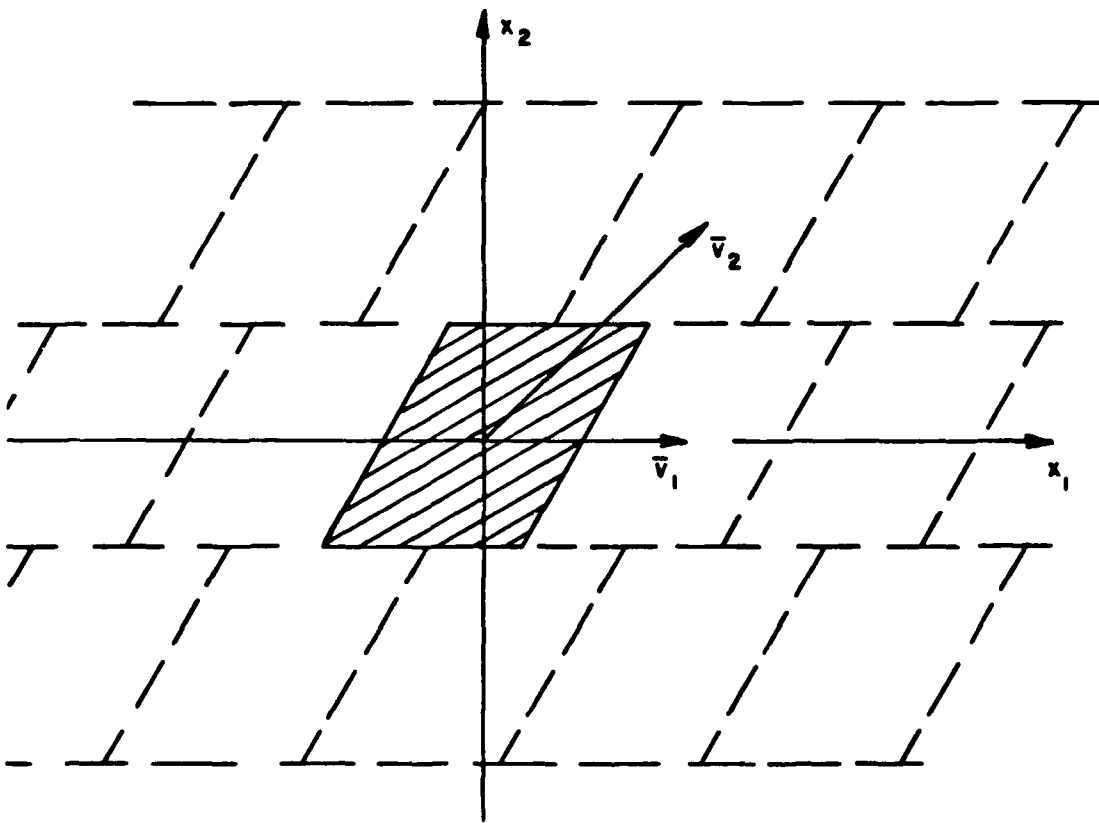


Figure 2-4. New \bar{v}_1 and \bar{v}_2 defining a similar periodicity as Figure 2-2 except the images are rotated around the unit.

The application of the sampling theorem for the reconstruction of the original signal needs only an interpolation formula, provided the non-overlapping condition is met. In this application, if one has the following:

- a) A signal limited in x-space and its images are specified by \bar{v}_1, \bar{v}_2 with non-overlapping condition met.
- b) The sampling lattice in k-space is defined by the vector:

$$l_1 \bar{u}_1 + l_2 \bar{u}_2, \text{ where } l_1, l_2 = 0, \pm 1, \pm 2, \pm 3, \dots$$

$$\text{with } \bar{v}_i \cdot \bar{u}_j = 2\pi \delta_{ij} : \delta_{ij} = \text{Kronecker delta}$$

or

$$U = 2\pi V^{-T}$$

where

$$U = [\bar{u}_1 | \bar{u}_2]$$

$$V = [\bar{v}_1 | \bar{v}_2]$$

$-T$ is the notation for the transpose of the matrix
inverse of V

- c) The interpolation formula

then one can reproduce the two dimensional impulse response. The procedures are:

- 1) Sample the k-space response at the sampling lattice for $F(l_1 \bar{u}_1 + l_2 \bar{u}_2)$.
- 2) Interpolate other required points, if necessary.

The interpolation formula taken from Petersen and Middleton [7].

$$F(\bar{k}_1, \bar{k}_2) = \sum_{l_1=-\infty}^{\infty} \sum_{l_2=-\infty}^{\infty} F(l_1\bar{u}_1 + l_2\bar{u}_2)G(k_1\hat{k}_1 + k_2\hat{k}_2 - l_1\bar{u}_1 - l_2\bar{u}_2) \quad (2-9)$$

where $\bar{k}_1 = k_1\hat{k}_1$

$$\bar{k}_2 = k_2\hat{k}_2$$

3) Inverse Fourier transform the k-space response to obtain the two dimensional impulse response.

$$f(x_1, x_2) = \frac{1}{4\pi^2} \iint_{-\infty}^{\infty} F(k_1, k_2) e^{j(k_1x_1 + k_2x_2)} dk_1 dk_2 \quad (2-10)$$

With the ease of calculation in mind, the periodicity of the object cell and its images are defined as in Figure 2-5 for this report. Its corresponding sampling lattice is shown in Figure 2-6.

The reconstruction function for the parallelogrammatic sampling [7]:

$$G(\omega_1, \omega_2) = \left(\frac{\sin \pi\omega_1}{\pi \omega_1} \right) \left(\frac{\sin \pi\omega_2}{\pi \omega_2} \right) \quad (2-11)$$

where

ω_1 is in the direction of \bar{u}_1

ω_2 is in the direction of \bar{u}_2

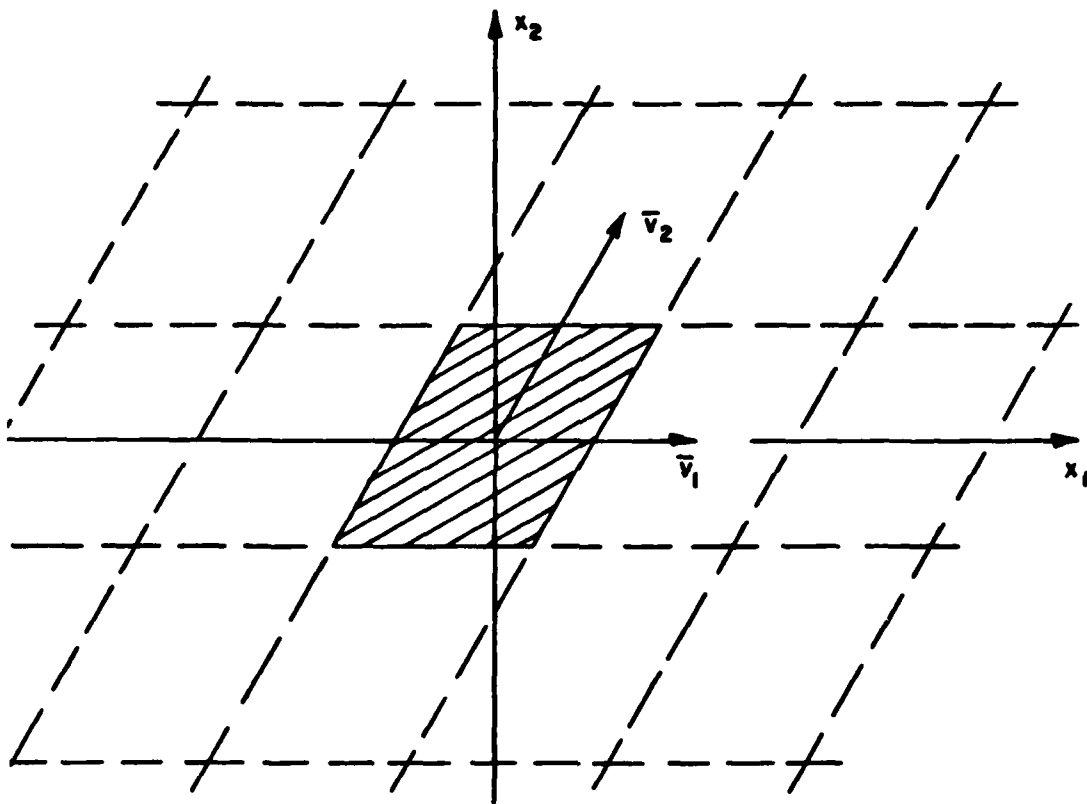


Figure 2-5. A choice of periodicity for the parallelogrammatic containment unit

For the sphere or isotropic confinement, the configuration is adopted from the concept of closest packing of spheres by Coxeter [9]. The configuration chosen for this report is as shown in Figure 2-7. The corresponding sampling lattice is shown in Figure 2-8.

For the two dimensional case [7,9]:

$$\bar{v}_1 = R \begin{bmatrix} \sqrt{3} \\ 2 \\ -1 \\ 2 \end{bmatrix} \quad \bar{v}_2 = R \begin{bmatrix} 0 \\ 1 \end{bmatrix} \quad (2-12)$$

$$\bar{u}_1 = (2\pi/R) \begin{bmatrix} 2 \\ \sqrt{3} \\ 0 \end{bmatrix} \quad \bar{u}_2 = (2\pi/R) \begin{bmatrix} 1 \\ \sqrt{3} \\ 1 \end{bmatrix}$$

where R is the radius of the isotropic cell. The reconstruction function [7]:

$$G(\omega_1, \omega_2) = \frac{1}{R^2 \omega_1 (\omega_1^2 - 3\omega_2^2)} \times \left\{ \begin{aligned} &2\omega_1 \cos(R\omega_1/\sqrt{3}) \cos(R\omega_2) \\ &-2\omega_1 \cos(2R\omega_1/\sqrt{3}) \\ &-2\sqrt{3}\omega_2 \sin(R\omega_1/\sqrt{3}) \sin(R\omega_2) \end{aligned} \right\} \quad (2-13)*$$

where

ω_1 is in the direction of \bar{u}_1

ω_2 is in the direction of \bar{u}_2

(* There is a ω_2 factor missing in the third term of this expression in reference [7]. See Appendix A for details of the derivation).

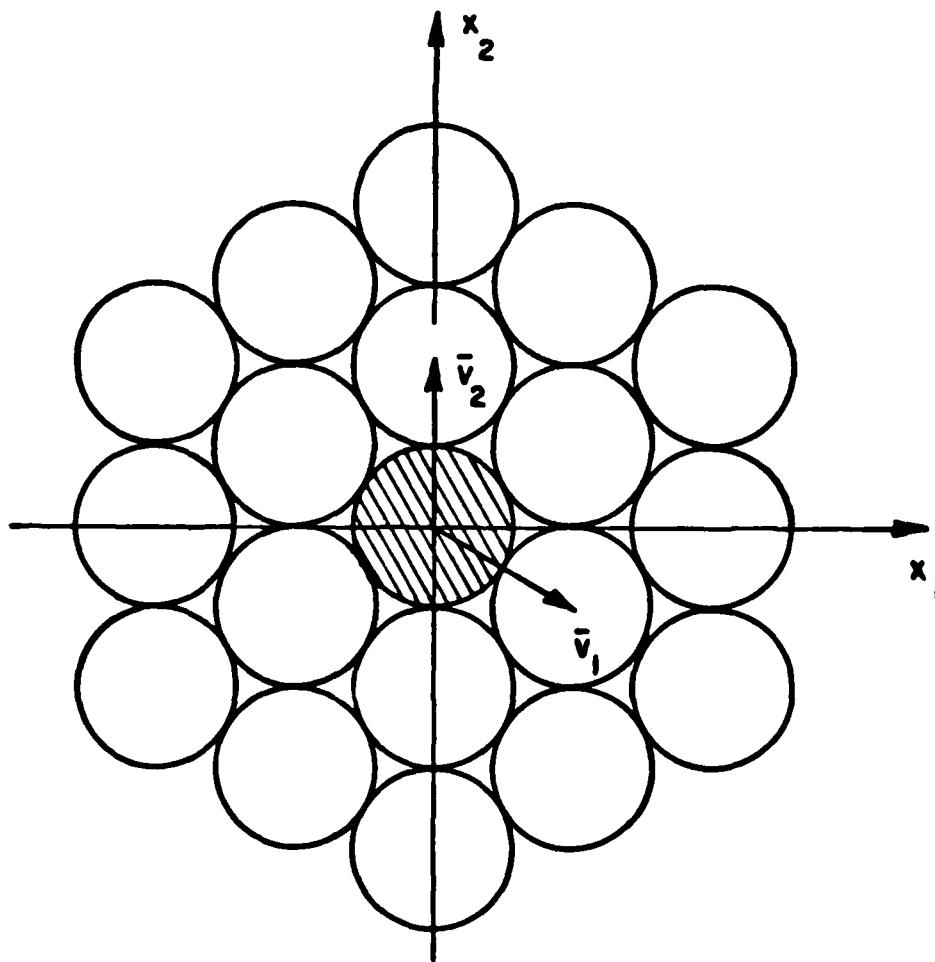


Figure 2-7. A choice of periodicity for the circular containment cell

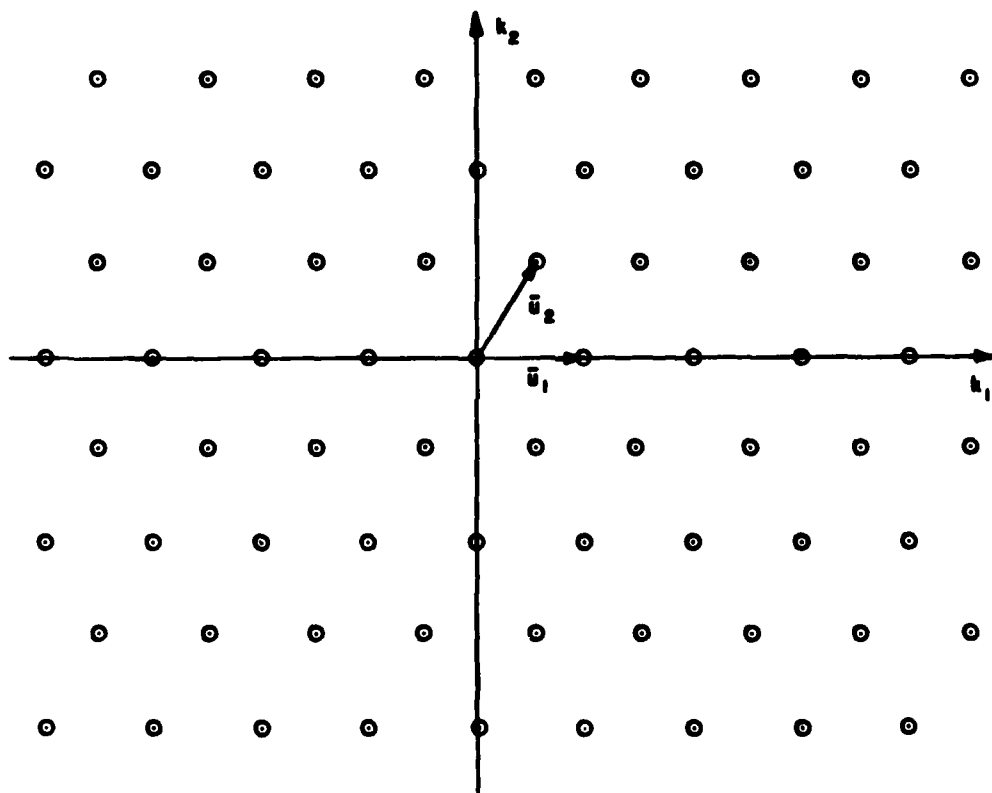


Figure 2-8. Sampling lattice defined by the choice of periodicity in Figure 2-7

Since this report only deals up to two dimensional sampling, the reader is referred to Petersen and Middleton's paper on the three dimensional reconstruction function $G(\omega_1, \omega_2, \omega_3)$.

The N dimensional sampling theorem gives the minimum sampling lattice or criterion which will sufficiently define the k-space signal. All other non sampled k-space values can be interpolated via an extension of Equation 2-9. The k-space signal can be inverse Fourier transformed into the spatial domain to give a representation of the spatial impulse response. In another words, the spatial signal is also characterized by those k-space lattice samples.

If one is interested only in the two dimensional impulse response, then Mensa et al. [8] presents a different view on the sampling criterion. Unfortunately, it is only applicable to the two dimensions. First, rectangular to polar coordinate transformation is applied to the two dimensional Fourier integral (Equation 2-10):

$$f(x_1, x_2) = \frac{1}{4\pi^2} \iint_{-\infty}^{\infty} F(k_1, k_2) e^{j(k_1 x_1 + k_2 x_2)} dk_1 dk_2 \quad (2-14)$$

$$\left\{ \begin{array}{ll} \text{Let } r^2 = k_1^2 + k_2^2 & ; \quad \phi = \tan^{-1}(k_2/k_1) \\ \rho^2 = x_1^2 + x_2^2 & ; \quad \theta = \tan^{-1}(x_2/x_1) \end{array} \right\} \quad (2-15)$$

$$= \frac{1}{4\pi^2} \int_{r=0}^{\infty} \int_{\phi=0}^{2\pi} r \tilde{F}(r, \phi) e^{j2\pi r \rho \cos(\phi - \theta)} dr d\phi \quad (2-16)$$

Then the double integral is reduced to a single integral by considering only a particular frequency ring (i.e. $\delta(r - \omega_i)$).

$$\tilde{f}_i(\rho, \theta) = \frac{\omega_i}{4\pi^2} \int_{\phi=0}^{2\pi} \tilde{F}(\omega_i, \phi) e^{j2\pi \omega_i \rho \cos(\phi - \theta)} d\phi \quad (2-17)$$

Thus, the two dimensional Fourier transformation is reduced to a convolution type integral. $F(k_1, k_2)$ is the frequency response of the target in the two dimensional k-space. The notion of $\delta(r - \omega_i)$ represents information taken only with one frequency. Subsequently, the two dimensional impulse response is obtainable via one integration. If information from other frequency rings are available, then superposition of every frequency ring response in the spatial domain will give a wide band two dimensional impulse response representation.

$$f_T(x_1, x_2) = \sum_i \tilde{f}_i(\rho, \theta) \quad (2-18)$$

where

$$x_1 = \rho \cos \theta$$

$$x_2 = \rho \sin \theta$$

Naturally, the Nyquist spacings between the frequency rings and between angular samples must be used, before the total two dimensional time response obtained can be considered a sufficient representation of the true two dimensional time response.

The angular increment which satisfies the Nyquist criterion is given by Mensa et al. [8]:

$$\Delta\theta \begin{cases} < \frac{\lambda}{2D} & \lambda \ll 2D \\ < \sin^{-1} \frac{\lambda}{(2D)} & \lambda < 2D \\ < \frac{\pi}{4} & \lambda > 2D \end{cases} \quad (2-19)$$

where D = maximum dimension of the object

λ = wavelength of the frequency to be used

(Assumption: The origin of the x-space coincides with the middle of the object.)

The author would like to propose the following for the frequency increment:

$$\Delta f < \frac{c}{2(1+K)D} \quad (2-20)$$

where D = maximum dimension of the object

c = speed of light

K = some safety factor

The aspect angle which has the longest dimension of the object is assumed to have the longest settling time in its impulse response. All other aspect angles require Nyquist frequency increments larger than or equal to this aspect angle. The value of the safety factor is the best estimation achievable by other means. The reason for the safety factor is not all impulse response signals are limited to the length of the object at any aspect angle. Furthermore, in the GTD sense, some of the

multiple scattering effects may be eliminated or included by employing a smaller or larger value of the safety factor. This is equivalent to truncation of the signal in time during measurement.

CHAPTER III

PRACTICAL CONSIDERATIONS

In this chapter, the practical aspects of the previously described theory are presented. Since negative frequencies cannot be physically generated, an assumption on the negative frequency response must be made. First, the assumption of a real measured signal is discussed. The frequency limits are then considered in relation to the object's size, its impulse response and the data processing requirement. For clarity, the practical aspects are discussed in one dimension. Extension to the higher dimensions can be easily accomplished.

In general, a true impulse is hard to generate; instead, a Gaussian pulse is often used. There are also times when good narrow Gaussian pulses are not readily available. In these cases, the approach of frequency sweeping may be used. The bandwidths of most oscillators, waveguide components, transmitting and receiving antennas are limited. In essence, the frequency band can only be swept from ω_L to ω_H (Figure 3-1). To overcome part of the problem, let's consider the one dimensional sampling theorem [1, 2]:

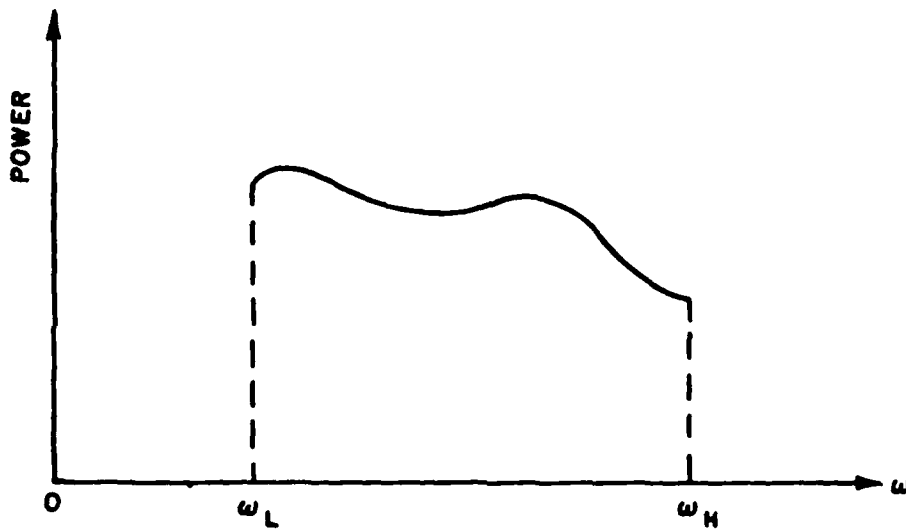


Figure 3-1. Frequency information available

If $f(t) = 0$ for $|t| > T$

then $F(\omega)$ can be uniquely determined from

$$F_n = F\left(\frac{n\pi}{T}\right)$$

and

$$F(\omega) = \sum_{n=-\infty}^{\infty} F\left(\frac{n\pi}{T}\right) \frac{\sin(\omega T - n\pi)}{\omega T - n\pi} \quad (3-1)$$

{Note: If $F(\omega)$ is even, then the required measurement information is $F\left(\frac{n\pi}{T}\right)$; for $n = 0, 1, 2, \dots$ }

Consider the inverse Fourier Transform

$$f(t) = \frac{1}{2\pi} \int_{-\infty}^{\infty} F(\omega) e^{j\omega t} d\omega \quad (3-2)$$

$$= \frac{1}{2\pi} \int_{-\infty}^{\infty} F(\omega) \cos(\omega t) d\omega + \frac{j}{2\pi} \int_{-\infty}^{\infty} F(\omega) \sin(\omega t) d\omega \quad (3-3)$$

If $F(\omega)$ is even, then the integrand in the second integral is an odd function of ω . It follows that the second integral is zero.

Therefore,

$$f(t) = \frac{1}{2\pi} \int_{-\infty}^{\infty} F(\omega) \cos(\omega t) d\omega \quad (3-4)$$

= real function, if $F(\omega)$ is even

(Note: If $F(\omega)$ is complex, then $\text{Re}[F(\omega)] = \text{Re}[F(-\omega)]$ and $\text{Im}[F(\omega)] = -\text{Im}[F(-\omega)]$ are the conditions for $f(t)$ to be real).

In this discussion, the object is real. It follows that $f(t)$ is also real. Now, information from $-\omega_H < \omega < -\omega_L$ and $\omega_L < \omega < \omega_H$ is available. (Figure 3-2)

Next, the Rayleigh Law is used to determine the scattered field at d.c. or zero frequency. From Kennaugh and Cosgriff [3]: "As the source frequency tends to zero, all finite scatterers follow the Rayleigh Law, giving a scattered field intensity which diminishes as the square of frequency." The scattered field intensity at d.c. will be zero.

If

$$\frac{\pi}{T} > \omega_L,$$

then

F_n is known for $-N < n < N$

where

$$N = I \left[\frac{\omega_H T}{\pi} \right] \quad (3-5)$$

$I[x]$ = truncation of x 's value after the decimal point

That is, if the first sampled location ($\frac{\pi}{T}$) is higher than or equal to ω_L , then information is available from $-\omega_H$ to ω_H , because one can interpolate the in between data points using the sampling theorem.

Let

x_S be the object size

K be some safety factor

then the settling time T_S is

$$T_S = 2(1+K) \frac{x_S}{c} \quad \text{with } T = T_S/2$$

One must have the condition:

$$\frac{\pi}{T} > \omega_L$$

$$\frac{2\pi c}{2(1+K)x_S} > \omega_L$$

$$\Leftrightarrow \frac{\pi c}{(1+K)x_S} > \frac{2\pi c}{\lambda_L}$$

$$\Leftrightarrow \lambda_L > 2(1+K)x_S \quad (3-6)$$

This puts a limit on the lowest frequency usable, or the largest object size assumed by a given ω_L .

The span ($\omega_H - \omega_L$) effectively determines the resolution of the impulse response signature. Let x_r be the desired resolution on the object, then the impulse response resolution is

$$t_r = \frac{2x_r}{c}$$

$$\Leftrightarrow \omega_r = \frac{2\pi c}{2x_r}$$

One has the condition:

$$\omega_H > \frac{2\pi c}{2x_r} = \omega_r$$

$$\Leftrightarrow \frac{2\pi c}{\lambda_H} > \frac{\pi c}{x_r}$$

$$\Leftrightarrow \lambda_H < 2x_r \tag{3-7}$$

Conditions 3-6 and 3-7 will help to decide how wide a frequency band may be used. If the bandwidth is wide enough, then the impulse response can be generated to a very good approximation.

A common problem during implementation may involve the inverse Fourier transform on the reconstructed frequency spectrum. This waveform may or may not be a well defined function which can be inverse Fourier transformed into a closed form solution. The common approach would be to approximate the integration using a summation on a digital computer. In effect, this approach will be a Fourier series representation which requires the time or frequency waveform to be periodic. Consequently, there are 2 more limitations:

- 1) The period (T_C) used in the digital computation must be greater than two times the settling time (T_S) of the impulse response.
(i.e., $T_C > 2T_S$)
- 2) The period (ω_C) used in the digital computation must be greater than two times the highest frequency (ω_H) swept.
(i.e., $\omega_C > 2\omega_H$)

Fortunately, a standard IBM subroutine FFT (Fast Fourier Transform) package is available to do the required Fourier analyses.

Furthermore, one dimensional impulse response requires a two dimensional plot. The two axis quantities are amplitude and time. Two dimensional impulse response requires a three dimensional plot. The three axis quantities are the amplitude and the plane axes. Should anyone consider three dimensional impulse response, one requires a plot in four dimensional space. Consequently, this report will only deal with impulse responses up to two dimensions. With the knowledge in one's mind that the spatial impulse response can easily be obtained by an extension of this two dimensional approach when there is an appropriate representation.

CHAPTER IV
ONE DIMENSIONAL IMPULSE RESPONSES

In this chapter, the interpolation of one dimensional impulse responses is presented; first, the result of interpolation using one dimensional data; then, using two dimensional data. The object is a six inch diameter metallic sphere. This object choice is because the Mie solution in frequency domain is readily available. In this first section, the Mie solution frequency data are sampled at different rates and interpolated either using a straight line or a sinc reconstruction function.

$$F(\omega) = \sum_{n=-N}^N F\left(\frac{n\pi}{T}\right) \frac{\sin(\omega T - n\pi)}{\omega T - n\pi} \quad (4-1)$$

where

$$N = I\left(\frac{\omega_H T}{\pi}\right)$$

$I(x)$ = truncation of x 's value after the decimal point

ω_H = highest frequency used

[Note: This is Equation (3-1) except the summation is from $-N$ to $+N$].

A cosine tapering weighting function [10]: (Figure 4-1) (for the convenience of the reader, all tables and figures of Chapter IV are grouped together at the end of the chapter)

$$W(n) \begin{cases} = 0.5[1+\cos(\frac{\pi n}{N_1})] & |n| < N_1 \\ = 0 & |n| > N_1 \end{cases} \quad (4-2)$$

is multiplied to the interpolated frequency data. The purpose of the weighting or filtering is to reduce the effect of the Gibb's phenomenon [2]. The resulting data are inverse Fourier transformed into the time domain discretely to give the impulse response in time.

Figure 4-2 represents a time domain impulse response plot obtained from the Mie solution for a six inch diameter metallic sphere using the frequency spectrum from 0 to 12 Ghz with a cosine tapering filter. The imperfect specular impulse and the ripples around it at the start of the response are caused by 1) finite bandwidth, and 2) Gibbs' phenomenon.

Figure 4-2 is considered to be the standard for comparison with the other responses. Its frequency samples are taken every 60 Mhz and linked together by straight lines. Figure 4-3 has frequency samples taken every 0.125 Ghz over the spectrum of 0 to 12 Ghz and interpolated the in between points using Equation (4-1). The differences of the impulse responses in this chapter from Figure 4-2 (the 'exact' solution) are shown in figures designated with their respective figure number plus an 'a' attached. For example, to obtain Figure 4-2 from Figure 4-3, one adds Figure 4-3a to Figure 4-3.

Figures 4-4, 4-5, and 4-6 are similar to Figure 4-3, except frequency samples are taken every 0.25 Ghz, 0.5 Ghz, and 0.75 Ghz respectively. Figure 4-5 is still recognizable to be Figure 4-2 but Figure 4-6 is not. Figure 4-6 does not have similar behavior because it employs a frequency sampling rate below the Nyquist rate. From Figure 4-2, one can estimate the settling time of the impulse response of the sphere to be about 1.5 nsec. Equally well, one could use a longer settling time depending on one's assumption of the noise amplitude. i.e.,

$$\begin{aligned}
 T &= 0.75E-9s \\
 f_s &> \frac{1}{2T} &= \frac{1}{1.5E-9s} \\
 &\cong 0.66 \text{ Ghz} \\
 &< 0.75 \text{ Ghz (Figure 4-6)}
 \end{aligned}$$

Figures 4-2 to 4-5 have sampling rate better than the Nyquist rate. If the sampling rate is high enough, then one may use straight line interpolation (Figure 4-2) instead of the sinc reconstruction function to save computer time on interpolation. On the other hand, if samples are scarce but still satisfy the Nyquist criterion, then the sinc reconstruction function (Equation (4-1)) is preferred for more pleasing results. (Figures 4-3, 4-4, 4-5)

Now, the reconstruction of the one dimensional impulse responses from data obtained on two dimensional isotropic and cubic sampling lattice is presented.

$$F(\bar{k}_1, \bar{k}_2) = \sum_{l_1} \sum_{l_2} F(l_1\bar{u}_1 + l_2\bar{u}_2)G(k_1\hat{k}_1 + k_2\hat{k}_2 - l_1\bar{u}_1 - l_2\bar{u}_2) \quad (4-3)$$

where

l_1 and l_2 are summed over l_1 and l_2 which satisfy

$$k_L < |l_1 \bar{u}_1 + l_2 \bar{u}_2| < k_H$$

and

k_L and k_H define the frequency bandwidth used.

(Note: This is Equation (2-9) with finite summation.)

Samples are taken out of the Mie's frequency solution on the isotropic sampling lattice defined by \bar{u}_1 and \bar{u}_2 in Equation (2-12), and the cubic sampling lattice defined by :

$$\bar{u}_1 = 2\pi \begin{bmatrix} 1 \\ 0 \end{bmatrix} \quad \bar{u}_2 = 2\pi \begin{bmatrix} 0 \\ 1 \end{bmatrix} \quad (4-4)$$

i.e.,

$$\text{samples are taken over } l_1 \bar{u}_1 + l_2 \bar{u}_2 \text{ for } l_1, l_2 = 0, \pm 1, \pm 2, \dots \quad (4-5)$$

This sampling lattice is generated by the program PTGRID (see Appendix B). The frequency response for an aspect angle is interpolated using Equation (4-3) in conjunction with either Equation (2-13) for isotropic sampling or Equation (2-11) for cubic sampling. This interpolation work is done by the program INTERPOL (see Appendix B). The resulting frequency response is again cosine tapering low pass filtered to reduce the Gibb's phenomenon. After the filtering, the frequency spectrum is inverse Fourier transformed discretely into the time domain to give an impulse response picture for the six inch metallic sphere. The

filtering and the discrete inverse Fourier transform are functions of FTRAN [11] (see Appendix B).

Sampling at every 0.5 Ghz for a six inch diameter metallic sphere, is equivalent to assuming a signal having four times the diameter of the sphere in one dimensional space. Therefore, the two dimensional confinement cell is assumed to contain the sphere and has a guard band of 1.5 times the maximum dimension of the sphere surrounding the sphere. The safety factor thus chosen is 1 (i.e., $2(1+K)=4 \Leftrightarrow K=1$). The frequency range sampled is 0 to 12 Ghz.

Figures 4-7, 4-8, 4-9, and 4-10 are one dimensional impulse responses reconstructed from two dimensional isotropic sampling data, for aspect angles of 0, 0.719, 1.438, 30 degree respectively. The CPU time taken for interpolating each waveform is about 5 minutes for 200 plotting points. Figures 4-11, 4-12, 4-13, 4-14 are reconstructed from cubic sampling data, for aspect angles of 0, 1.193, 2.386, 45 degrees. The CPU time taken for these waveforms is about 2.5 minutes for 200 plotting points. Less time in interpolation for cubic sampled data is probably due to the simplicity of the reconstruction function (Equation (2-11) versus (2-13)). These angular choices are arbitrarily chosen. One should note the close resemblance of all these figures (4-7 to 4-14) with Figure 4-5. Next, let's consider the case of more samples taken. Effectively, the safety factor is changed from one to three but the frequency range remains the same. Figures 4-15, 4-16, and 4-17 are reconstructed one dimensional impulse responses using isotropic samples for aspect angles of 0, 0.352, 30 degrees respectively. Again discrepancy is not high (Figures 4-15a, 4-16a, and 4-17a). Since the

density of samples taken is finer, or more samples participated in the interpolation, the CPU time has increased to about 20 minutes for 200 plotting points.

If both the isotropic and cubic sampling can perform competitively, how does one decide on which sampling grid? The answer lies in the efficiency definition defined previously. However, the area is considered in a plane instead of the volume in a three dimensional space.

i.e., one modifies Equations (2-6) and (2-7) to

$$\text{Efficiency} = \frac{\text{AREA OF A CROSS-SECTION ON THE OBJECT}}{\text{AREA OF THE SAME CROSS-SECTION ON THE TWO DIMENSIONAL ENCLOSURE}} \quad (4-6)$$

but the decision rule: Equation (2-8), remains the same.

Efficiency, as mentioned before, is defined as a minimum sampling requirement. Three objects: a six inch diameter sphere, a $3\sqrt{2}$ inch cube and a sphere cap cylinder are shown in Figure 4-18 on their major axis cross-section. Their respective cross-sectional areas; closest circular, squared, rectangular enclosure cross-sectional areas; and efficiencies are tabulated in Table 4-1.

The definition of Equation (4-5) is used to locate the sampling lattice. The number of these locations over a frequency range is summed to give the minimum number of sampling, defined by the sampling theorem, to sufficiently characterize the spatial impulse response in that frequency range. This work is done by the program PTGRID (see Appendix B). The numbers are tabulated in Table 4-2 and plotted in Figures 4-19,

4-20, and 4-21. A safety factor of one is used in the computation. The sizes of the objects are chosen such that the circular enclosure is the same for all three objects for easy comparison in the graphs.

As the frequency range becomes larger and larger, the significance of the efficient sampling grid becomes more and more important. Let's take the example of the sphere cap cylinder (Figure 4-19). The use of the rectangular enclosure will provide an efficiency of 0.96. The number of samples required over 0 to 12 Ghz is 696. The use of the squared enclosure can only give an efficiency of 0.38. The number of samples required is 2.5 times that of the rectangular enclosure. The use of the circular enclosure has an efficiency of 0.45. The number of samples is about 2.3 times that of the rectangular enclosure. As the frequency range is expanded, saving in measurement time by the proper choice of the enclosure becomes very substantial.

TABLE 4-1

EFFICIENCY COMPARISON ON 3 OBJECTS USING 3 TYPES OF CONTAINMENT CELLS

Object	SPHERE	CUBE	SPHERE CAP CYLINDER
Area on major axis	182.4	116.1	82.2
Area of closest circular enclosure	182.4	182.4	182.4
Area of closest squared enclosure	232.3	116.1	214.7
Area of closest rectangular enclosure	232.3	116.1	85.9
Efficiency of circular enclosure	1	0.64	0.45
Efficiency of squared enclosure	0.79	1	0.38
Efficiency of rectangular enclosure	0.79	1	0.96

(Note: the areas are in units of squared centimeters)

TABLE 4-2

THE NUMBER OF SAMPLING POINTS FOR 3 TYPES OF SAMPLING
ON 3 OBJECTS OVER VARIOUS FREQUENCY RANGES

Object	SPHERE		CUBE	SPHERE CAP CYLINDER	
Type of enclosure	circular	squared	squared	rectangular	squared
Frequency ranges from 0 up to (Ghz)					
1	12	12	8	2	8
2	42	48	24	20	44
3	96	120	60	46	108
4	186	212	100	80	192
5	282	324	160	116	292
6	408	472	240	174	436
7	558	640	324	236	592
8	720	828	420	310	768
9	912	1048	516	384	972
10	1134	1304	656	476	1200
11	1368	1564	776	582	1456
12	1626	1876	940	696	1740
Plotted in Figure	4-19	-	-	4-19	4-19
	4-20	4-20	-	-	-
	4-21	-	4-21	-	-
Notation:	x	o	o	□	o

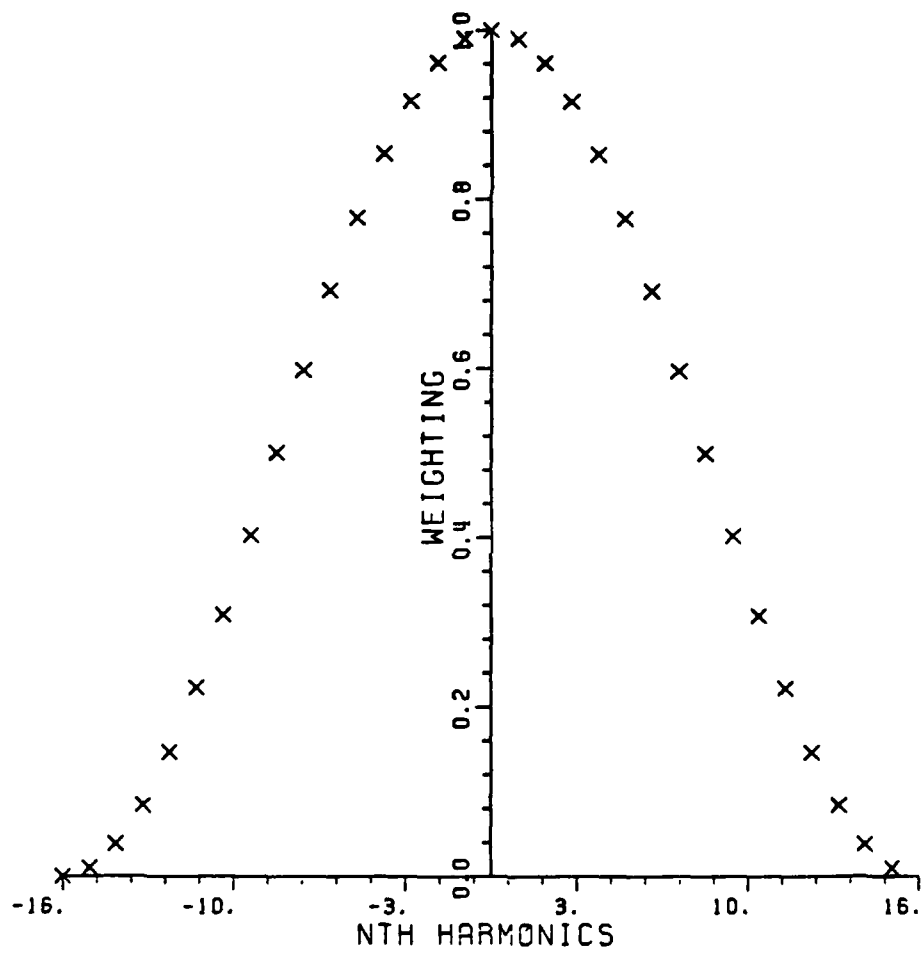


Figure 4-1. Cosine tapering weighting
(Equation (4-2) with $N_1 = 16$)

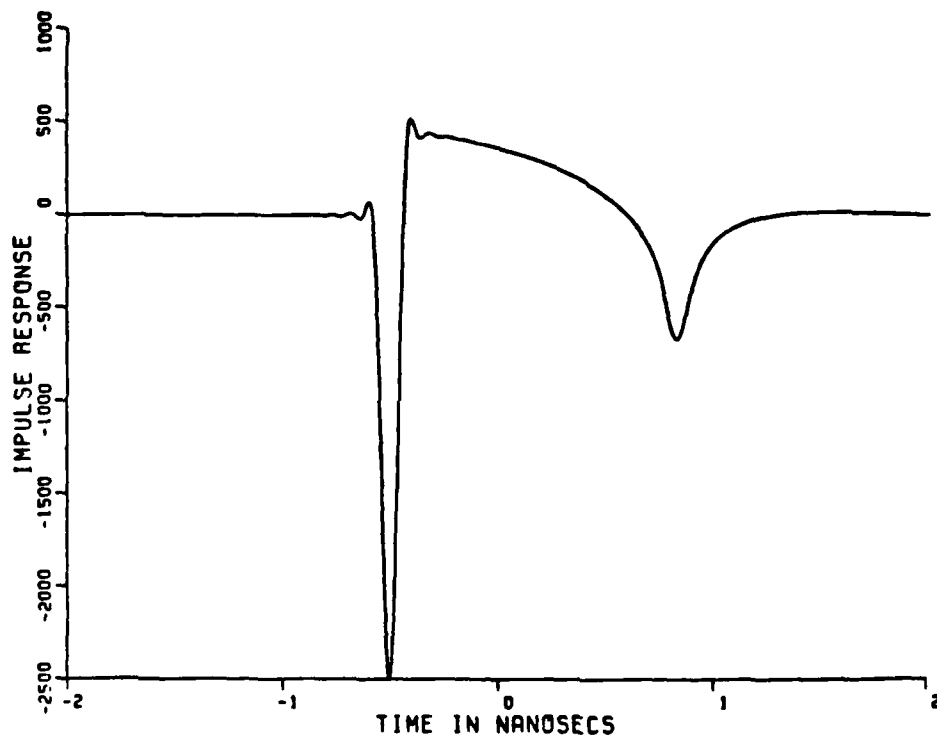


Figure 4-2. Impulse response of a 6" metallic sphere with frequency samples taken every 60 Mhz over the range of 0 to 12 Ghz

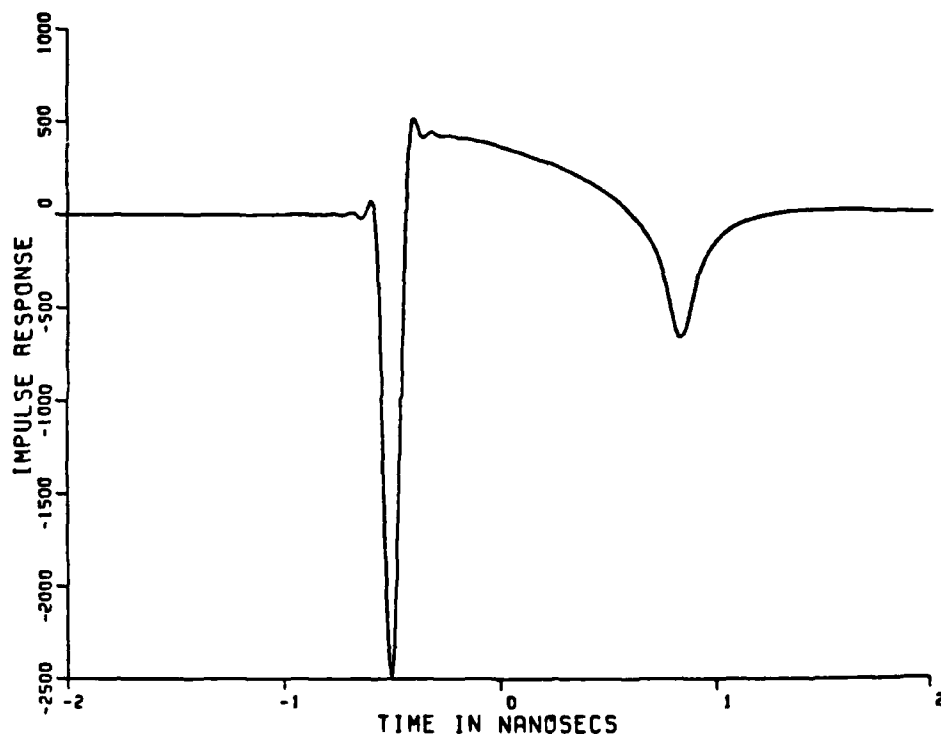


Figure 4-3. Impulse response of a 6" metallic sphere with frequency samples taken every 125 Mhz over the range of 0 to 12 Ghz and interpolated using Equation (4-1)

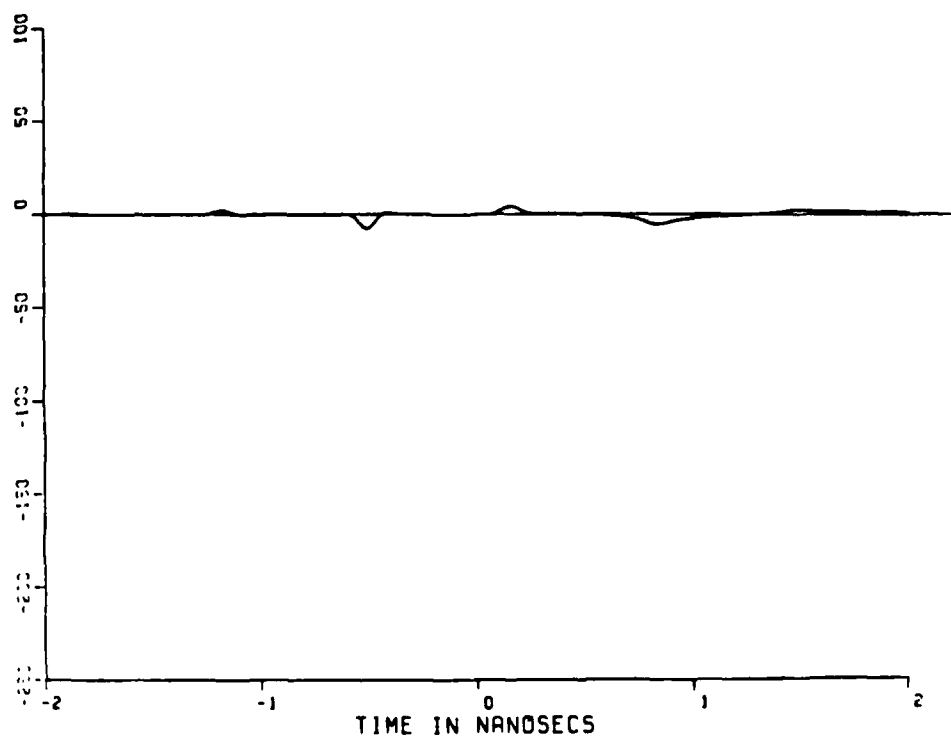


Figure 4-3a. Error of Figure 4-3 from Figure 4-2
(Magnification = 10x)

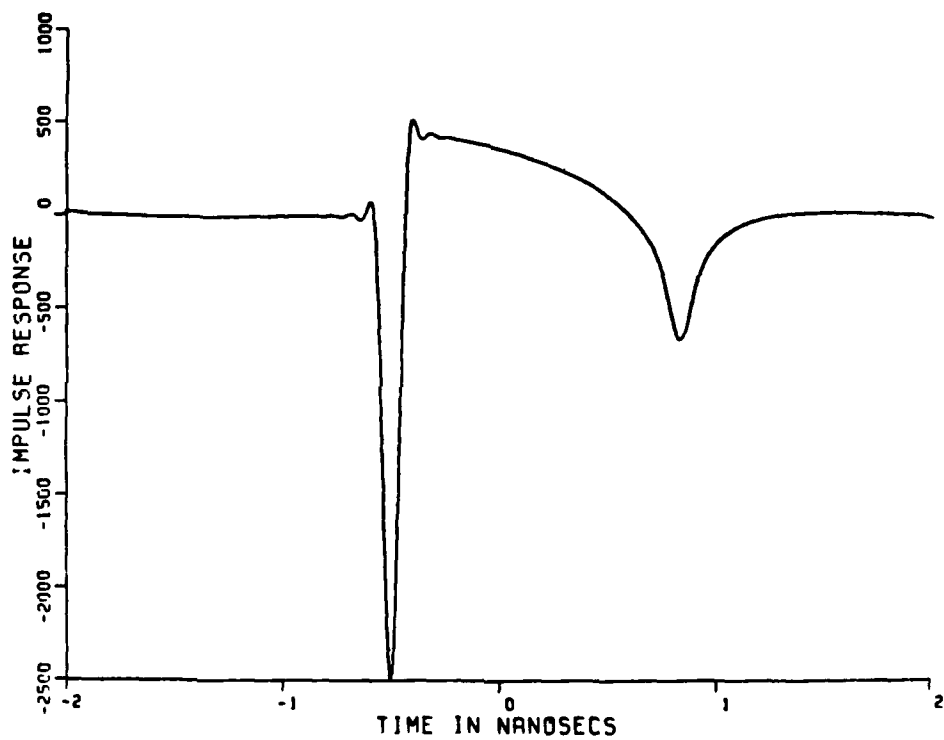


Figure 4-4. Similar description as Figure 4-3, except frequency samples are taken every 250 Mhz

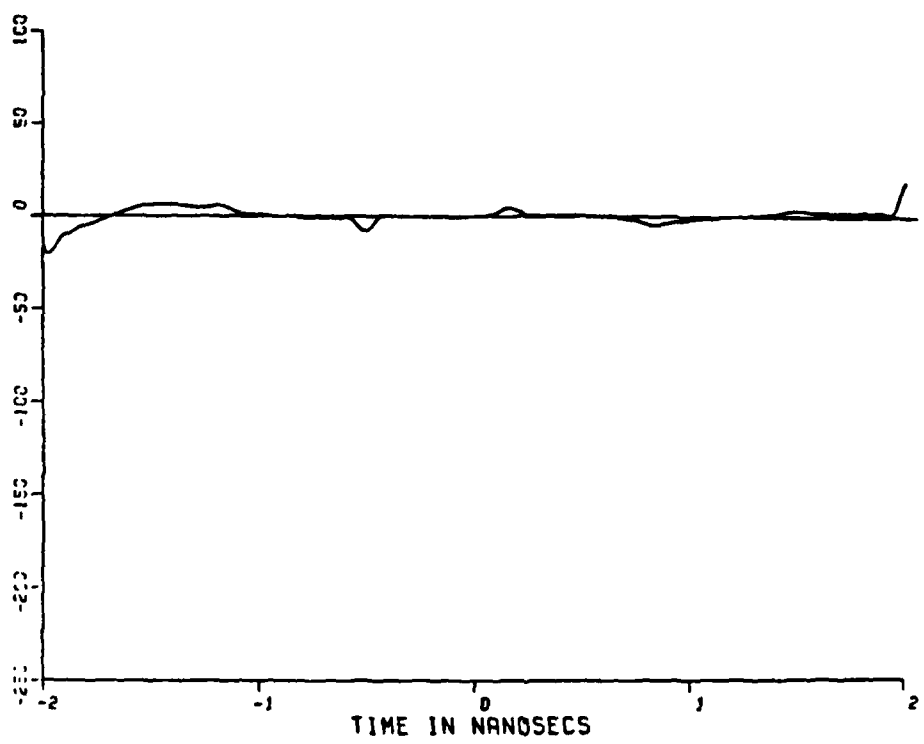


Figure 4-4a. Error of Figure 4-4 from Figure 4-2
(Magnification = 10x)

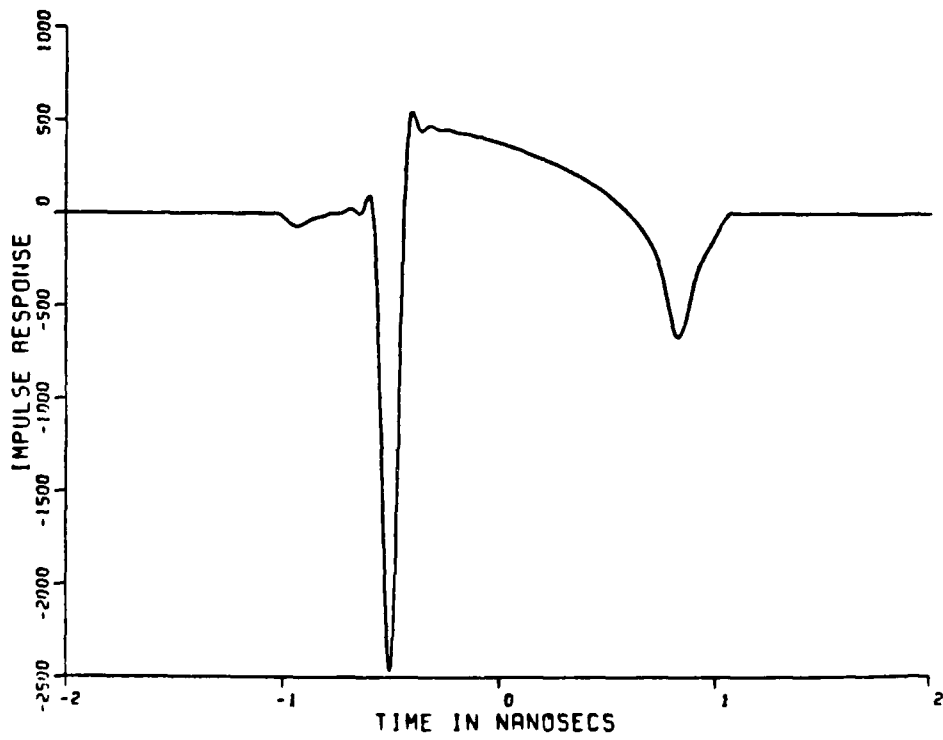


Figure 4-5. Similar description as Figure 4-3, except frequency samples are taken every 500 Mhz

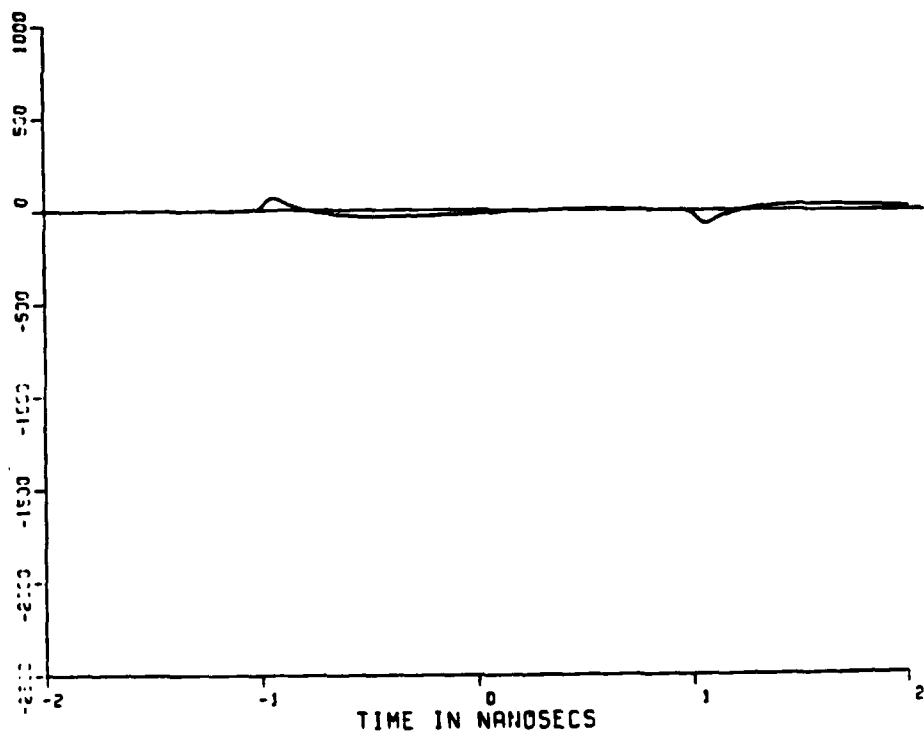


Figure 4-5a. Error of Figure 4-5 from Figure 4-2
(No magnification)

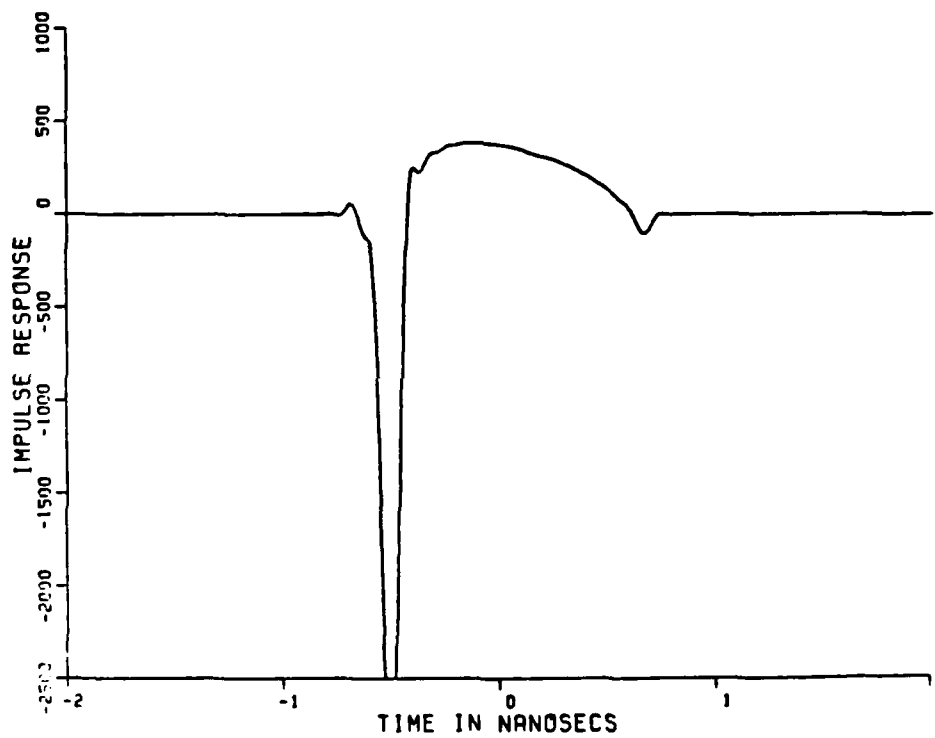


Figure 4-6. Similar description as Figure 4-3, except frequency samples are taken every 750 Mhz

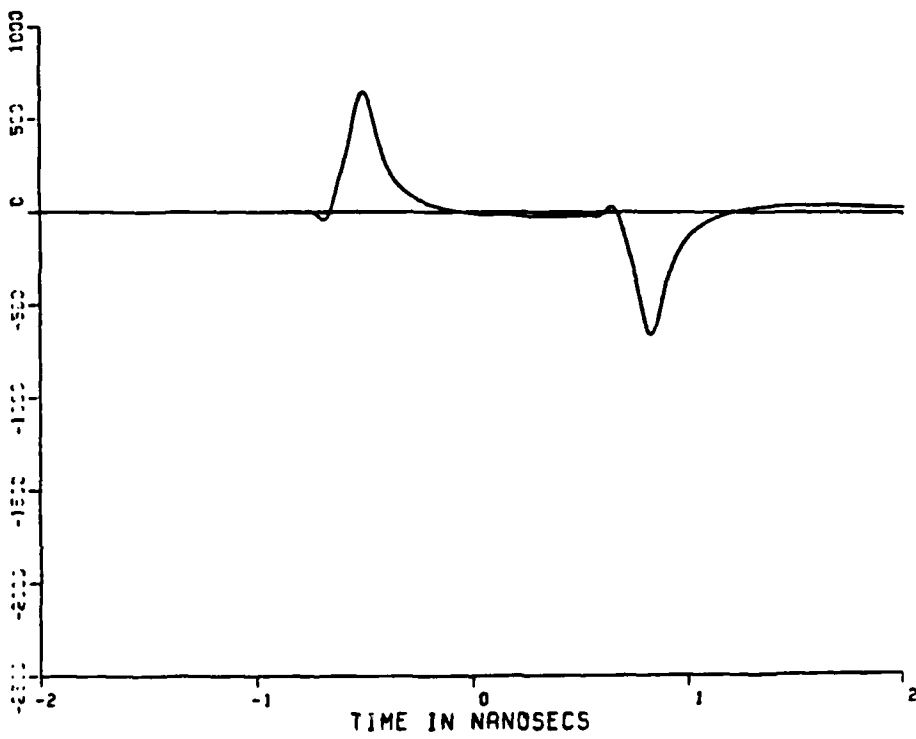


Figure 4-6a. Error of Figure 4-6 from Figure 4-2
(No magnification)

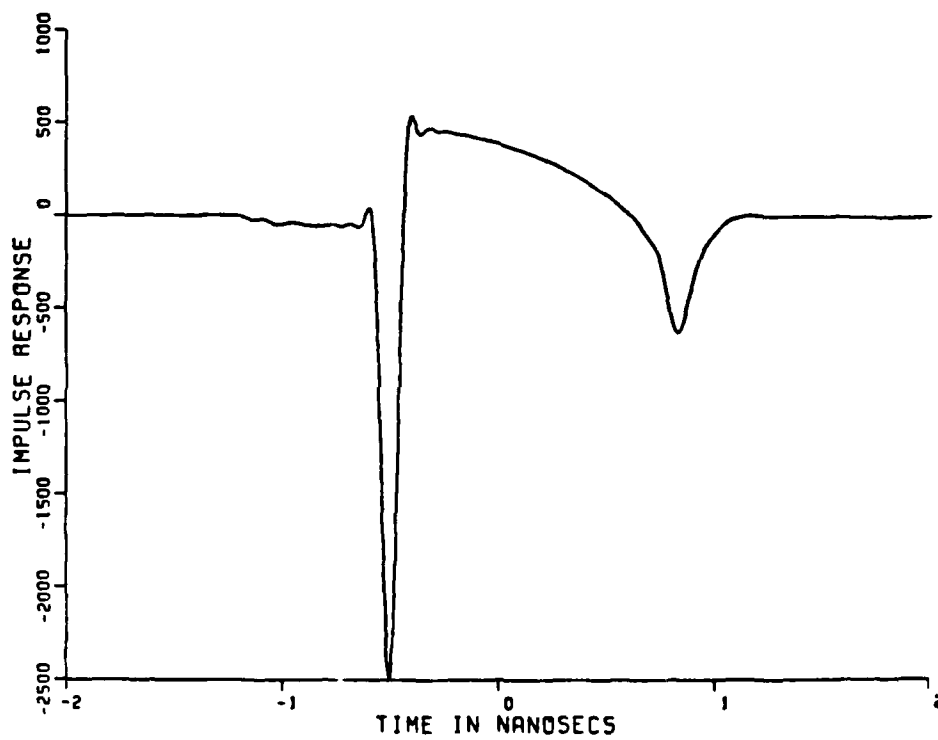


Figure 4-7. Impulse response of a 6" metallic sphere at 0° aspect angle with the 1-D frequency response interpolated from 2-D isotropic lattice samples taken with a safety factor of 1 over the range of 0 to 12 Ghz using Equation (4-3) and (2-13)

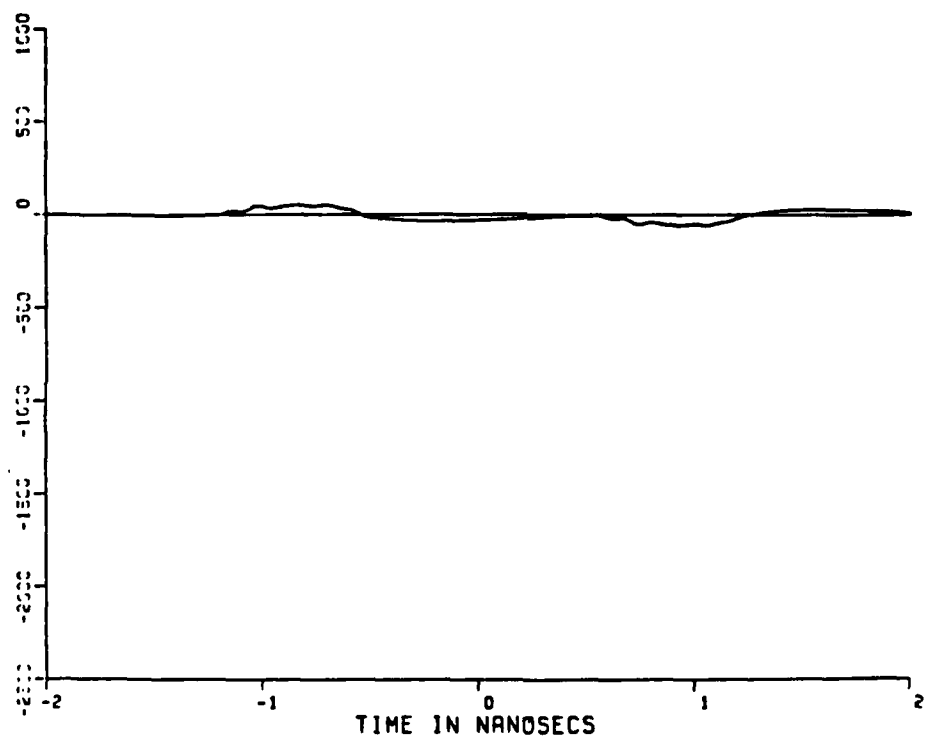


Figure 4-7a. Error of Figure 4-7 from Figure 4-2

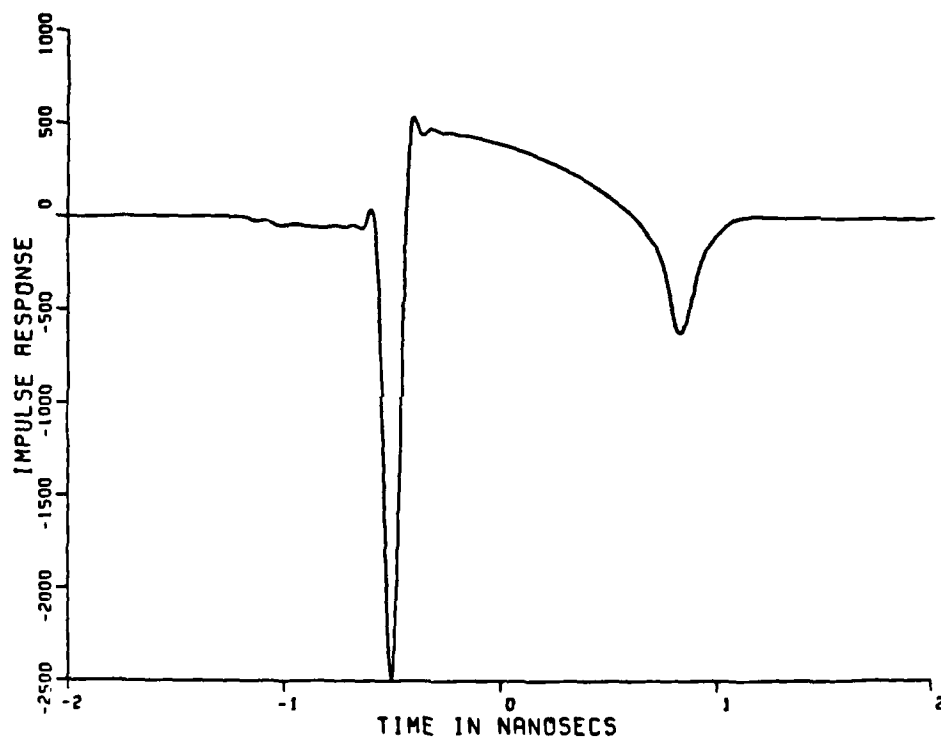


Figure 4-8. Similar description as Figure 4-7, except the aspect angle is $.72^\circ$

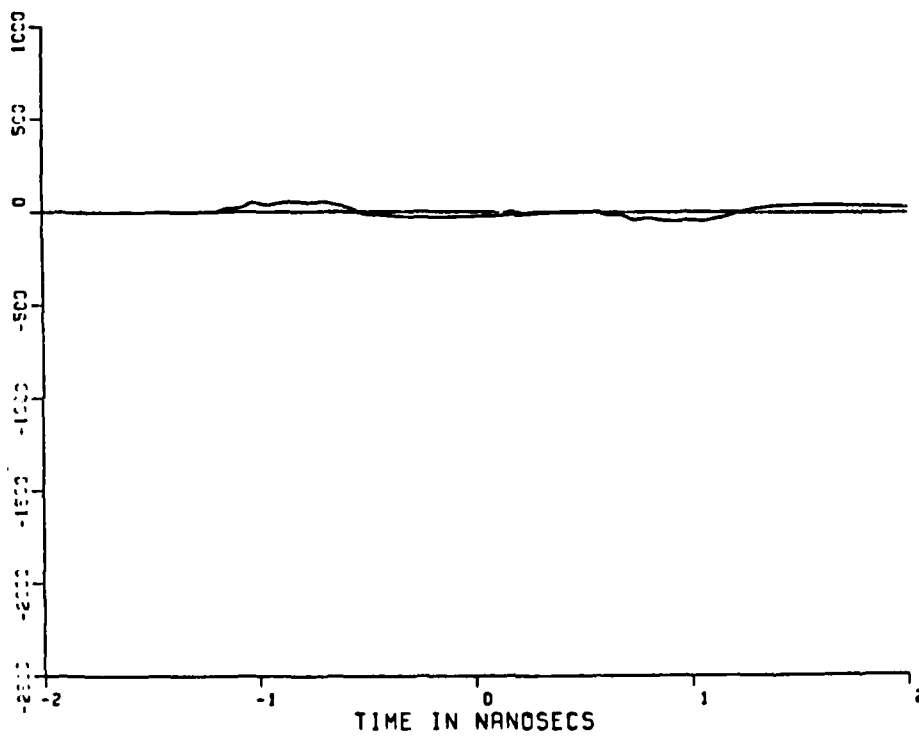


Figure 4-8a. Error of Figure 4-8 from Figure 4-2

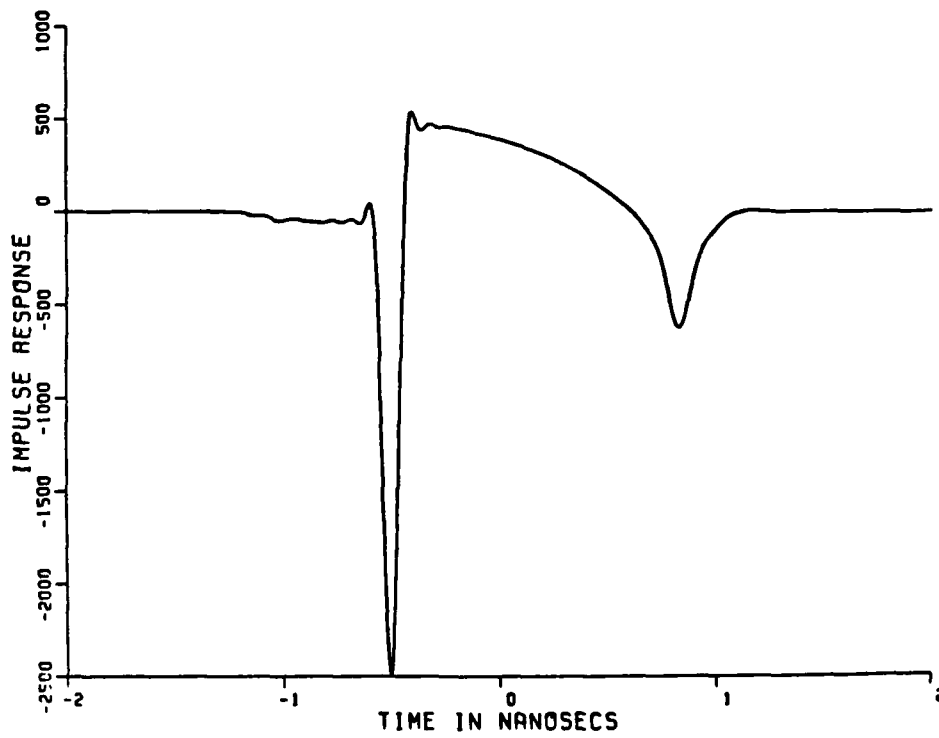


Figure 4-9. Similar description as Figure 4-7, except the aspect angle is 1.44°

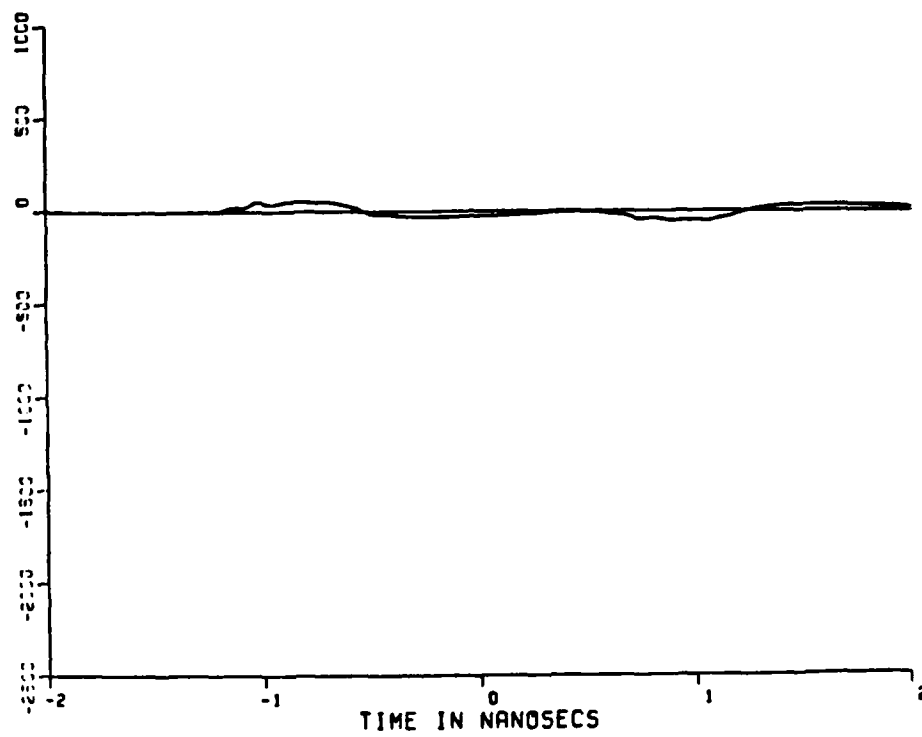


Figure 4-9a. Error of Figure 4-9 from Figure 4-2

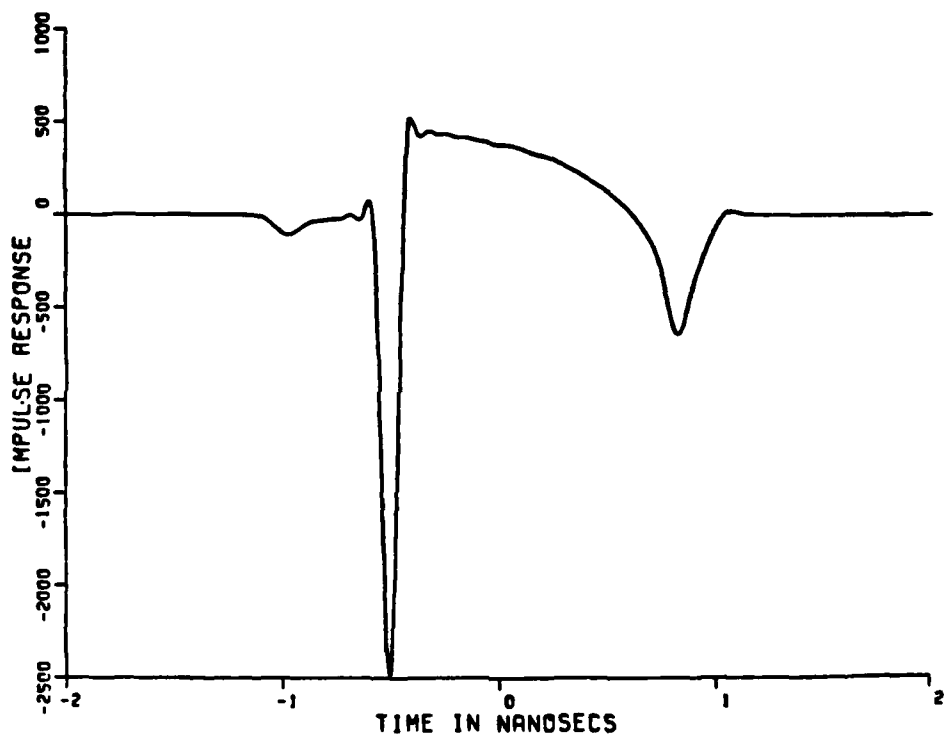


Figure 4-10. Similar description as Figure 4-7, except the aspect angle is 30°

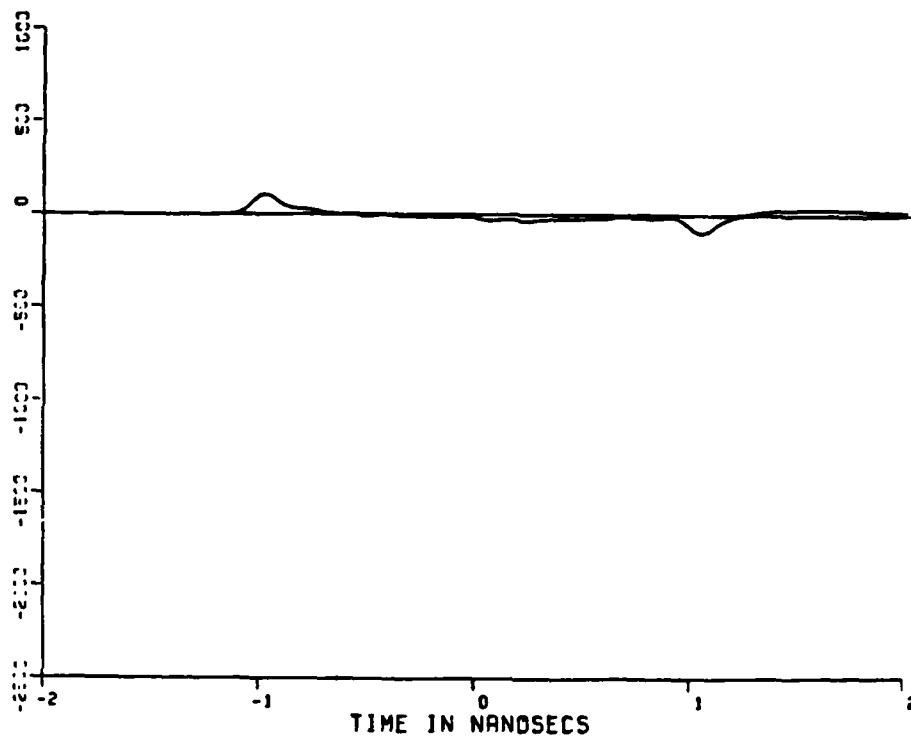


Figure 4-10a. Error of Figure 4-10 from Figure 4-2

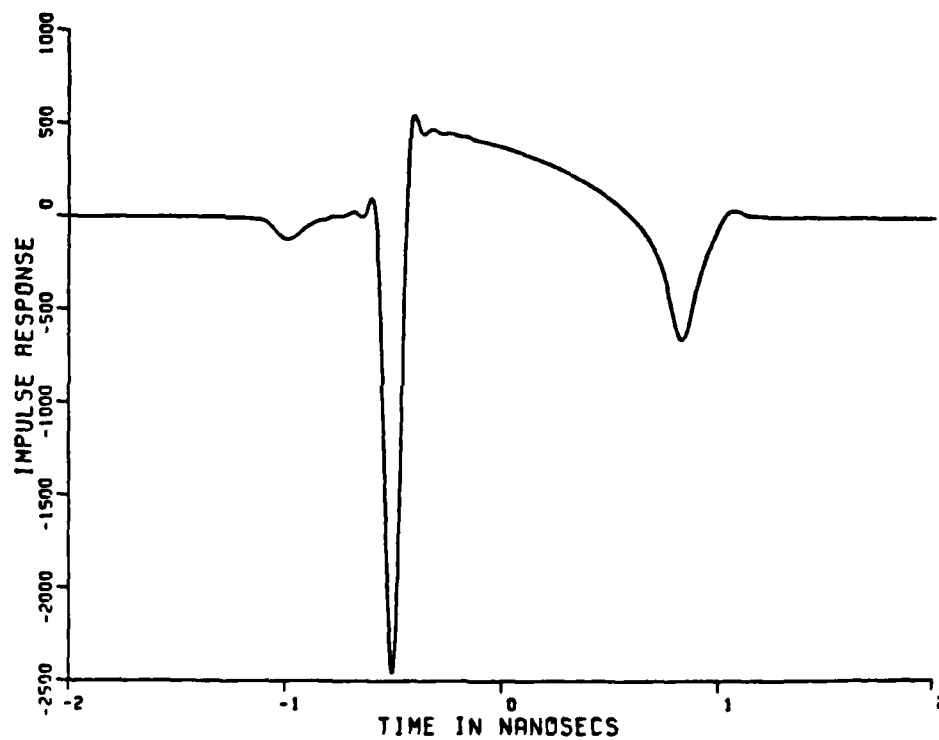


Figure 4-11. Impulse response of a 6" metallic sphere at 0° aspect angle with the 1-D frequency response interpolated from 2-D cubic lattice samples taken with a safety factor of 1 over the range of 0 to 12 Ghz using Equation (4-3) and (2-11)

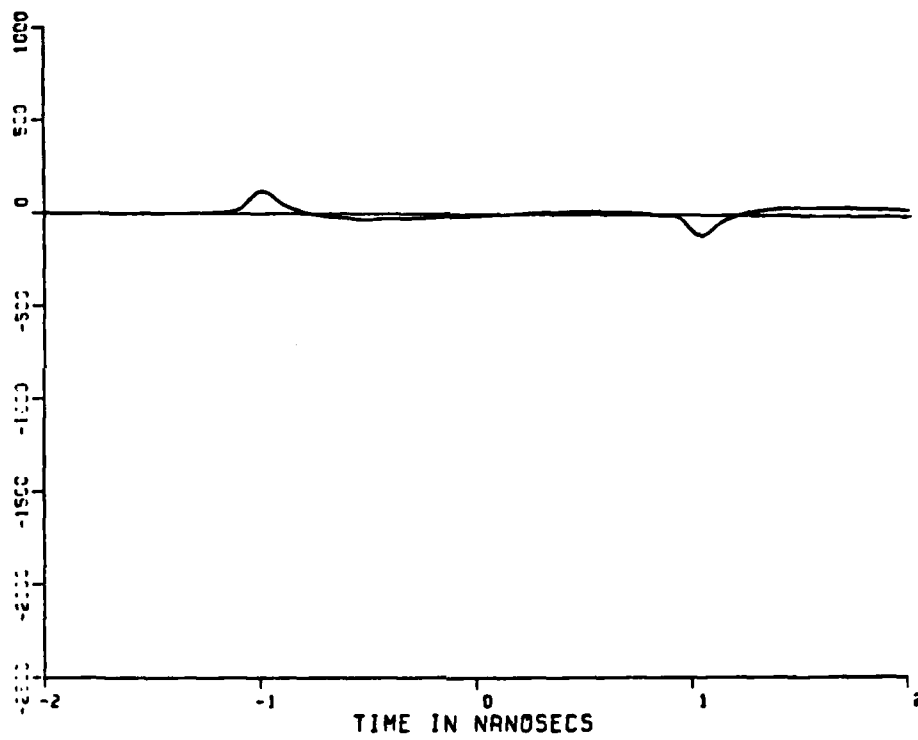


Figure 4-11a. Error of Figure 4-11 from Figure 4-2

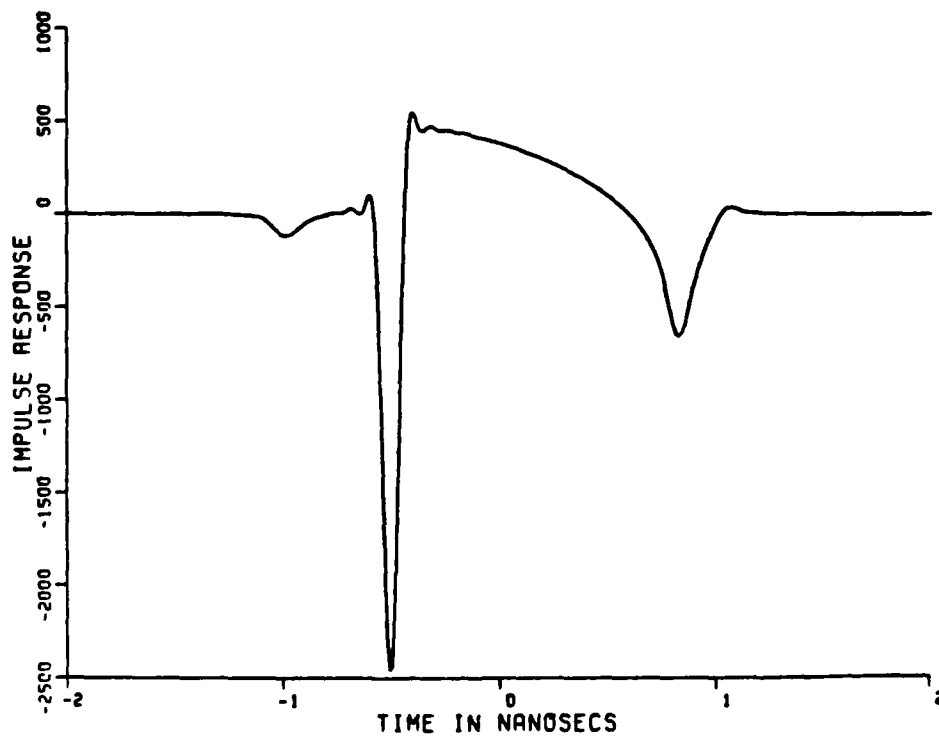


Figure 4-12. Similar description as Figure 4-11, except the aspect angle is 1.19°

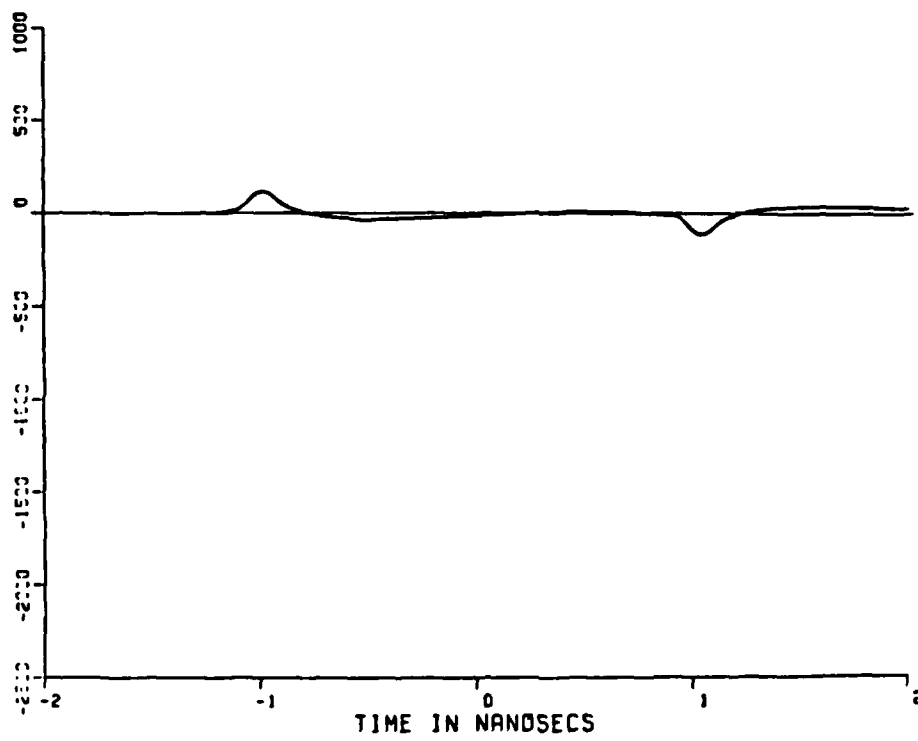


Figure 4-12a. Error of Figure 4-12 from Figure 4-2

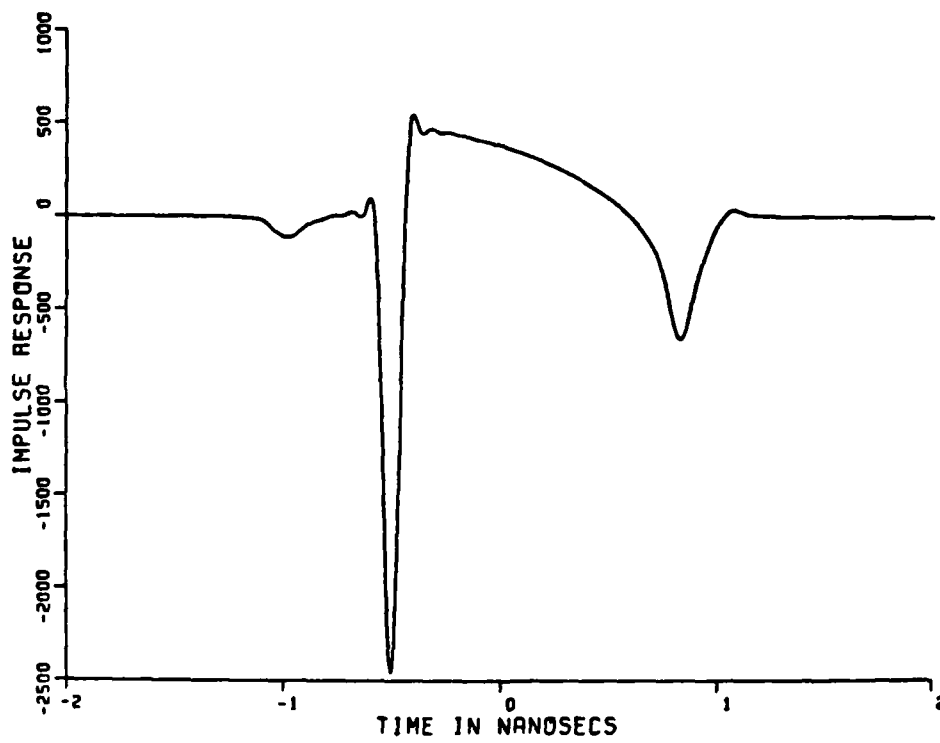


Figure 4-13. Similar description as Figure 4-11, except the aspect angle is 2.39°

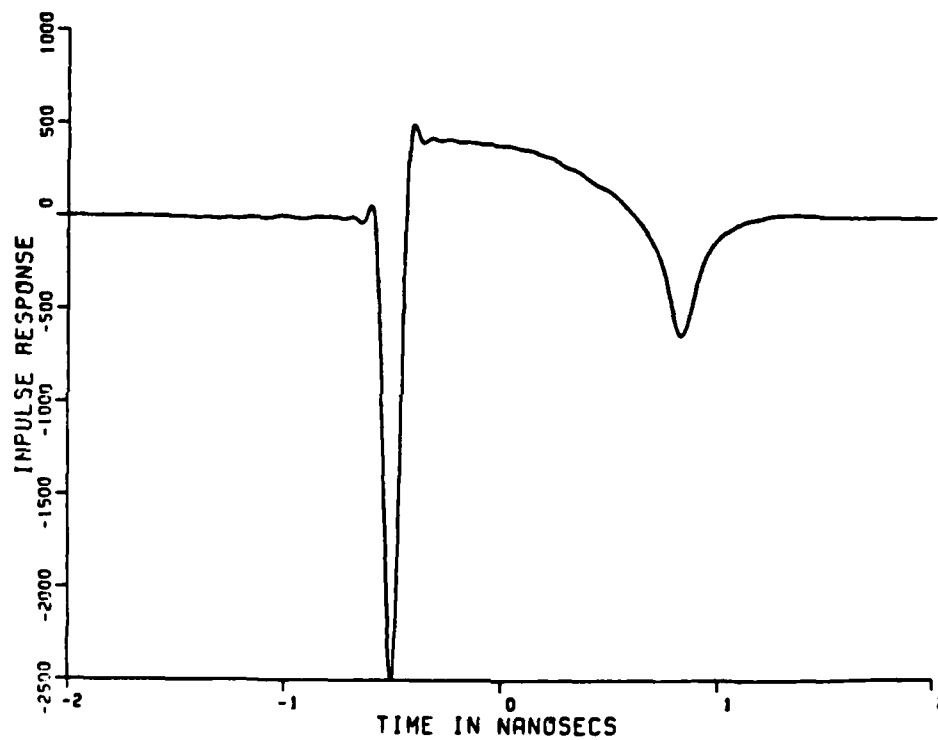


Figure 4-14. Similar description as Figure 4-11, except the aspect angle is 45°

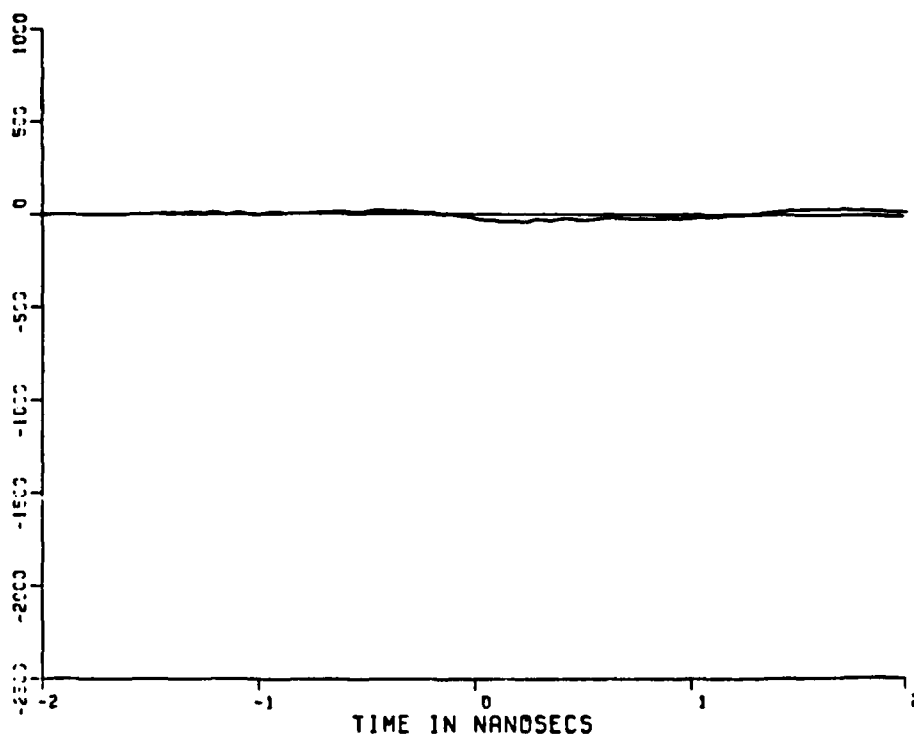


Figure 4-14a. Error of Figure 4-14 from Figure 4-2

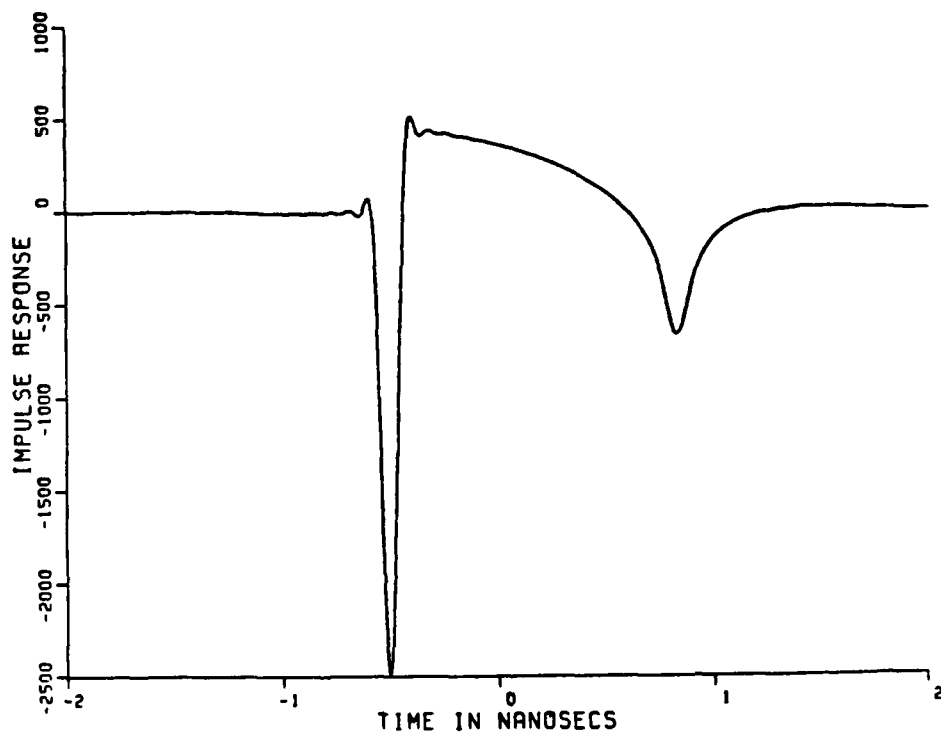


Figure 4-15. Impulse response of a 6" metallic sphere at 0° aspect angle with the 1-D frequency response interpolated from a 2-D isotropic lattice samples taken with a safety factor of 3 over the range of 0 to 12 Ghz using Equation (4-3) and (2-13)

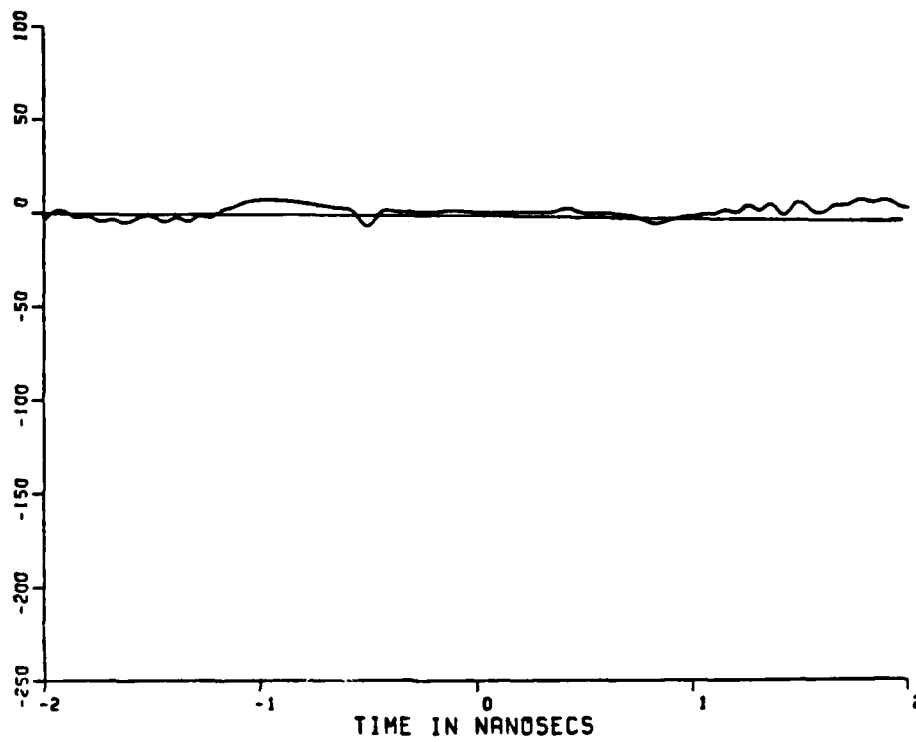


Figure 4-15a. Error of Figure 4-15 from Figure 4-2
(Magnification = 10x)

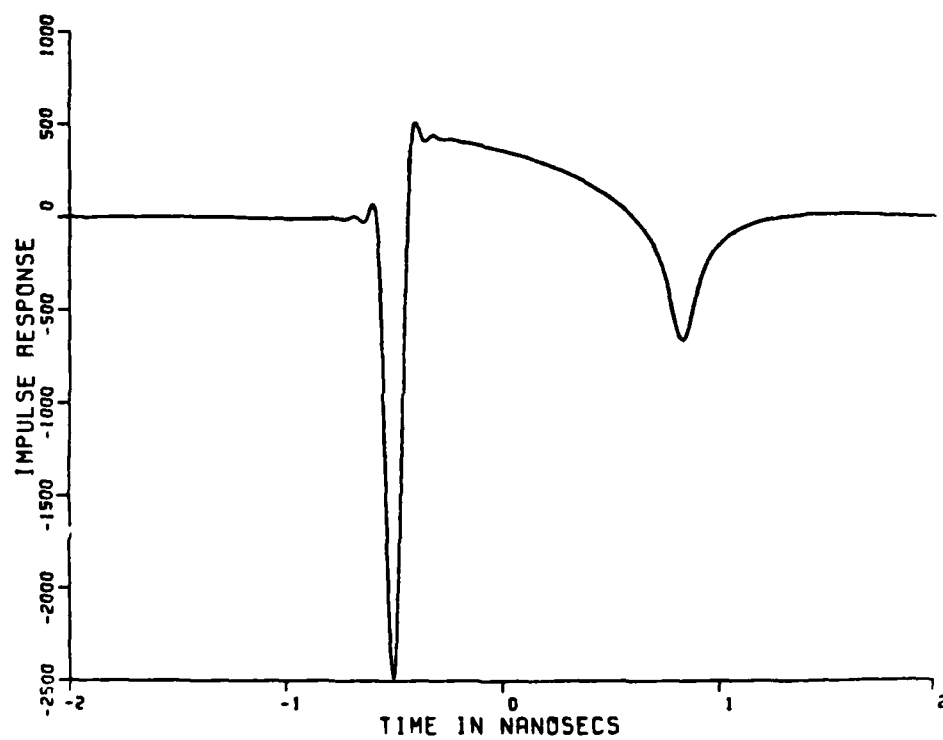


Figure 4-16. Similar description as Figure 4-15, except the aspect angle is 0.35°

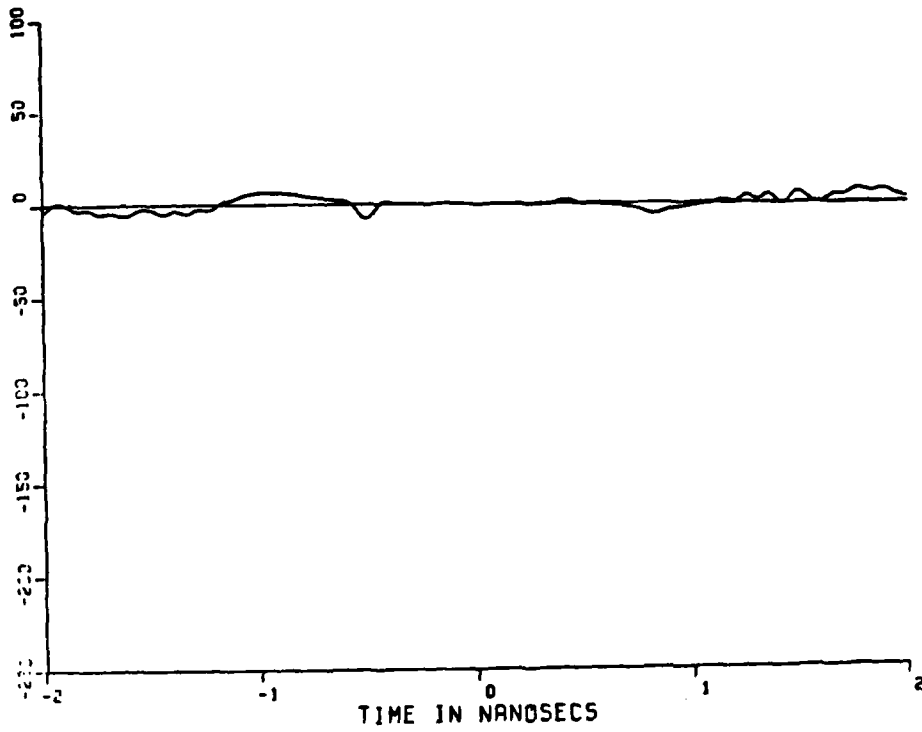


Figure 4-16a. Error of Figure 4-16 from Figure 4-2
(Magnification = 10x)

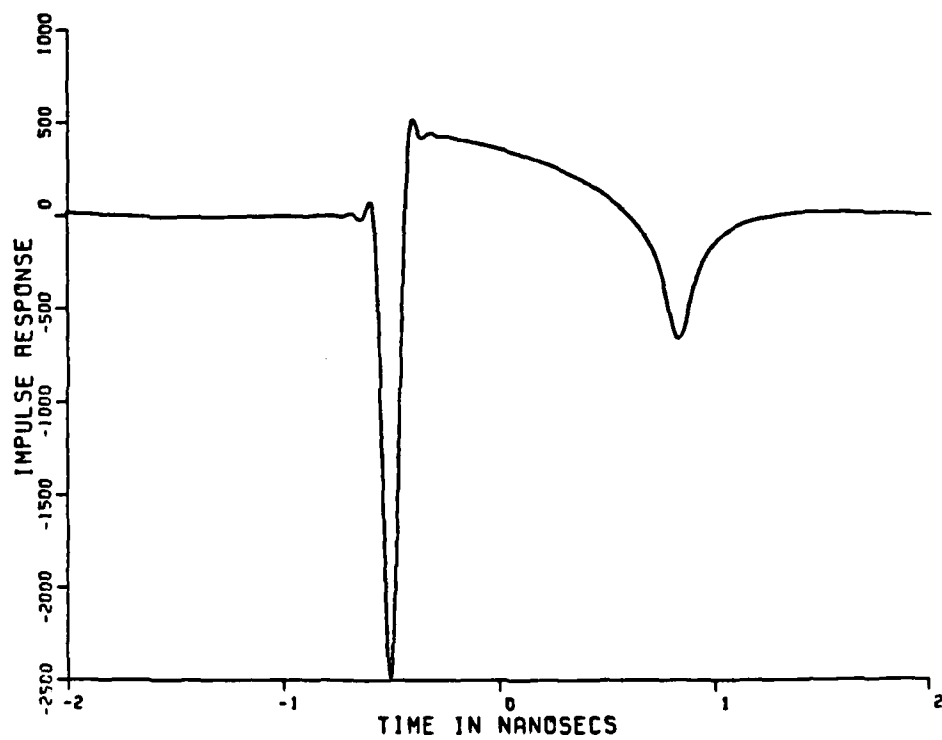


Figure 4-17. Similar description as Figure 4-15, except the aspect angle is 30°

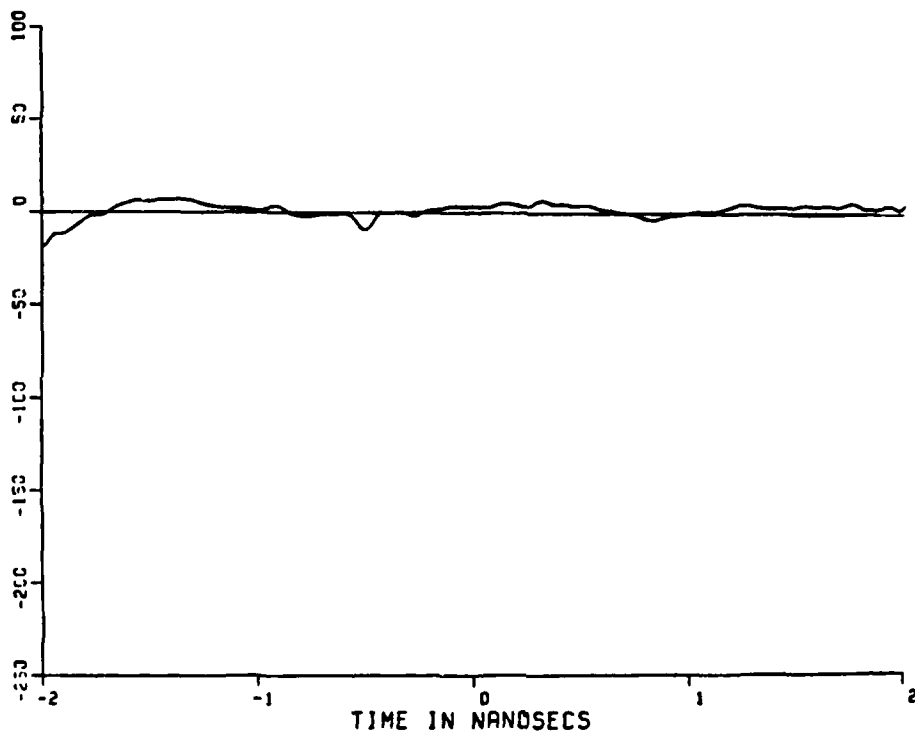


Figure 4-17a. Error of Figure 4-17 from Figure 4-2
(Magnification = 10x)

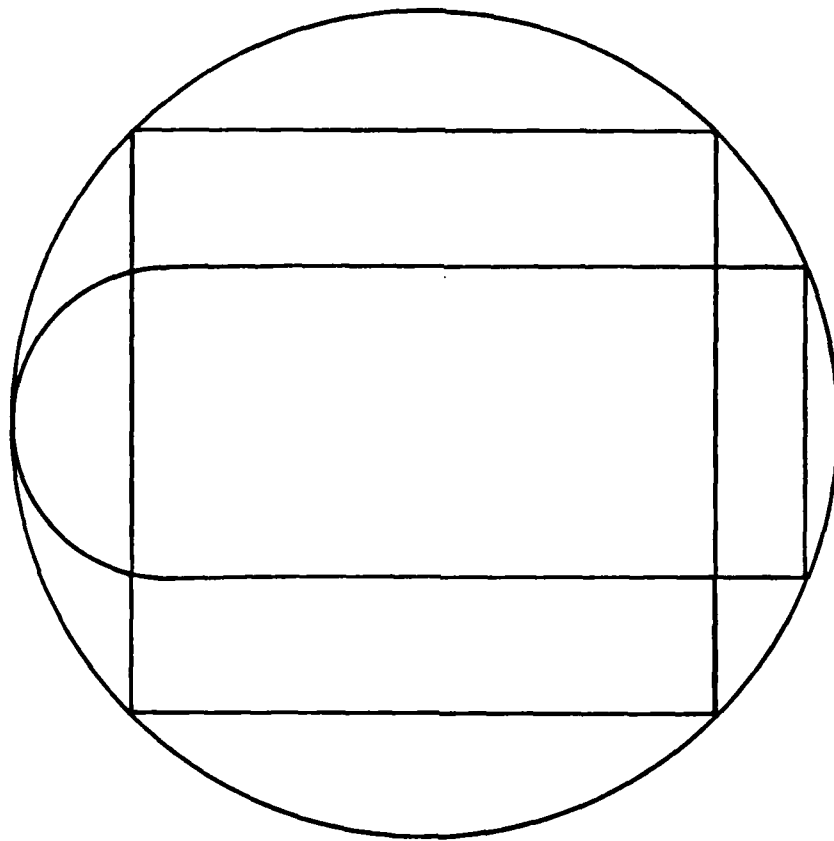


Figure 4-18. Dimensional perspective among the sphere, cube and sphere cap cylinder used in the example (Diameter of sphere = 6 inches)

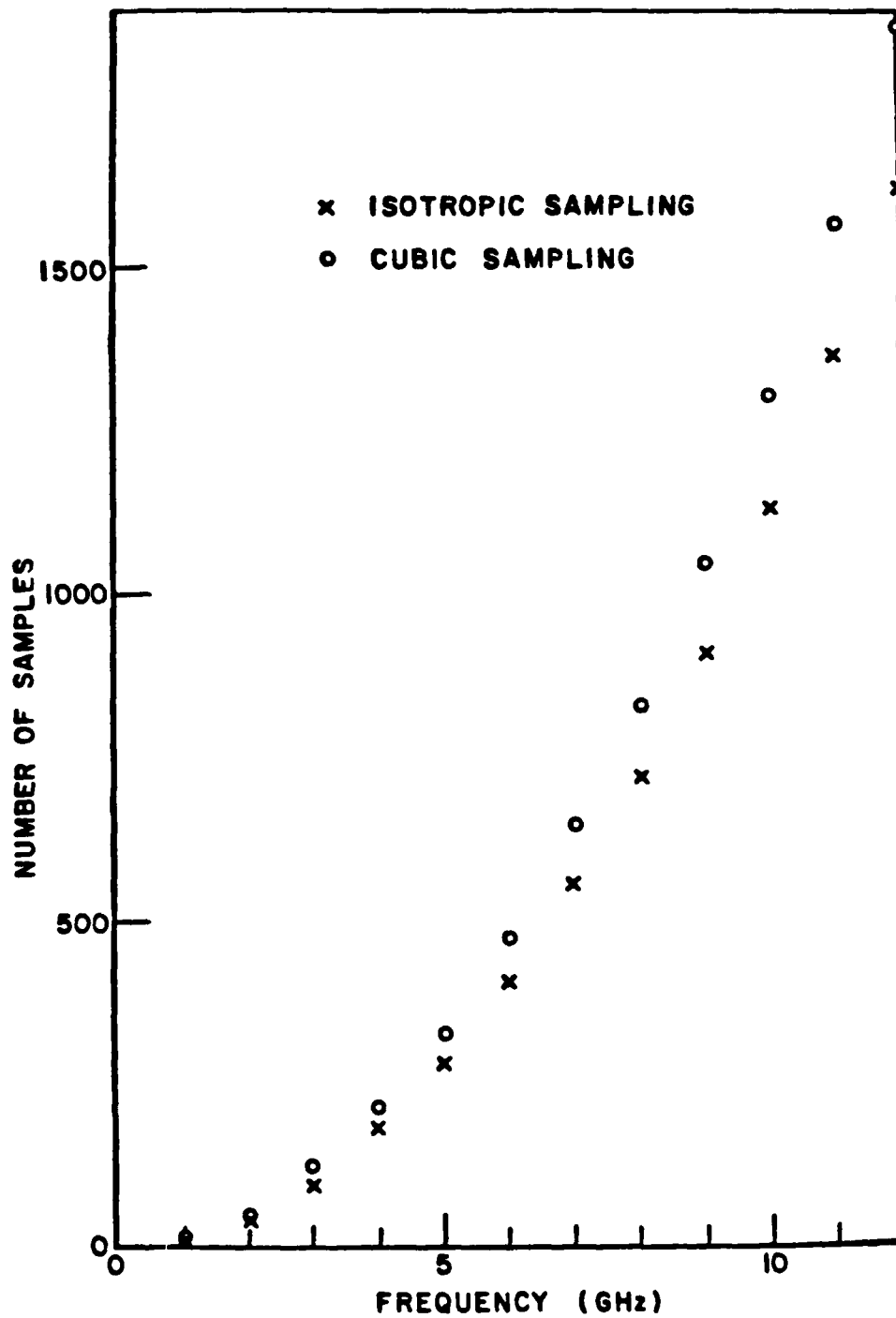


Figure 4-20. The number of samples specified by two types of sampling lattices on a 6" sphere

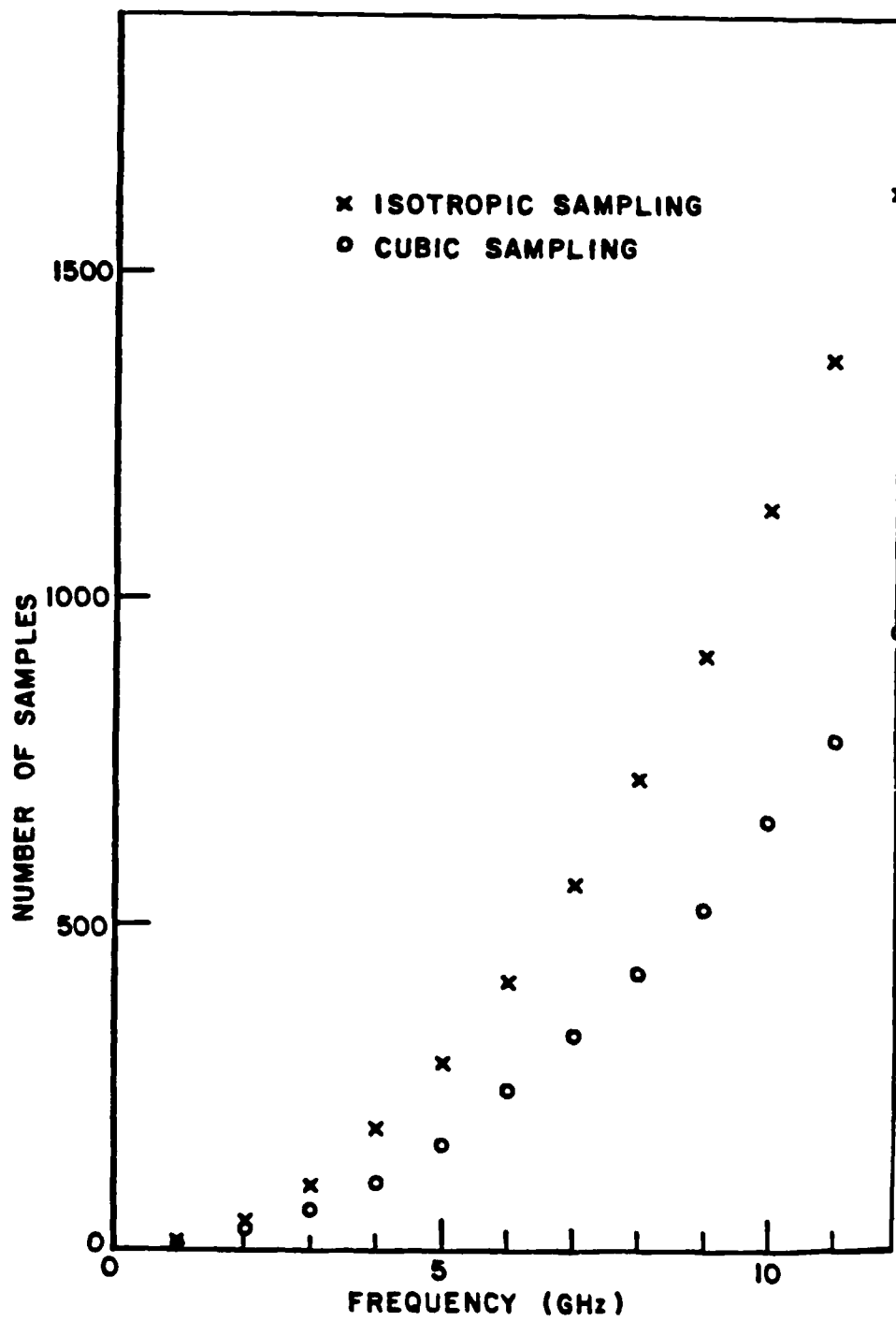


Figure 4-21. The number of samples specified by two types of sampling lattices on the cube described in Figure 4-18

CHAPTER V
TWO DIMENSIONAL IMPULSE RESPONSES

Thus far, the discussion has focused only on the number of samples required. The smaller the number of samples, the less measurement time is required. However, if the two dimensional impulse response is of interest, then the transform method must also be considered. This chapter will discuss the potential time consumption problem of multi-dimensional Fourier transform plus some possible solutions. Image reconstruction using the spatial impulse response is also considered.

While an isotropic enclosure may be more efficient to enclose a sphere than a cube, it is not as easy to do three dimensional discrete Fourier analyses as the cubic enclosure. Most of the discrete Fourier transform techniques are developed to fit equally spaced data. In another words, programs are written to perform readily on the cubic sampling lattice. Any other sampling grid data must be interpolated to the cubic grid either before or after the discrete Fourier transform step; otherwise, the proper representation cannot be achieved. Sometimes, interpolation may also be desired for the cubic sampling grid data, as in the case of higher resolution requirement than

measured. This type of interpolation requires a lot of computer time as pointed out in Mensa et al.'s paper [8].

Let's consider an example to estimate the time involved.

From Chapter IV:

- 1) Interpolation for 200 plotting points using 1626 isotropic samples is about 5 mins.
- 2) Interpolation for 200 plotting points using 1876 cubic samples is about 2.5 mins.
- 3) The number of samples required on a sphere cap cylinder for circular, rectangular and squared enclosures are 1626, 696, 1740 respectively.

(Table 4-2)

Compact range measurement facility at O. S. U. per Walton [12]:

The measurement system response time is about:

- 1) 0.2s/data point, if frequency scan is used.
- 2) 1 min/frequency ring, if angular scan is used.

The time estimation for each type of the sampling measurement on the sphere cap cylinder and two dimensional interpolation is presented in Table 5-1. (For the convenience of the reader, all tables and figures of Chapter V are grouped together at the end of the chapter.) The interpolation time for the rectangular enclosure data may also be considered zero. By remembering a scale factor, the data can be processed as in a squared grid. If the proper signal representation or a finer resolution is required, the interpolation step is still

unavoidable. Therefore, the numbers in the table do give a fair comparison, as all data are brought to the same level - squared grid representation. The interpolation step plays an important role on the decision of which type of sampling to use. The saving in measurement time is sometimes balanced out by the data processing time.

The Nyquist criteria (Equations (2-19), (2-20)) plus the polar transformation (Equation (2-15)) described earlier give new perspective for the efficient but non-cubic enclosure. Now one only needs to interpolate for a sufficient number of frequency rings. This work is done by program INTERPOL (see Appendix B). Each frequency ring is transformed to the spatial domain individually and summed together to get the total time response. The former is the work of program INTEGFFT (see Appendix B); the latter is the job of program SUM3D (see Appendix B). The interpolation performed this way may require as much time as the interpolation onto the squared grid. It nevertheless gives an alternative way to the solution of the problem. Now, another question may be raised: Why perform interpolation if it is so time consuming?

The interpolation may be avoided, if the two dimensional time response is the only interest. All one has to do is to measure the frequency rings and then process the data as described before. However, if one desires the impulse response of a target at a particular aspect angle or the response over a frequency ring other than those measured, one is required to develop a different interpolation scheme than the one described in the theory section. A possible way to reduce the

interpolation time is to derive a faster interpolation scheme or a general multi-dimensional Fourier transform technique which operates on any grid. A parallel processor which uses optics may be another possibility in terms of hardware. A lens system has a Fourier transform relationship between the source and the image [13].

The Mie solution for a sphere is a very good data example; except its backscattered response is isotropic. A proper choice of test object must have non-isotropic property. The sphere shifted off the centre of the plane is one possibility, but it only has variation in the phase term and not in the magnitude term. Since most of the other exact solutions are not readily available, a first order UTD solution for a finite circular cylinder [14] is used; with the caution that UTD gives a valid approximation to the exact solution at high frequency.

The size of the circular cylinder is chosen to be six inches in length and three inches in diameter. Having chosen the size of the cylinder, one has defined the low frequency limit of this UTD model to about 2 Ghz. Since the step and ramp response of an object reduce the need for the high frequency information, only the impulse response of this cylinder solution is considered here.

Figure 5-1 is the two dimensional impulse response (Equation (2-9)) for the above circular cylinder. The frequency samples are first generated on the grid points defined by Equation (4-5) over only 180°. In this case, the spatial impulse response is assumed to settle after the wave has passed over four times the length of the object at every aspect angle. The rectangle so designated has dimensions: 24" in

length and 12" in diameter. The periodic lattice is chosen as in Figure 2-3. Consequently,

$$\bar{v}_1 = 24'' \begin{bmatrix} 1 \\ 0 \end{bmatrix} \quad \bar{v}_2 = 12'' \begin{bmatrix} 0 \\ 1 \end{bmatrix}$$

The guard band is 9" on each side of the cap of the cylinder and 4.5" on the circular surface. Then,

$$\bar{u}_1 = \frac{2\pi}{24''} \begin{bmatrix} 1 \\ 0 \end{bmatrix} \quad \bar{u}_2 = \frac{2\pi}{12''} \begin{bmatrix} 0 \\ 1 \end{bmatrix}$$

Since,

$$l_1 \bar{u}_1 = l_1 |\bar{u}_1| \hat{k}_1$$

$$l_2 \bar{u}_2 = l_2 |\bar{u}_2| \hat{k}_2$$

where

$$l_1, l_2 = 0, \pm 1, \pm 2, \pm 3, \dots$$

Therefore, the sampling lattice is defined by:

$$l_1 \bar{u}_1 + l_2 \bar{u}_2 = l_1 |\bar{u}_1| \hat{k}_1 + l_2 |\bar{u}_2| \hat{k}_2$$

<=> points on the k-plane:

$$k_1 = l_1 |\bar{u}_1| \quad \text{and} \quad k_2 = l_2 |\bar{u}_2|$$

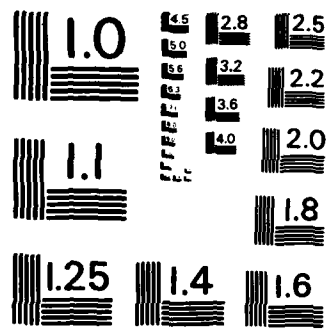
where

$$l_1, l_2 = 0, \pm 1, \pm 2, \pm 3, \dots$$

Then the sampled data are Fourier transformed discretely into the spatial domain. The discrete two dimensional Fourier transform is performed by an IBM subroutine HARM (see Appendix B). The frequency range used is 2 to 5 Ghz. The safety factor of one is used. The vertical polarization data are taken from the UTD solution on a major axis cut. Figure 5-1a is the contour plot of Figure 5-1. Figure 5-2 is also a two dimensional impulse response for a cylinder solution that has the same previous description. The differences are the technique of the Fourier transformation and the sampling locations in the frequency plane. It employs Mensa et al.'s method on 6 different frequency rings: 2.5, 3, 3.5, 4, 4.5, 5 Ghz. (Equation (2-18)) The samples are taken so that Equations (2-19) and (2-20) are satisfied. Again the samples are taken over 180°. Figure 5-2a is the contour plot of Figure 5-2.

Comparing Figures 5-1 and 5-2, one can see many similarities. The differences can be deduced by recalling their respective generating methods. Figure 5-1 has information scattered all over the frequency range; while, Figure 5-2 has vaules only over those frequency rings mentioned before. There is also the processing error involved.

One interesting thing is to be noted in Figure 5-1, or 5-2. If one records just the highest points within its neighborhood, one can trace out a rectangle. This may be easier to see on a contour plot (Figure 5-1a, 5-2a). This looks like one cross-section of the target. If 2π



MICROCOPY RESOLUTION TEST CHART
NATIONAL BUREAU OF STANDARDS-1963-A

solid angle information is available, then an image of the target can indeed be produced. Of course, the resolution is still governed by the highest frequency used. In this case the bandwidth used is quite narrow; hence, the resulting resolution is not high.

Figure 5-3 is generated similarly as Figure 5-2. It is generated using Mensa et al.'s method on 16 different frequency rings: 2.5, 3, 3.5, 4, 4.5, 5, 5.5, 6, 6.5, 7, 7.5, 8, 8.5, 9, 9.5, 10 Ghz. Figure 5-3a is the contour plot of Figure 5-3. The dimensions of the rectangle defined by the high peaks do correspond to the major axis cross-section of the circular cylinder described earlier. One may wonder how a rectangle is concluded from Figure 5-3a. There are a few clues available. The T_j 's are quite obvious from the high peaks on the illuminated side. The final time (T_f) of the one dimensional impulse response, as one recalls, is defined by the beginning of the exponential decay of the signal. The final peaks at the coordinates (5,3) and (5,-3) are indeed higher than any point $x_1 > 5$. The ridges and valleys on the shadow side ($x_1 > 5$) of the cylinder is fairly straight.

Let's consider the case where this imaging theory converges to Lewis-Bojarski's work. Figure 5-4 is the same as Figure 5-3 except data are taken over 360° , or illuminated in every direction on the two dimensional plane. Figure 5-4a is the contour plot of Figure 5-4. As expected, the peaks (or T_j 's) in the figure trace out a rectangle which is the major axis cut of the circular cylinder. One may note that literature today usually presents data plots using the absolute value of the amplitude. One must be careful when confronted by these plots.

As Figures 5-5 and 5-5a have shown, the absolute value of the amplitude does not usually tell the whole picture. Figure 5-5 plots the absolute value of the amplitude in Figure 5-4. Figure 5-5a is the contour plot of Figure 5-5. The major axis cross-section is no longer as well defined by the peaks as in Figure 5-4 or 5-4a. Nevertheless, producing an image using the spatial impulse response is very promising.

Although this thesis' imaging theory is not as 'rigorous' as Lewis and Bojarski's work, the theory is more flexible in application. The object is only required to be illuminated at the aspect angles over a 2π solid angle. The shadowed side information is also employed in the image reconstruction process. There is no need for any assumption on the object's shadowed side geometry. If the start and the end of the object's one dimensional impulse response for every aspect angle over half of the 4π solid angle are well defined by T_i 's (illuminated) and T_f 's (shadowed) as described earlier, then an image of the object may be produced using the T_i 's and T_f 's. For T_i 's and T_f 's not defined distinctly, careful interpretation on the spatial impulse response must be used. In the case of a full 4π illumination, the image may be reconstructed using only T_i 's information. This converges to Lewis-Bojarski's identity. This theory is better in utilizing data information available but it lacks a concrete proof.

Let's investigate this imaging possibility further using a six inch diameter metallic sphere whose centre is located three inches off the centre of the reference plane on the x_1 -axis. The cubic sampling

lattice used has a safety factor of three. The frequency range used is 0 to 12 Ghz. Again, the frequency data are taken out of the Mie solution. The sampling lattice is defined by Equation (4-5) over half of the plane ($\pi < \theta < 2\pi$). The data are weighted by the two dimensional cosine tapering function. The two dimensional version of Equation (4-2) is replacing the variable n by the radial distance from the centre of the k -space. The shape of the function is Figure 4-1 rotated around the weighting axis. The weighted data are Fourier transformed into the spatial domain and presented as Figure 5-6. Figure 5-6a is the contour plot of Figure 5-6.

Again the initial speculars trace the illuminated side of the sphere nicely. The T_f 's are not as well defined as the finite cylinder case. More interpretation work is required. The valley on the shadow side shows a curvature. This may be indicating the back side of the object having a curvature. The radius of the valley's curvature is about 3π inches, which is the equivalent distance a wave would creep before scattering back in the transmitting direction (Figure 5-7). The radius of the curvature created by the initial speculars is about six inches, which is the $2R$ distance travelled by the wave. The first R is the distance travelled to the target. The second R is the distance travelled by the wave scattering back from the target. Using this information, the circle with the three inch radius can be formed.

Of course, if one uses data over the full plane as Lewis-Bojarski's work, then there is no need for the previously described type of pattern recognition interpretation. The initial speculars usually define the perimeter of the object, if it is a smooth convex body. The perimeter indicated is only one cross-section of the target on the major axis. If more cross-sectional information of the target is available, then an image of the whole object may be produced. The potential on the image reconstruction is high, but more research work is required in the area; particularly in the pattern recognition area.

TABLE 5-1

AN EXAMPLE: TIME ESTIMATION

Type of enclosure	Measurement time (mins)	Interpolation time (mins)	Total time (mins)
circular	5.42	40.09	45.51
rectangular	2.32	8.47	10.79
squared	5.80	-	5.80

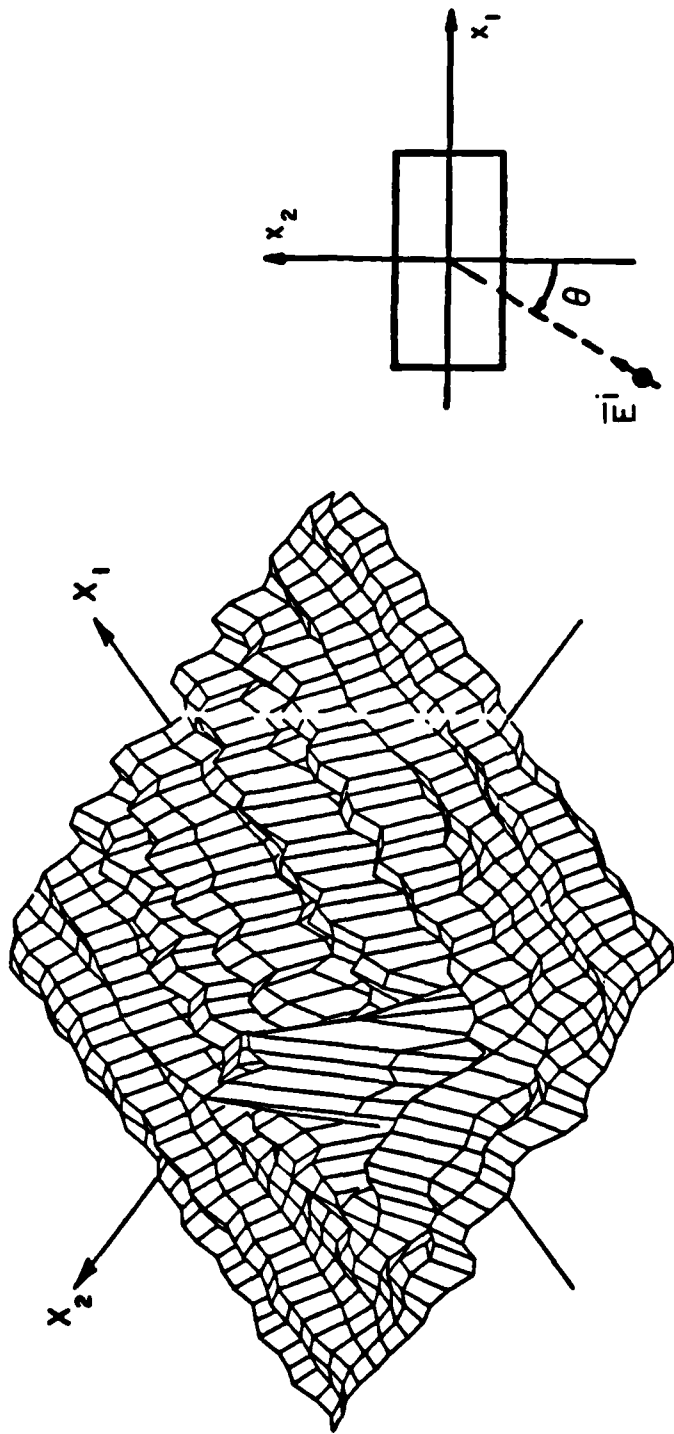


Figure 5-1. 2-D impulse response of a finite metallic cylindrical cylinder with 6" in length and 3" in diameter. Frequency samples are taken at the cubic sampling lattice over the range of 2 to 5 Ghz and Fourier transformed discretely into the spatial domain. Data are taken over the half plane: $0 \leq \theta \leq \pi$

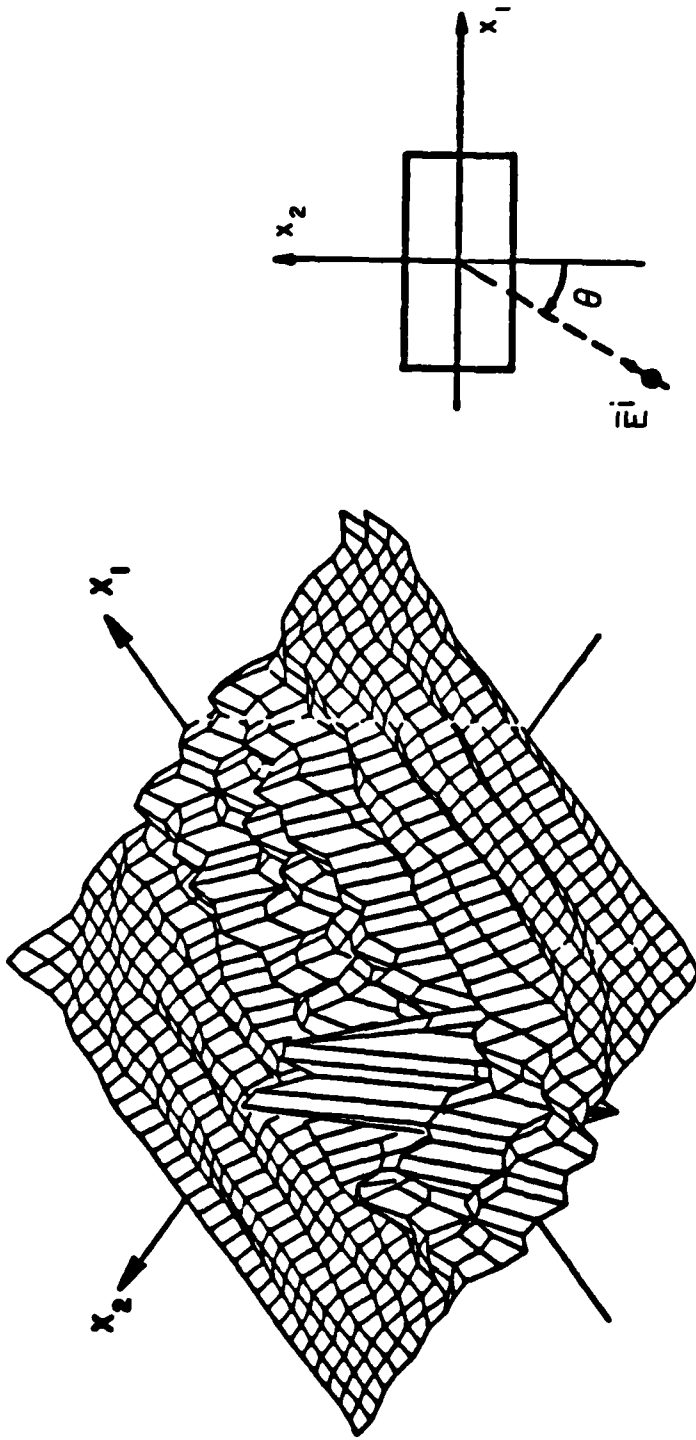


Figure 5-2. 2-D impulse response of a finite metallic cylindrical cylinder with 6" in length and 3" in diameter. Frequency samples are taken over 6 rings: 2.5, 3, 3.5, 4, 4.5, 5 Ghz and transformed into the spatial domain via Mensa et al.'s method. Data are taken over the half plane: $0 < \theta < \pi$

11 00 110 000 001 002 003 004 005 006 007 008 009 010 011 012 013 014 015 016 017 018 019 020 021 022 023 024 025 026 027 028 029 030 031 032 033 034 035 036 037 038 039 040 041 042 043 044 045 046 047 048 049 050 051 052 053 054 055 056 057 058 059 060 061 062 063 064 065 066 067 068 069 070 071 072 073 074 075 076 077 078 079 080 081 082 083 084 085 086 087 088 089 090 091 092 093 094 095 096 097 098 099 100

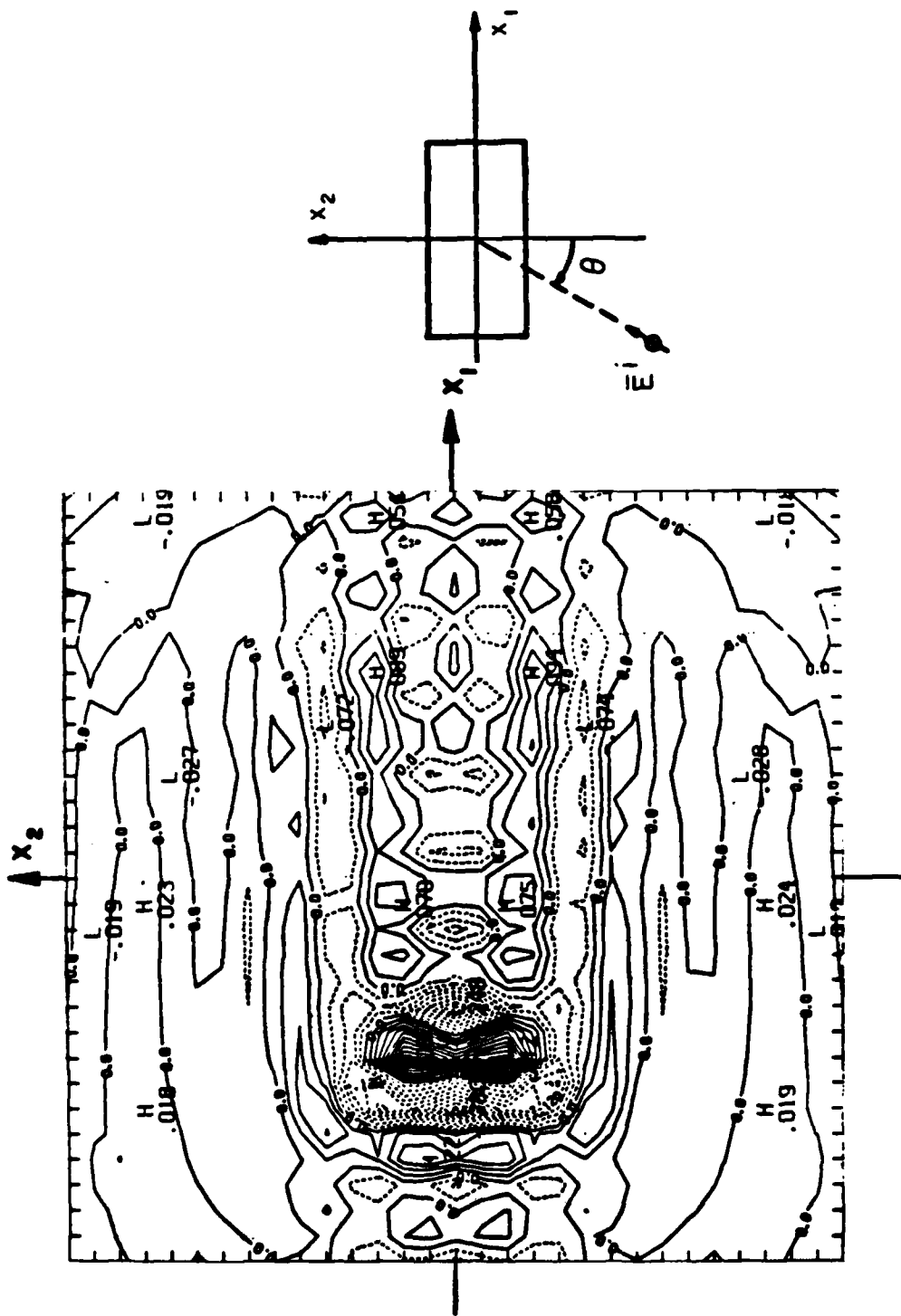


Figure 5-2a. Contour plot of Figure 5-2

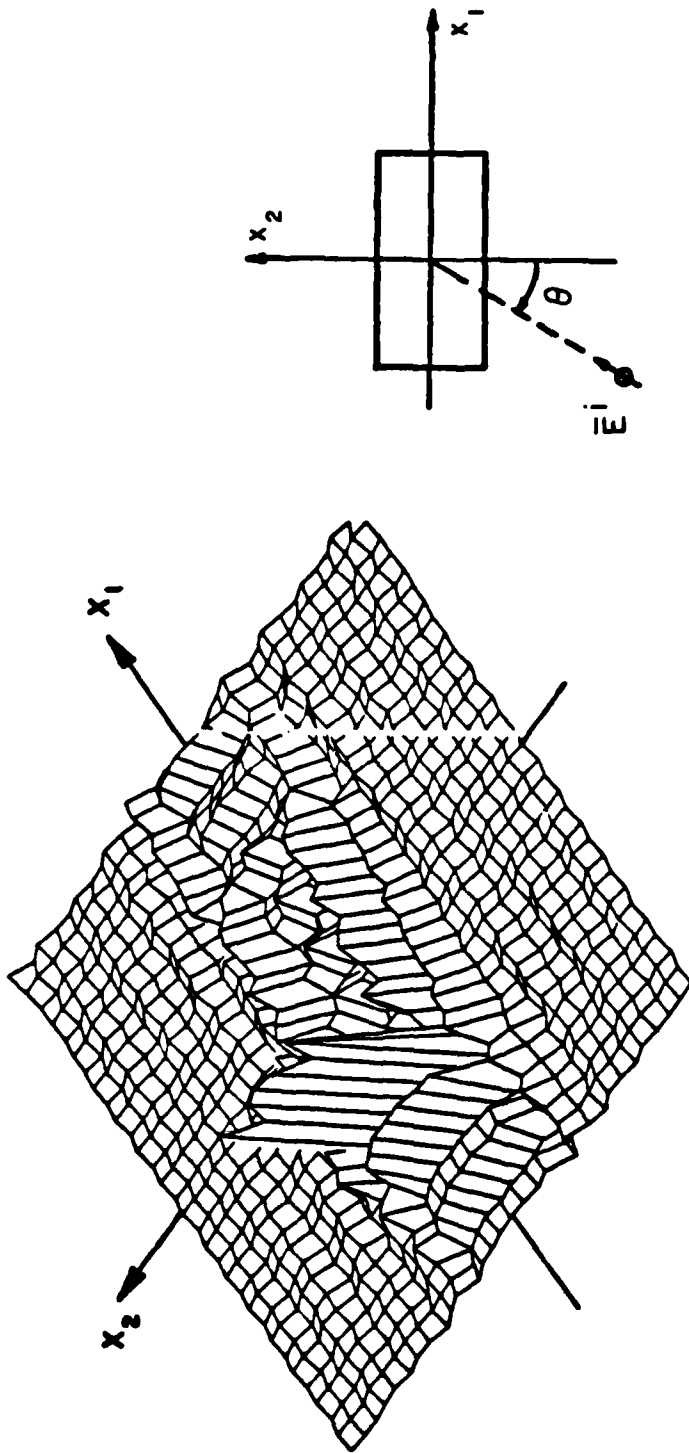


Figure b-3. Similar description as Figure 5-2 with 10 additional frequency rings: 5.5, 6, 6.5, 7, 7.5, 8, 8.5, 9, 9.5, 10 Ghz

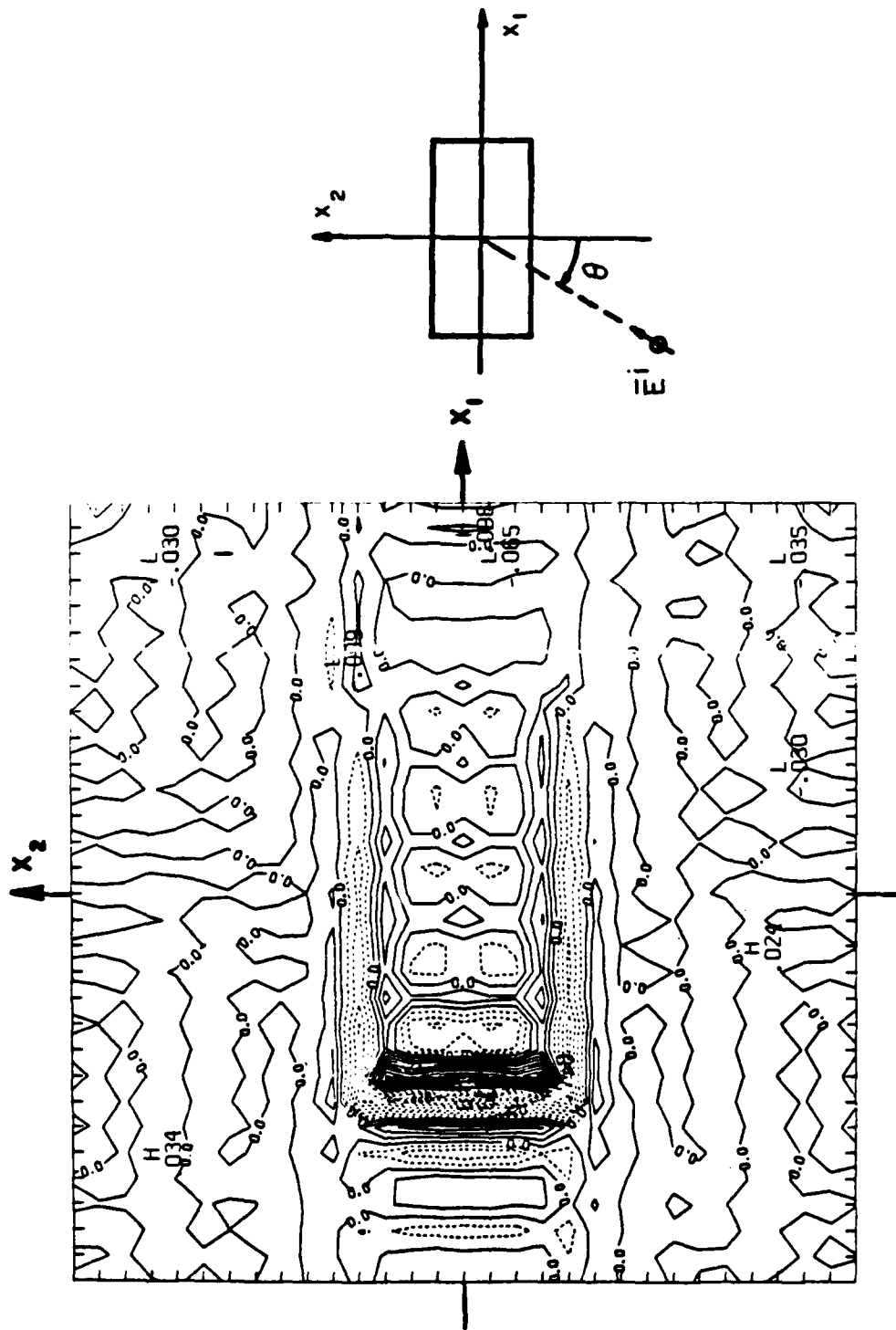


Figure 5-3a. Contour plot of Figure 5-3

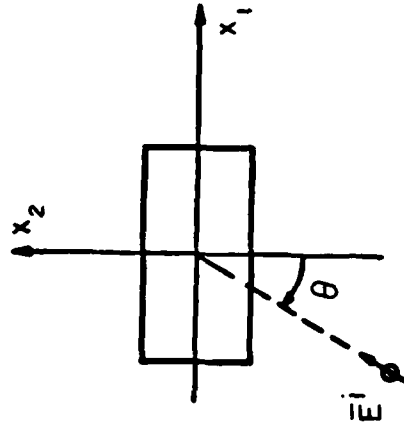
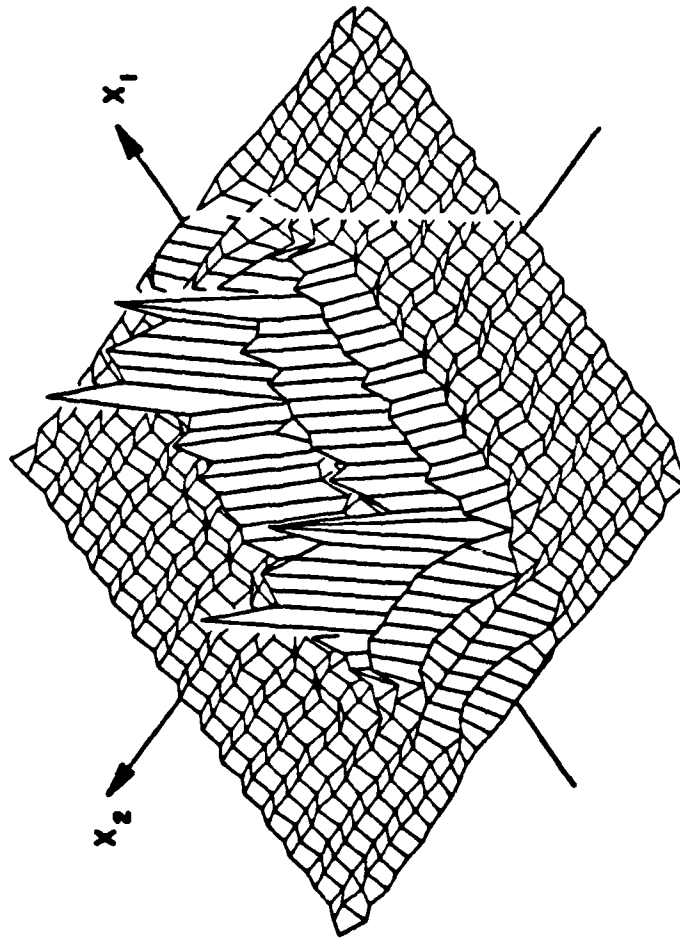


Figure 5-4. Similar description as Figure 5-3, except the data are taken over the full 360° plane

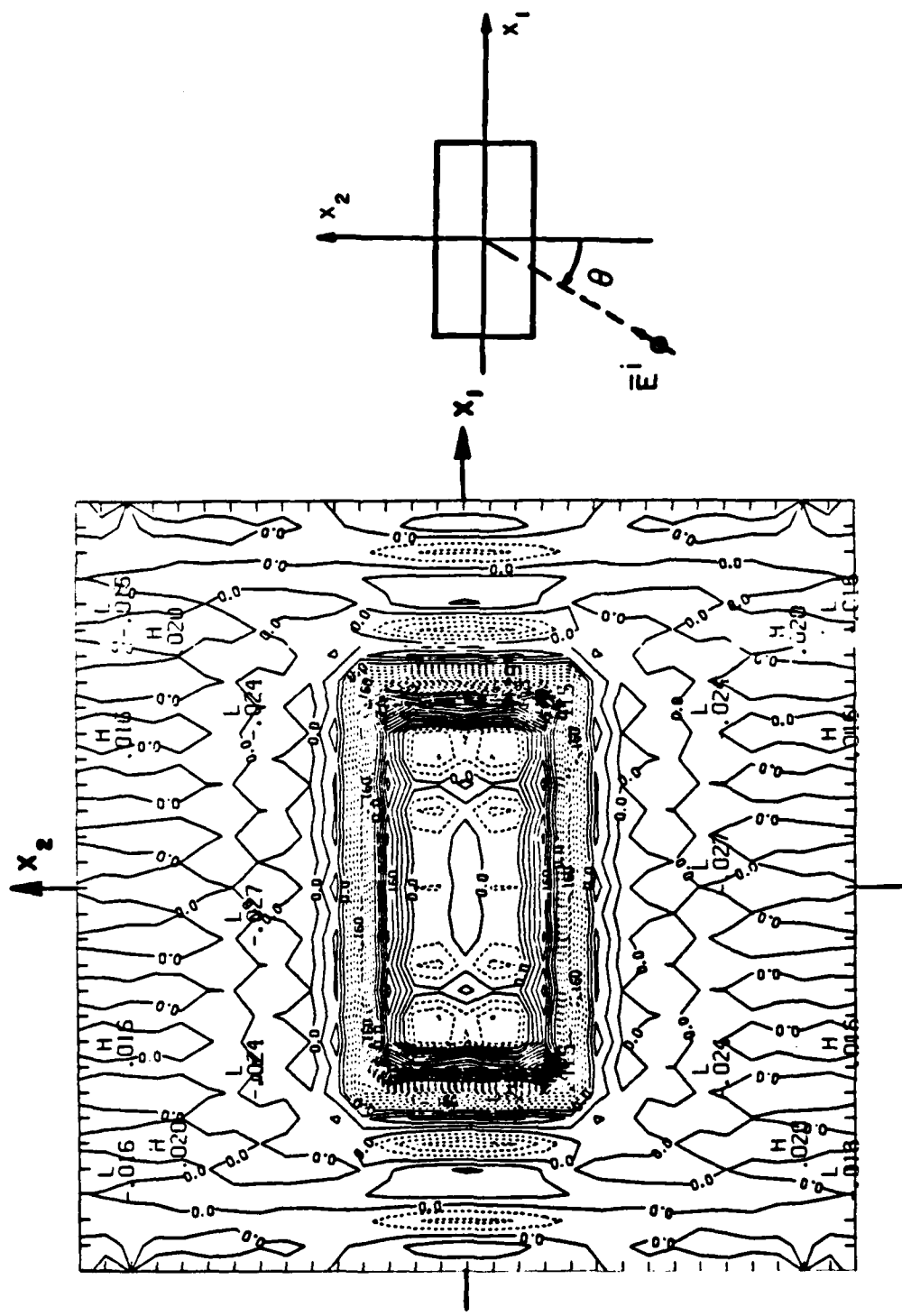


Figure 5-4a. Contour plot of Figure 5-4

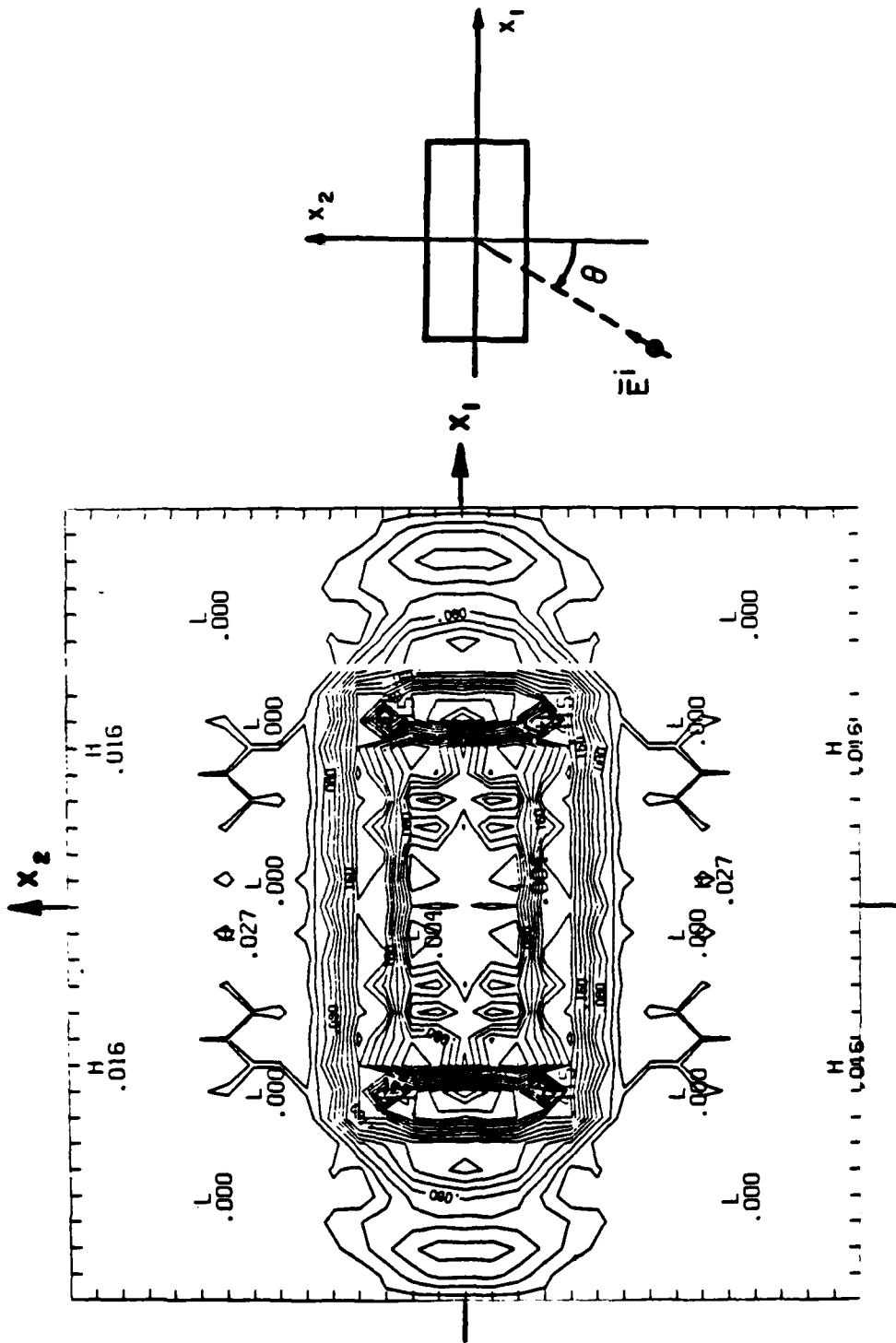


Figure 5-5a. Contour plot of Figure 5-5

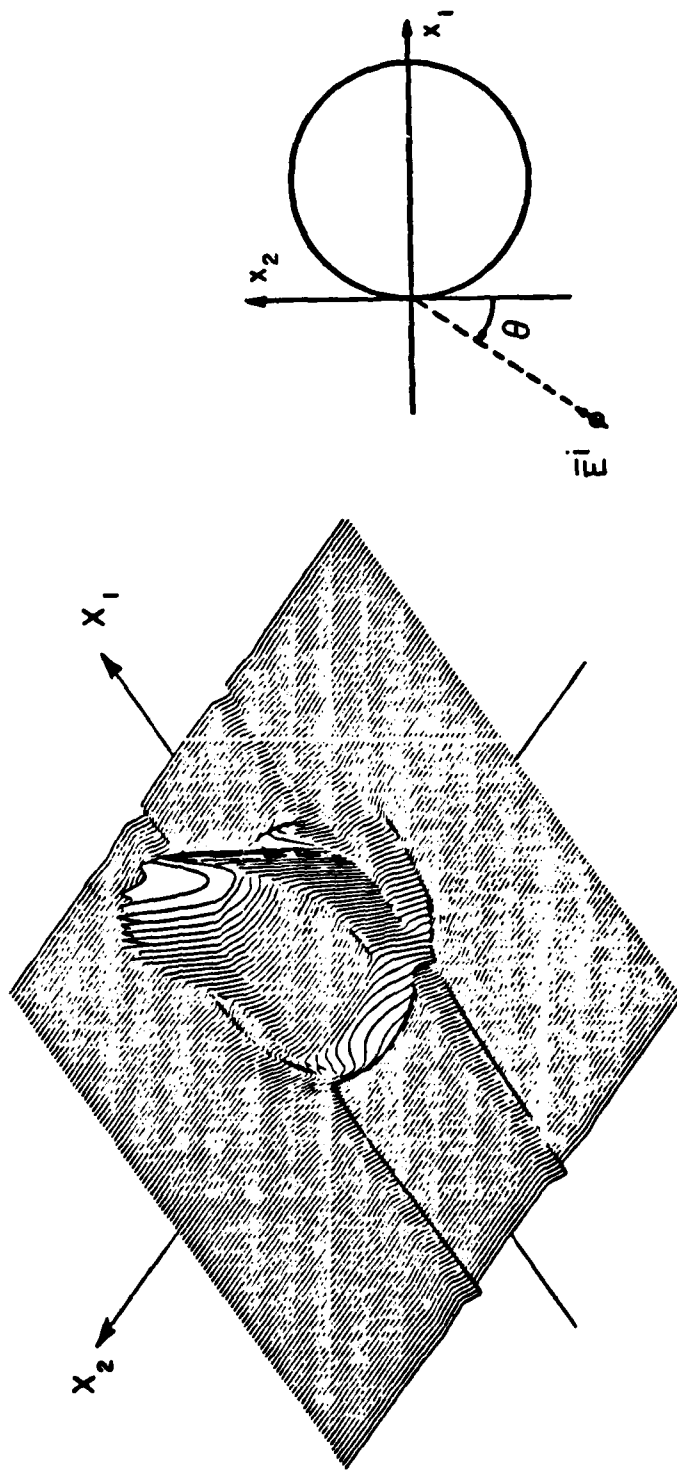


Figure 5-6. 2-D impulse response of a 6" metallic sphere with its centre situated at (3", 0). Frequency samples are taken at the cubic sampling lattice over the range of 0 to 12 Ghz. The data are cosine tapering weighted before Fourier transformed discretely into the spatial domain. Data are taken over the half plane: $\pi < \theta < 2\pi$

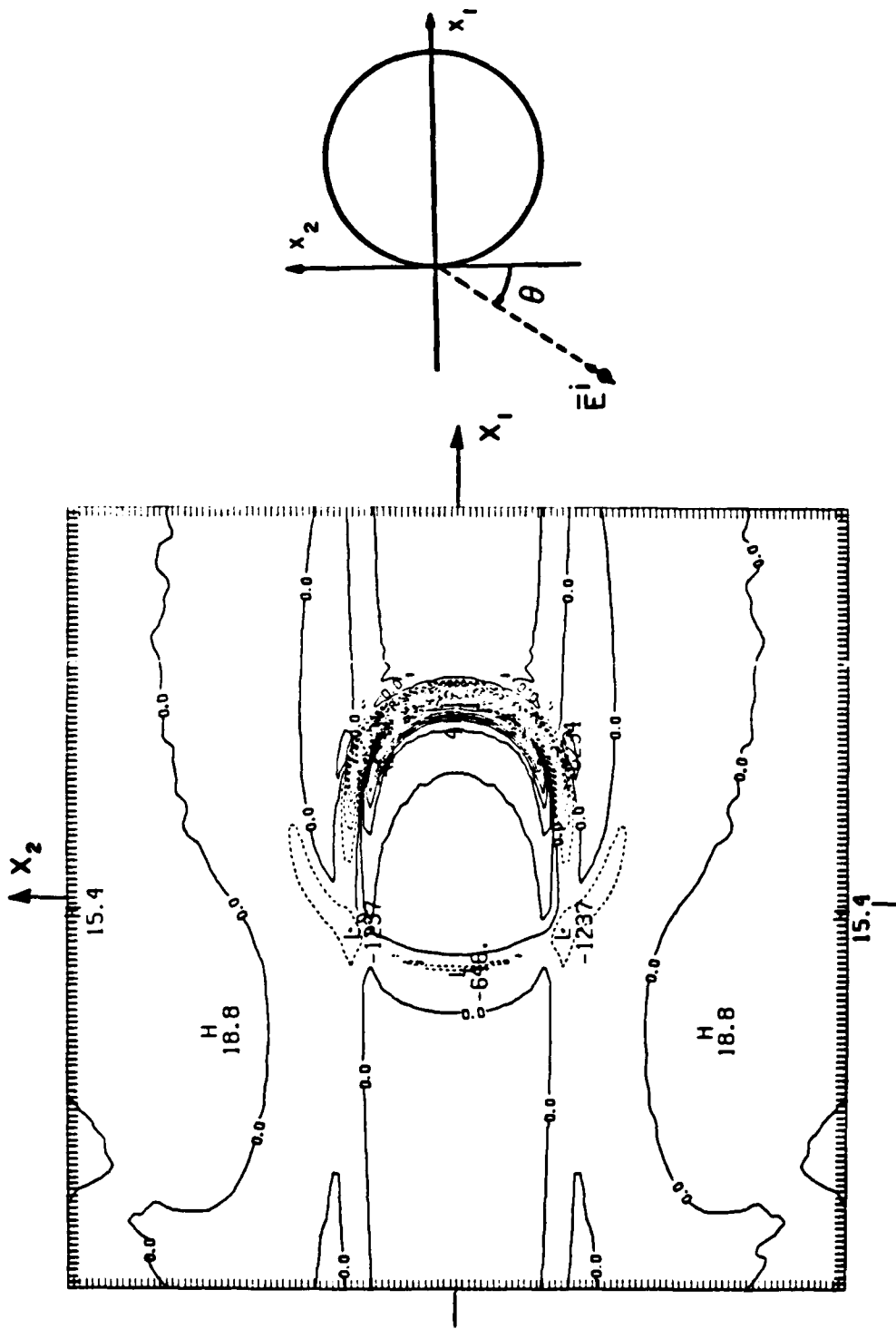


Figure 5-6a. Contour plot of Figure 5-6

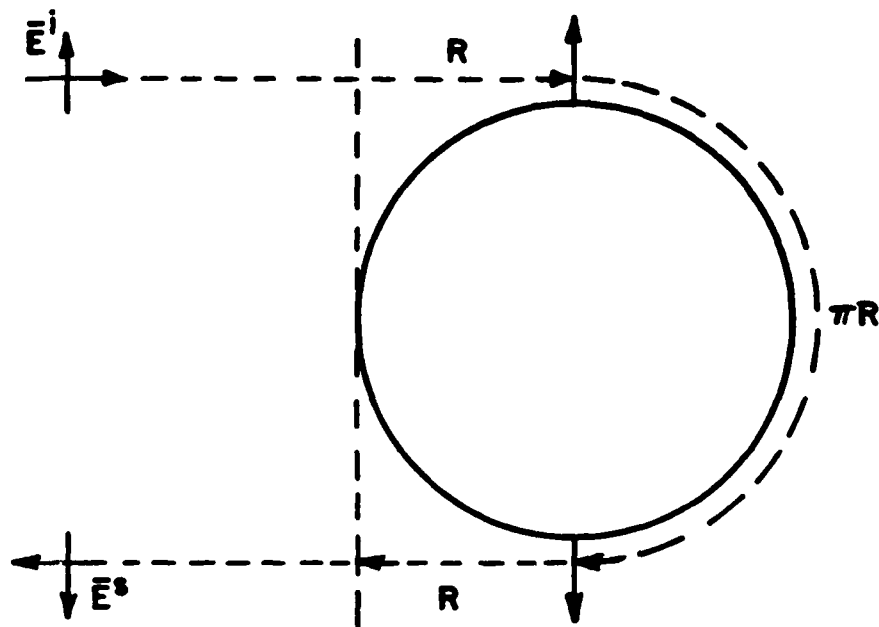


Figure 5-7. Path length of a creeping wave on a metallic sphere

CHAPTER VI

CONCLUSIONS

If a signal is limited in the spatial domain (or wave number domain), this signal is sufficiently characterized by its values over the discrete sampling lattice in the wave number domain (or the spatial domain). In the two dimensional case, the sampling locations in the wave number space are specified by the vector:

$$[l_1 \bar{u}_1 + l_2 \bar{u}_2]$$

where

$$l_1, l_2 = 0, \pm 1, \pm 2, \pm 3, \dots$$

The \bar{u}_1 and \bar{u}_2 are related to \bar{v}_1 and \bar{v}_2 by the following:

$$[\bar{u}_1 | \bar{u}_2] = 2\pi [\bar{v}_1 | \bar{v}_2]^{-T}$$

where

$-T$:the transpose of the inverse of the matrix formed

The \bar{v}_1 and \bar{v}_2 are specified by one's choice on how the space limited signal is assumed to repeat itself in its domain. \bar{v}_1 is pointed to the centre of one of the closest images in the periodic lattice. \bar{v}_2 is independent of \bar{v}_1 , and it points at the centre of another close image. By defining the settling time as the end of the impulse response, one has a space limited three dimensional impulse response signal. In the finite circular cylinder data presented in Chapter V, the signal is assumed to be 4 times the size of the cylinder in the two dimensional spatial plane. The choice of 4 is equivalent to choosing the one dimensional impulse response of having a settling time four times as long as the wave would travel over the length of the object at any aspect angle. Or the safety factor is chosen to be one. (i.e., $2(1+K) = 4 \Leftrightarrow K = 1$) This factor provides sufficient results in both Chapter IV and V.

In Chapter V, the example of the finite circular cylinder with dimensions: 6" in length and 3" in diameter, the two dimensional containment unit is chosen to be a square. The squared repetitive lattice in the spatial domain is defined by,

$$\bar{v}_1 = R \begin{bmatrix} 1 \\ 0 \end{bmatrix} \quad \bar{v}_2 = R \begin{bmatrix} 0 \\ 1 \end{bmatrix}$$

where

$$R = 6''$$

and the safety factor K is chosen to be 1. With these inputs to the program PTGRID (see Appendix B), the program outputs the sampling lattice defined by \bar{u}_1 and \bar{u}_2 . The data output is arranged with the

aspect angles and the corresponding frequency increment. One makes the necessary data extraction at the proper aspect angles, and increments the frequency until the highest frequency is reached. One could also have defined a rectangular repetitive lattice. Then

$$\bar{v}_1 = R \begin{bmatrix} 1 \\ 0 \end{bmatrix} \quad \bar{v}_2 = R \begin{bmatrix} 0 \\ 0.5 \end{bmatrix}$$

where

$$R = 6''$$

Or, for a circular repetitive lattice,

$$\bar{v}_1 = R \begin{bmatrix} \sqrt{3} \\ 2 \\ \frac{1}{-2} \end{bmatrix} \quad \bar{v}_2 = R \begin{bmatrix} 0 \\ 1 \end{bmatrix}$$

where

$$R = \sqrt{(6'')^2 + (3'')^2}$$

$$= 6.708''$$

Again these \bar{v}_1 and \bar{v}_2 values can be input into the program PTGRID (see Appendix B) to obtain the sampling lattice.

Thus, one can sample discretely and interpolate in the wave number space to reproduce the frequency response of an object. Fourier transforming this wave number signal into the spatial domain gives a representation of the spatial impulse response of the object. The

spatial impulse response is defined as the image function obtained by three dimensional Fourier transforming the far field frequency response of a finite object at all aspect angles defined over the 4π solid angle. Since most objects have different shapes, sizes, and orientations, their corresponding spatial impulse responses are different. Their corresponding sampling lattices will also be different. One general sampling lattice that is applicable to a set of objects is desirable. This is accomplished by introducing different types of canonical containment units to confine the spatial impulse responses. Two common canonical cells are parallelepiped and sphere. Two dimensional examples are shown in Figures 2-5 and 2-7, with their corresponding sampling lattices shown in Figures 2-6 and 2-8 respectively.

In Chapter IV, a six inch metallic sphere is chosen as an example to compare two types of sampling lattices -cubic and isotropic. The comparison is performed on the interpolated one dimensional impulse responses at different aspect angles using the interpolation scheme defined in the sampling theorem. As one expects, the results turn out to be competitive for the two types of sampling. Efficiencies, in the sense of the least number of sampling points, are different for different canonical containment cells used on the same object.

Efficiency in using one type of canonical containment cell:

$$\eta = \frac{\text{CONSERVATIVE ESTIMATE OF THE OBJECT'S VOLUME}}{\text{VOLUME OF THE SMALLEST CANONICAL CONTAINMENT CELL ENCLOSING THE OBJECT}}$$

Efficiencies among a sphere cap cylinder, a sphere and a cube using cubic, isotropic, and rectangular box confinement units are presented in Chapter IV. The efficiency definition proves to be a very good concept in deciding the type of sampling lattice for an object or a group of objects. This is under the assumption that the settling time of the spatial impulse response is shaped similarly to the object; e.g., the settling time of the impulse response of a sphere is the same in every aspect angle.

To obtain an approximation to the spatial impulse response from the sampled data over a finite frequency range, one can use the discrete Fourier transform. Because of today's digital computer design, the different sufficient characterization cannot be readily processed without interpolation; except, of course, the cubic lattice data sets. The interpolation step which most people like to avoid, is very time consuming. This may be referred back to the time estimation example on a sphere cap cylinder presented in Chapter V. The interpolation step is another factor that affects an engineering decision. The avoidance helps Mensa et al. to arrive at the time response faster. The price they paid is the limitation of their method's application to two dimensional Fourier transform. Their approach is thus not recommended because of its inability to be expanded into higher dimensions. The sampling criteria accompanying their method are,

the angular increment:

$$\Delta \theta \begin{cases} < \frac{\lambda}{2D} & \lambda \ll 2D \\ < \sin^{-1}\left(\frac{\lambda}{2D}\right) & \lambda < 2D \\ < \frac{\pi}{4} & \lambda > 2D \end{cases}$$

the frequency increment:

$$\Delta f < \frac{c}{2(1+K)D}$$

where

D = maximum dimension of the object

λ = wavelength of the frequency used

c = speed of light

K = some safety factor

In the finite circular cylinder example,

$$D = 17.04 \text{ cm}$$

$$K = 0.75$$

$$\Delta f < 0.503 \text{ Ghz}$$

at the highest frequency of 10 Ghz,

$$\lambda = 3 \text{ cm}$$

$$\Delta \theta < 5 \text{ degrees}$$

Therefore,

the frequency increment chosen = 0.5 Ghz

the angular increment chosen = 1 degree

Nevertheless, processed results from UTD solution on a finite circular cylinder support the convergence of Mensa et al.'s method to two dimensional discrete Fourier transform.

Lewis-Bojarski's identity requires either the object be illuminated at all angles or assumption be made on the shadowed side. Results on a finite metallic circular cylinder and a metallic sphere indicate that the spatial impulse response approach does not have the above restriction, though proper interpretation may be required. Furthermore, the use of the spatial impulse response to imaging can converge to Lewis-Bojarski's results. There is also an indication that the presentation in the form of the absolute value of the amplitude does not necessarily provide the proper picture for pattern recognition. The plain amplitude representation with positive and negative values is sometimes more appropriate. This is concluded by comparing the Figure 5-4, or 5-4a with 5-5 or 5-5a. The perimeter of a major axis cross-section of a finite circular cylinder is shown more distinctly using the plain amplitude presentation. Judging from the two dimensional impulse responses, one can deduce the substantial potential of the spatial impulse response in image reconstruction.

The spatial impulse response has numerous applications including target identification and imaging. Although smooth convex metallic body examples are considered here, tomographic applications on other types of bodies are possible. In all, the N dimensional sampling theorem provides new insights into the sampling criteria in the wave number space for a finite object. The potential in reduced management time on

two or three dimensional data is enormous. The two dimensional impulse response also projects a promising target imaging technique using the spatial impulse response.

CHAPTER VII

RECOMMENDATIONS

Traditionally, two and three dimensional data are presented in cubic lattices, for which present day digital computers are designed. Although the digital computer of today manages data in cubic lattices, the cubic lattices are not necessarily the most efficient in terms of the least number of data samples. The most general approach to solve this computer problem requires the cubic data management structure of the digital computer be modified into a more general data structure. In another words, data organized in any random fashion can be processed by this computer. If this general approach is not practical, the next best step is a faster interpolation scheme either in hardware or software. The lowest level on the hierarchy of improvement is the improvement for specific application. In this thesis, a general Fourier transform that can perform on any data lattice, fits into this category.

After some of the computer problems are solved, the next step in the development is to account for the experimental noise. How does one extract the true information that is embedded in noise? Without this

generalization, this report is only useful in information storage and retrieval on noise free data. Noise free is in the sense that the noise effect in measurement is eliminated before storage. The full development of this report's theory will enable significant reduction in time on data measurement, processing and storage.

The whole report is focused on the monostatic data. It would be interesting to see how this theory holds up with the bistatic data. Using the definition of the three dimensional Fourier transform, one can derive a similar method that parallels Mensa et al.'s approach.

By converting the k-space coordinates into spherical coordinates:

$$k_1 = \rho \sin \theta \cos \phi \quad k_2 = \rho \sin \theta \sin \phi \quad k_3 = \rho \cos \theta \quad (7-1)$$

equation (1-1) becomes:

$$f(\bar{x}) = \frac{1}{8\pi^3} \int_{\rho=0}^{\infty} \int_{\theta=0}^{\pi} \int_{\phi=0}^{2\pi} \tilde{F}(\rho, \theta, \phi) e^{j|\bar{x}| \rho \cos < (\bar{x}, \rho)} \rho^2 \sin \theta d\phi d\theta d\rho \quad (7-2)$$

where

$$|\bar{x}| = \sqrt{x_1^2 + x_2^2 + x_3^2}$$

(Rotate the k-space coordinate system so that the k_3 -axis is in line with \bar{x} : $\Rightarrow < (\bar{x}, \rho) = \theta$).

Then,

$$f(\bar{x}) = \frac{1}{8\pi^3} \int_{\rho=0}^{\infty} \int_{\theta=0}^{\pi} \int_{\phi=0}^{2\pi} \tilde{F}(\rho, \theta, \phi) e^{j|\bar{x}|\rho \cos \theta} \rho^2 \sin \theta d\phi d\theta d\rho \quad (7-3)$$

By considering one particular aspect angle: ϕ_m, θ_i

$$f_{im}(\bar{x}) = \frac{\sin \theta_i}{8\pi^3} \int_{\rho=0}^{\infty} \tilde{F}(\rho, \theta_i, \phi_m) e^{j|\bar{x}|\rho \cos \theta_i} \rho^2 d\rho \quad (7-4)$$

With all aspect angular data,

$$f(\bar{x}) = \sum_{i=1}^{\infty} \sum_{m=1}^{\infty} f_{im}(\bar{x}) \quad (7-5)$$

= the impulse response of the finite object at \bar{x}

Even though Equation (7-4) requires the integration over all frequencies, the integral can be approximated over three regions: the Rayleigh, the resonance, and the optical. Thus, the integral in Equation (7-4) is not impossible to be solved. There are problems associated with this approach. The Nyquist angular requirement is frequency dependent (Equation (2-17)). In order to satisfy the Nyquist angular requirement at high frequency, the signal is excessively sampled at the low frequency spectrum, but sampled only adequately at the high frequency spectrum for a finite frequency range of interest. Nonetheless, the approach is viable if one does not intend to extend the bandwidth of the approximated spatial impulse response.

With the help of the different sampling criteria, the infinite number of samples required to reconstruct the impulse response over a finite frequency range has changed to a finite number. Though the number is finite, the measurement time can be very substantial when an expanded frequency range in two dimensions, or three dimensions is required. Professor Leon Peters suggested another approach to further reduce the measurement time [15]. At high frequency, a target's frequency response is mostly contributed by its major scattering centres. If one can make a set of different canonical scattering centre measurement, then most targets' high frequency response can be built using the proper phase shift factors. For most scattering centres, their frequency responses are relatively simple. As a result, the Nyquist criteria for these centres in the frequency domain are more relaxed than complete structures. These canonical scattering centre data can be reused to reconstruct the high frequency response of other targets. In another words, after the canonical scattering centre data are available, one only measures the low frequency spectrum before the one dimensional, two dimensional, or three dimensional impulse response of an object can be reconstructed. This would be another interesting area for further exploration. However, more development work is required in all these described areas to extend this report into a more useful engineering tool.

APPENDIX A

THE DERIVATION OF EQUATION (2-13)

$$G(\omega_1, \omega_2) = \frac{1}{R^2 \omega_1 (\omega_1^2 - 3\omega_2^2)} \times \left\{ \begin{array}{l} 2\omega_1 \cos\left(\frac{R\omega_1}{\sqrt{3}}\right) \cos(R\omega_2) \\ -2\omega_1 \cos\left(\frac{2R\omega_1}{\sqrt{3}}\right) \\ -2\sqrt{3} \omega_2 \sin\left(\frac{R\omega_1}{\sqrt{3}}\right) \sin(R\omega_2) \end{array} \right\}$$

Equation (65) of Petersen and Middleton [7]:

$$G(\bar{\omega}) = \left(\frac{1}{R^2}\right) \left(\frac{1}{2\sqrt{3}}\right) \iint_{\text{Regular Hexagon}} e^{j\bar{\omega} \cdot \bar{x}} dx$$

Equation description for the regular hexagon: (see Figure A-1)

$$\textcircled{1} \left\{ \begin{array}{l} x_2 = R \\ \left(\frac{-R}{\sqrt{3}}\right) < x_1 < \left(\frac{R}{\sqrt{3}}\right) \end{array} \right.$$

$$\textcircled{2} \left\{ \begin{array}{l} x_2 = -\sqrt{3} x_1 + 2R \\ \left(\frac{R}{\sqrt{3}}\right) < x_1 < \left(\frac{2R}{\sqrt{3}}\right) \end{array} \right.$$

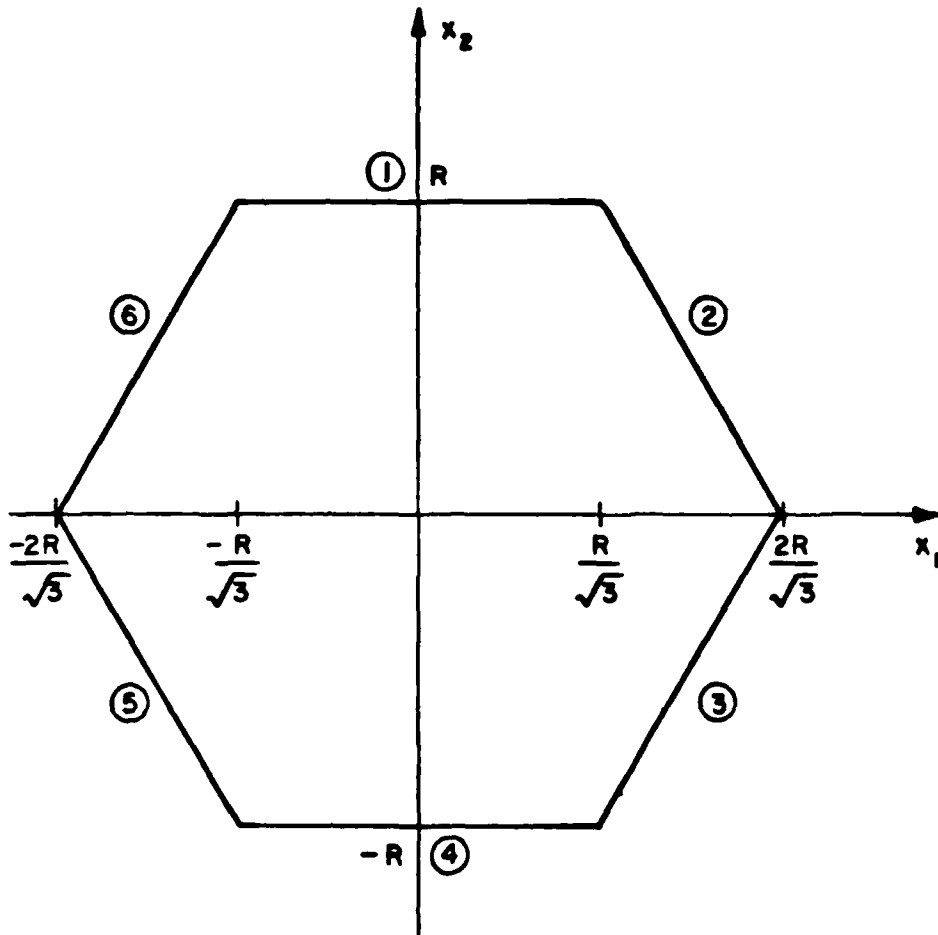


Figure A-1. Hexagonal integration limit

$$\textcircled{3} \begin{cases} x_2 = \sqrt{3} x_1 - 2R \\ \left(\frac{R}{\sqrt{3}}\right) < x_1 < \left(\frac{2R}{\sqrt{3}}\right) \end{cases}$$

$$\textcircled{4} \begin{cases} x_2 = -R \\ \left(\frac{-R}{\sqrt{3}}\right) < x_1 < \left(\frac{R}{\sqrt{3}}\right) \end{cases}$$

$$\textcircled{5} \begin{cases} x_2 = -\sqrt{3} x_1 - 2R \\ \left(\frac{-2R}{\sqrt{3}}\right) < x_1 < \left(\frac{-R}{\sqrt{3}}\right) \end{cases}$$

$$\textcircled{6} \begin{cases} x_2 = \sqrt{3} x_1 + 2R \\ \left(\frac{-2R}{\sqrt{3}}\right) < x_1 < \left(\frac{-R}{\sqrt{3}}\right) \end{cases}$$

then

$$G(\bar{\omega}) = \frac{1}{2\sqrt{3}R^2} (I_1 + I_2 + I_3) \quad (\text{A-1})$$

where

$$I_1 = \int_{\left(\frac{-R}{\sqrt{3}}\right)}^{\left(\frac{R}{\sqrt{3}}\right)} \int_{\textcircled{6}}^{\textcircled{5}} e^{j(\omega_1 x_1 + \omega_2 x_2)} dx_2 dx_1 \quad (\text{A-2})$$

$$x_1 = \left(\frac{-2R}{\sqrt{3}}\right) \quad x_2 = \textcircled{5}$$

$$I_2 = \int_{\left(\frac{-R}{\sqrt{3}}\right)}^{\left(\frac{R}{\sqrt{3}}\right)} \int_{\textcircled{4}}^{\textcircled{3}} e^{j(\omega_1 x_1 + \omega_2 x_2)} dx_2 dx_1 \quad (\text{A-3})$$

$$x_1 = \left(\frac{-R}{\sqrt{3}}\right) \quad x_2 = -R$$

$$I_3 = \int_{x_1 = \left(\frac{R}{\sqrt{3}}\right)}^{\left(\frac{2R}{\sqrt{3}}\right)} \int_{x_2 = \textcircled{3}} e^{j(\omega_1 x_1 + \omega_2 x_2)} dx_2 dx_1 \quad (\text{A-4})$$

Equation (A-2):

$$I_1 = \int_{x_1 = \left(\frac{-2R}{\sqrt{3}}\right)}^{\left(\frac{-R}{\sqrt{3}}\right)} \int_{x_2 = -\sqrt{3}x_1 - 2R}^{\sqrt{3}x_1 + 2R} e^{j\omega_1 x_1} \cdot e^{j\omega_2 x_2} dx_2 dx_1$$

$$= \int_{x_1 = \left(\frac{-2R}{\sqrt{3}}\right)}^{\left(\frac{-R}{\sqrt{3}}\right)} e^{j\omega_1 x_1} \left[\frac{e^{j\omega_2 x_2}}{j\omega_2} \right]_{-(\sqrt{3}x_1 + 2R)}^{(\sqrt{3}x_1 + 2R)} dx_1$$

$$= \frac{1}{j\omega_2} \int_{x_1 = \left(\frac{-2R}{\sqrt{3}}\right)}^{\left(\frac{-R}{\sqrt{3}}\right)} e^{j\omega_1 x_1} \left\{ e^{j\omega_2(\sqrt{3}x_1 + 2R)} - e^{-j\omega_2(\sqrt{3}x_1 + 2R)} \right\} dx_1$$

$$= \frac{1}{j\omega_2} \int_{x_1 = \left(\frac{-2R}{\sqrt{3}}\right)}^{\left(\frac{-R}{\sqrt{3}}\right)} \left\{ e^{j(\omega_1 + \sqrt{3}\omega_2)x_1} + 2jR\omega_2 e^{-j(\omega_1 - \sqrt{3}\omega_2)x_1} - 2j\omega_2 R \right\} dx_1$$

$$= \frac{1}{j\omega_2} \left\{ \left[\begin{array}{c} j(\omega_1 + \sqrt{3}\omega_2)x_1 + 2jR\omega_2 \\ e \\ j(\omega_1 + \sqrt{3}\omega_2) \end{array} \right] \begin{array}{l} -R \\ \sqrt{3} \\ -2R \\ \sqrt{3} \end{array} \right. \\
\left. - \left[\begin{array}{c} j(\omega_1 - \sqrt{3}\omega_2)x_1 - 2jR\omega_2 \\ e \\ j(\omega_1 - \sqrt{3}\omega_2) \end{array} \right] \begin{array}{l} -R \\ \sqrt{3} \\ -2R \\ \sqrt{3} \end{array} \right\}$$

Therefore,

$$I_1 = \frac{e^{2jR\omega_2}}{\omega_2(\omega_1 + \sqrt{3}\omega_2)} \left[\begin{array}{cc} -j(\omega_1 + \sqrt{3}\omega_2)\left(\frac{2R}{\sqrt{3}}\right) & -j(\omega_1 + \sqrt{3}\omega_2)\left(\frac{R}{\sqrt{3}}\right) \\ e & -e \end{array} \right] \\
+ \frac{e^{-2jR\omega_2}}{\omega_2(\omega_1 - \sqrt{3}\omega_2)} \left[\begin{array}{cc} -j(\omega_1 - \sqrt{3}\omega_2)\left(\frac{R}{\sqrt{3}}\right) & -j(\omega_1 - \sqrt{3}\omega_2)\left(\frac{2R}{\sqrt{3}}\right) \\ e & -e \end{array} \right]$$

Equation (A-3):

$$I_2 = \int_{x_1 = \frac{-R}{\sqrt{3}}}^{\frac{R}{\sqrt{3}}} \int_{x_2 = -R}^R e^{j(\omega_1 x_1 + \omega_2 x_2)} dx_2 dx_1$$

$$= \int_{x_1 = \left(\frac{-R}{\sqrt{3}}\right)}^{\left(\frac{R}{\sqrt{3}}\right)} e^{j\omega_1 x_1} dx_1 \int_{x_2 = -R}^R e^{j\omega_2 x_2} dx_2$$

$$= \left[\frac{e^{j\omega_1 x_1}}{j\omega_1} \right]_{\frac{-R}{\sqrt{3}}}^{\frac{R}{\sqrt{3}}} \left[\frac{e^{j\omega_2 x_2}}{j\omega_2} \right]_{-R}^R$$

$$= \left[\left(\frac{2}{\omega_1} \right) \sin \left(\frac{\omega_1 R}{\sqrt{3}} \right) \right] \left[\left(\frac{2}{\omega_2} \right) \sin (\omega_2 R) \right]$$

Therefore,

$$I_2 = \left(\frac{4}{\omega_1 \omega_2} \right) \sin (\omega_2 R) \sin \left(\frac{\omega_1 R}{\sqrt{3}} \right)$$

Equation (A-4),

$$I_3 = \int_{x_1 = \left(\frac{R}{\sqrt{3}}\right)}^{\left(\frac{2R}{\sqrt{3}}\right)} \int_{x_2 = \sqrt{3}x_1 - 2R}^{-\sqrt{3}x_1 + 2R} e^{j(\omega_1 x_1 + \omega_2 x_2)} dx_2 dx_1$$

$$= \int_{x_1 = \left(\frac{R}{\sqrt{3}}\right)}^{\left(\frac{2R}{\sqrt{3}}\right)} e^{j\omega_1 x_1} \left[\frac{e^{j\omega_2 x_2}}{j\omega_2} \right]_{\sqrt{3}x_1 - 2R}^{-\sqrt{3}x_1 + 2R} dx_1$$

$$= \frac{1}{j\omega_2} \int_{x_1 = \left(\frac{R}{\sqrt{3}}\right)}^{\left(\frac{2R}{\sqrt{3}}\right)} e^{j\omega_1 x_1} \left[e^{j\omega_2(-\sqrt{3}x_1 + 2R)} - e^{j\omega_2(\sqrt{3}x_1 - 2R)} \right] dx_1$$

$$= \frac{1}{j\omega_2} \int_{x_1 = \left(\frac{R}{\sqrt{3}}\right)}^{\left(\frac{2R}{\sqrt{3}}\right)} \left[e^{j(\omega_1 - \sqrt{3}\omega_2)x_1 + 2jR\omega_2} - e^{j(\omega_1 + \sqrt{3}\omega_2)x_1 - 2jR\omega_2} \right] dx_1$$

$$= \frac{1}{j\omega_2} \left\{ \left[\frac{e^{j(\omega_1 - \sqrt{3}\omega_2)x_1 + 2jR\omega_2}}{j(\omega_1 - \sqrt{3}\omega_2)} \right] \begin{matrix} \frac{2R}{\sqrt{3}} \\ \\ \\ \frac{R}{\sqrt{3}} \end{matrix} \right. \\ \left. - \left[\frac{e^{j(\omega_1 + \sqrt{3}\omega_2)x_1 - 2jR\omega_2}}{j(\omega_1 + \sqrt{3}\omega_2)} \right] \begin{matrix} \frac{2R}{\sqrt{3}} \\ \\ \\ \frac{R}{\sqrt{3}} \end{matrix} \right\}$$

Therefore,

$$I_3 = \frac{e^{2jR\omega_2}}{\omega_2(\omega_1 - \sqrt{3}\omega_2)} \left[\begin{matrix} j(\omega_1 - \sqrt{3}\omega_2)\left(\frac{R}{\sqrt{3}}\right) & j(\omega_1 - \sqrt{3}\omega_2)\left(\frac{2R}{\sqrt{3}}\right) \\ e & -e \end{matrix} \right] \\ + \frac{e^{-2jR\omega_2}}{\omega_2(\omega_1 + \sqrt{3}\omega_2)} \left[\begin{matrix} j(\omega_1 + \sqrt{3}\omega_2)\left(\frac{2R}{\sqrt{3}}\right) & j(\omega_1 + \sqrt{3}\omega_2)\left(\frac{R}{\sqrt{3}}\right) \\ e & -e \end{matrix} \right]$$

Now,

$$I_1 + I_3$$

$$= \frac{1}{\omega_2(\omega_1 + \sqrt{3}\omega_2)} \left\{ e^{-j[(\omega_1 + \sqrt{3}\omega_2)\frac{2R}{\sqrt{3}} - 2R\omega_2]} + e^{j[(\omega_1 + \sqrt{3}\omega_2)\frac{2R}{\sqrt{3}} - 2R\omega_2]} \right.$$

$$\left. - e^{-j[(\omega_1 + \sqrt{3}\omega_2)\frac{R}{\sqrt{3}} - 2R\omega_2]} - e^{j[(\omega_1 + \sqrt{3}\omega_2)\frac{R}{\sqrt{3}} - 2R\omega_2]} \right\}$$

$$+ \frac{1}{\omega_2(\omega_1 - \sqrt{3}\omega_2)} \left\{ e^{-j[(\omega_1 - \sqrt{3}\omega_2)\frac{R}{\sqrt{3}} + 2R\omega_2]} + e^{j[(\omega_1 - \sqrt{3}\omega_2)\frac{R}{\sqrt{3}} + 2R\omega_2]} \right.$$

$$\left. - e^{-j[(\omega_1 - \sqrt{3}\omega_2)\frac{2R}{\sqrt{3}} + 2R\omega_2]} - e^{j[(\omega_1 - \sqrt{3}\omega_2)\frac{2R}{\sqrt{3}} + 2R\omega_2]} \right\}$$

$$= \frac{1}{\omega_2(\omega_1 + \sqrt{3}\omega_2)} \left\{ 2\cos \left[(\omega_1 + \sqrt{3}\omega_2)\frac{2R}{\sqrt{3}} - 2R\omega_2 \right] \right.$$

$$\left. - 2\cos \left[(\omega_1 + \sqrt{3}\omega_2)\frac{R}{\sqrt{3}} - 2R\omega_2 \right] \right\}$$

(This expression continues on the next page.)

$$+ \frac{1}{\omega_2(\omega_1 - \sqrt{3}\omega_2)} \left\{ 2\cos \left[(\omega_1 - \sqrt{3}\omega_2) \frac{R}{\sqrt{3}} + 2R\omega_2 \right] - 2\cos \left[(\omega_1 - \sqrt{3}\omega_2) \frac{2R}{\sqrt{3}} + 2R\omega_2 \right] \right\}$$

[Since: $\cos \alpha - \cos \beta = -2 \sin \frac{1}{2} (\alpha + \beta) \sin \frac{1}{2} (\alpha - \beta)$]

$$= \frac{-4}{\omega_2(\omega_1 + \sqrt{3}\omega_2)} \left\{ \sin \frac{1}{2} \left[\left(\frac{3R}{\sqrt{3}} \right) (\omega_1 + \sqrt{3}\omega_2) - 4R\omega_2 \right] \sin \frac{1}{2} \left[\left(\frac{R}{\sqrt{3}} \right) (\omega_1 + \sqrt{3}\omega_2) \right] \right\}$$

$$+ \frac{4}{\omega_2(\omega_1 - \sqrt{3}\omega_2)} \left\{ \sin \frac{1}{2} \left[\left(\frac{3R}{\sqrt{3}} \right) (\omega_1 - \sqrt{3}\omega_2) + 4R\omega_2 \right] \sin \frac{1}{2} \left[\left(\frac{R}{\sqrt{3}} \right) (\omega_1 - \sqrt{3}\omega_2) \right] \right\}$$

$$= \frac{-4}{\omega_2(\omega_1 + \sqrt{3}\omega_2)} \left\{ \sin \left(\frac{\sqrt{3}R\omega_1}{2} - \frac{R\omega_2}{2} \right) \sin \left(\frac{R\omega_1}{2\sqrt{3}} + \frac{R\omega_2}{2} \right) \right\}$$

$$+ \frac{4}{\omega_2(\omega_1 - \sqrt{3}\omega_2)} \left\{ \sin \left(\frac{R\sqrt{3}\omega_1}{2} + \frac{R\omega_2}{2} \right) \sin \left(\frac{R\omega_1}{2\sqrt{3}} - \frac{R\omega_2}{2} \right) \right\}$$

$$[\text{Since: } \sin \alpha \sin \beta = \frac{1}{2} \cos (\alpha - \beta) - \frac{1}{2} \cos (\alpha + \beta)]$$

$$= \frac{-2}{\omega_2(\omega_1 + \sqrt{3}\omega_2)} \left\{ \cos \left[\left(\sqrt{3} - \frac{1}{\sqrt{3}} \right) \left(\frac{R\omega_1}{2} \right) - R\omega_2 \right] - \cos \left[\left(\sqrt{3} + \frac{1}{\sqrt{3}} \right) \frac{R\omega_1}{2} \right] \right\}$$

$$+ \frac{2}{\omega_2(\omega_1 - \sqrt{3}\omega_2)} \left\{ \cos \left[\left(\sqrt{3} - \frac{1}{\sqrt{3}} \right) \left(\frac{R\omega_1}{2} \right) + R\omega_2 \right] - \cos \left[\left(\sqrt{3} + \frac{1}{\sqrt{3}} \right) \frac{R\omega_1}{2} \right] \right\}$$

$$= \frac{-2}{\omega_2(\omega_1 + \sqrt{3}\omega_2)} \left\{ \cos \left(\frac{R\omega_1}{\sqrt{3}} - R\omega_2 \right) - \cos \left(\frac{2R\omega_1}{\sqrt{3}} \right) \right\}$$

$$+ \frac{2}{\omega_2(\omega_1 - \sqrt{3}\omega_2)} \left\{ \cos \left(\frac{R\omega_1}{\sqrt{3}} + R\omega_2 \right) - \cos \left(\frac{2R\omega_1}{\sqrt{3}} \right) \right\}$$

$$\begin{aligned}
&= \frac{-2}{\omega_2(\omega_1^2 - 3\omega_2^2)} \left\{ (\omega_1 - \sqrt{3}\omega_2) \cos\left(\frac{R\omega_1}{\sqrt{3}} - R\omega_2\right) \right. \\
&\quad - (\omega_1 - \sqrt{3}\omega_2) \cos\left(\frac{2R\omega_1}{\sqrt{3}}\right) \\
&\quad - (\omega_1 + \sqrt{3}\omega_2) \cos\left(\frac{R\omega_1}{\sqrt{3}} + R\omega_2\right) \\
&\quad \left. + (\omega_1 + \sqrt{3}\omega_2) \cos\left(\frac{2R\omega_1}{\sqrt{3}}\right) \right\} \\
&= \frac{-2}{\omega_2(\omega_1^2 - 3\omega_2^2)} \left\{ \omega_1 \left[\cos\left(\frac{R\omega_1}{\sqrt{3}} - R\omega_2\right) - \cos\left(\frac{R\omega_1}{\sqrt{3}} + R\omega_2\right) \right] \right. \\
&\quad - \sqrt{3} \omega_2 \left[\cos\left(\frac{R\omega_1}{\sqrt{3}} - R\omega_2\right) + \cos\left(\frac{R\omega_1}{\sqrt{3}} + R\omega_2\right) \right] \\
&\quad \left. + 2 \sqrt{3} \omega_2 \cos\left(\frac{2R\omega_1}{\sqrt{3}}\right) \right\}
\end{aligned}$$

$$\left[\begin{array}{l} \text{Since: } \cos \alpha + \cos \beta = 2 \cos \frac{1}{2} (\alpha + \beta) \cos \frac{1}{2} (\alpha - \beta) \\ \cos \alpha - \cos \beta = -2 \sin \frac{1}{2} (\alpha + \beta) \sin \frac{1}{2} (\alpha - \beta) \end{array} \right]$$

$$= \frac{-2}{\omega_2(\omega_1^2 - 3\omega_2^2)} \left\{ \begin{aligned} &\omega_1 \left[2 \sin \frac{1}{2} \left(\frac{2R\omega_1}{\sqrt{3}} \right) \sin \frac{1}{2} (2R\omega_2) \right] \\ &- \sqrt{3} \omega_2 \left[2 \cos \frac{1}{2} \left(\frac{2R\omega_1}{\sqrt{3}} \right) \cos \frac{1}{2} (-2R\omega_2) \right] \\ &+ 2\sqrt{3} \omega_2 \cos \left(\frac{2R\omega_1}{\sqrt{3}} \right) \end{aligned} \right\}$$

Therefore, $I_1 + I_3$

$$= \frac{-4}{\omega_2(\omega_1^2 - 3\omega_2^2)} \left\{ \begin{aligned} &\omega_1 \sin \left(\frac{R\omega_1}{\sqrt{3}} \right) \sin (R\omega_2) \\ &- \sqrt{3} \omega_2 \cos \left(\frac{R\omega_1}{\sqrt{3}} \right) \cos (R\omega_2) \\ &+ \sqrt{3} \omega_2 \cos \left(\frac{2R\omega_1}{\sqrt{3}} \right) \end{aligned} \right\}$$

Now, $I_1 + I_2 + I_3$

$$= \frac{-4}{\omega_1\omega_2(\omega_1^2 - 3\omega_2^2)} \left\{ \begin{aligned} &\sqrt{3}\omega_2\omega_1 \cos \left(\frac{2R\omega_1}{\sqrt{3}} \right) + \omega_1^2 \sin \left(\frac{R\omega_1}{\sqrt{3}} \right) \sin (R\omega_2) \\ &- \sqrt{3} \omega_1\omega_2 \cos \left(\frac{R\omega_1}{\sqrt{3}} \right) \cos (R\omega_2) \\ &- \omega_1^2 \sin (\omega_2 R) \sin \left(\frac{\omega_1 R}{\sqrt{3}} \right) \\ &+ 3 \omega_2^2 \sin (\omega_2 R) \sin \left(\frac{\omega_1 R}{\sqrt{3}} \right) \end{aligned} \right\}$$

$$= \frac{-4}{\omega_1 (\omega_1^2 - 3\omega_2^2)} \left\{ \begin{array}{l} \sqrt{3} \omega_1 \cos\left(\frac{2R\omega_1}{\sqrt{3}}\right) - \sqrt{3} \omega_1 \cos\left(\frac{R\omega_1}{\sqrt{3}}\right) \cos(R\omega_2) \\ + 3 \omega_2 \sin(\omega_2 R) \sin\left(\frac{\omega_1 R}{\sqrt{3}}\right) \end{array} \right\}$$

Equation (A-1),

$$G(\bar{\omega}) = \frac{1}{2\sqrt{3}R} (I_1 + I_2 + I_3)$$

$$= \frac{1}{R \omega_1 (\omega_1^2 - 3\omega_2^2)} \times \left\{ \begin{array}{l} 2 \omega_1 \cos\left(\frac{R\omega_1}{\sqrt{3}}\right) \cos(R\omega_2) \\ - 2 \omega_1 \cos\left(\frac{2R\omega_1}{\sqrt{3}}\right) \\ - 2 \sqrt{3} \omega_2 \sin\left(\frac{R\omega_1}{\sqrt{3}}\right) \sin(R\omega_2) \end{array} \right\}$$

= Equation (2-13).

APPENDIX B

PROGRAMS DEVELOPED

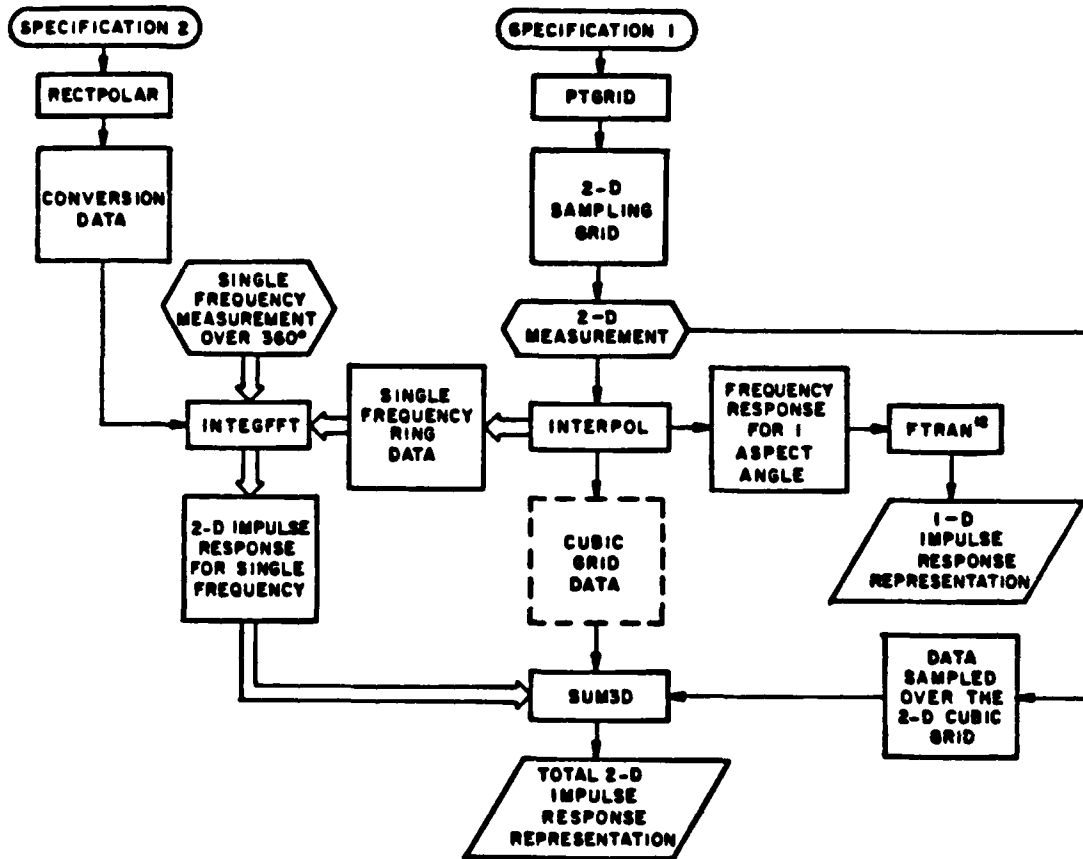


Figure B-1. Flow chart showing the relationship among the written programs

```

C
C PROGRAM: RECONST1D
C
C THIS PROGRAM WILL TAKE A DATA SET: 'COEFF' IN REAL AND IMAGINARY FORMAT
C AND INTERPOLATE THE POINTS IN BETWEEN SAMPLES USING SAMPLING THEOREM
C APPROACH. PRESENTLY, THIS
C PROGRAM IS ALLOWED TO TAKE 100 SAMPLES. IF MORE IS REQUIRED, PLEASE
C CHANGE THE ARRAY SIZE OF COEFF AND THE VALUE OF NUM.
C MSIZE:THE ARRAY SIZE=2*(NUMBER OF SAMPLES) +1
C NUM:NUMBER OF SAMPLES
C XINC: INCREMENT
C THE SAMPLES ARE TAKEN AT DELTA FREQUENCY OF 'FREQ'.
C THE FREQUENCY RANGE FOR INTERPOLATION IS SPECIFIED BY 'INITIAL'
C AND 'LAST'. THE NUMBER OF POINTS IN 'DATA' IS 'NP1'. THE
C OUTPUT FILE IS SPECIFIED BY 'FNAME2'.
C
C THIS PROGRAM WILL LINK WITH SINC, JPL0T, SUM1D AND 'FLOTLIB
C
C REAL INITIAL, LAST
C COMPLEX COEFF(201),SUM,DATA(200)
C CHARACTER*10 FNAME1.FNAME2
C CHARACTER COM1
C NUM=100
C MSIZE=2*NUM +1
C NSTEP=200
C INITIAL=6.E7
C LAST=12.E9
C XINC=(LAST-INITIAL)/(NSTEP-1)
C PI=3.14159265
C
C THE SUMMATION IS FROM -N TO +N
C COEFF - THE ARRAY OF COEFFICIENTS FOR ITH TERM IN THE SUMMATION
C WHERE THE INDEX -N IS REPRESENTED BY 1
C +N IS REPRESENTED BY 2*N +1
C T - ASSUMED CUTOFF TIME= 1/(2*SAMPLING FREQUENCY)
C
C DATA STRUCTURE OF FNAME1
C N :NUMBER OF POINTS IN THE FILE (*)
C FMIN :SMALLEST FREQUENCY USED(*)
C FREQ :SAMPLING FREQUENCY (*)
C COEFF(I):(REAL-IMAGINARY) (*)
C
C TYPE *,'TYPE FILE NAME CONTAINING COMPLEX COEFFICIENTS'
C ACCEPT 2.FNAME1
2 FORMAT (A10)
C OPEN (UNIT=8,NAME=FNAME1,TYPE='OLD')
C READ(8,*) N
C READ(8,*) FMIN
C READ(8,*) FREQ
C T=1./(2.*FREQ)
C IF (N.GT.NUM) GO TO 8888

```

```

NDIM=2*N +1
C
C   INITIALIZATION
C
DO 5 I=1,MSIZE
    COEFF(I)=(0.,0.)
5   CONTINUE
    READ(8,*) COEFF(NUM)
    DO 10 I=1,N-1
        READ(8,*) COEFF(NUM+I+1)
C
C   FILL IN COMPLEX CONJUGATE FOR THE NEGATIVE FREQUENCY
C
        COEFF(NUM+1-I)=CONJG(COEFF(NUM+I+1))
10  CONTINUE
    CLOSE (UNIT=8,DISP='SAVE')
    NZERO=0
C
C   SET ANY FREQUENCY INTERPOLATION SPECIFIED BELOW FMIN TO ZERO
C   NZERO: NUMBER OF ZEROS TO BE PLACED
C
    IF (FMIN.LE.FREQ) GO TO 127
    NZERO=INT(FMIN/XINC)
    DO 123 I=1,NZERO
        DATA(I)=(0.,0.)
123 CONTINUE
C
C   STARTS THE INTERPOLATION
C   (THE SUMMATION IS PERFORMED BY FUNCTION SUM1D)
C
127 ILAST=INT((N-1)*FREQ/XINC)
    IF (ILAST.LT.NSTEP) INDEX=ILAST
    IF (ILAST.GE.NSTEP) INDEX=NSTEP
    DO 20 I=NZERO +1,INDEX
        DATA(I) = SUM1D(((I-1)*XINC+INITIAL)*T*2.*PI,COEFF,MSIZE,NDIM)
20  CONTINUE
C
C   SET ANY SPECIFIED FREQUENCY INTERPOLATION HIGHER THAN FMIN+N*FREQ
C   TO ZERO
C
    DO 133 I=INDEX +1,NSTEP
        DATA(I)=(0.,0.)
133 CONTINUE
C
C   PLOT AND OPTIONAL WRITE INTO A FILE: FNAME2
C
    CALL JPLOT(DATA,NSTEP,INITIAL.XINC,0.NSTEP-1)
23  WRITE(6,*) 'WRITE THE INTERPOLATED DATA INTO A FILE?'
    WRITE(6,*) '1) YES, IN AMPLITUDE AND PHASE (RADIAN) FORM'
    WRITE(6,*) '2) YES, IN REAL AND IMAGINARY FORM'
    WRITE(6,*) '3) NO, FORGET IT!'

```

```

ACCEPT 25,COM1
25  FORMAT(A1)
    IF (COM1.EQ.'3') GO TO 9999
    IF ((COM1.NE.'1').AND.(COM1.NE.'2')) GO TO 23
    WRITE(6,*) 'STORAGE FILE NAME:'
    ACCEPT 30,FNAME2
30  FORMAT(A10)
    IF (COM1.EQ.'2') GO TO 35
C
C   CONVERT TO AMPLITUDE (LINEAR) AND PHASE (RADIAN)
C
DO 33 I=1,NSTEP
    XREAL=CABS(DATA(I))
    XIMAG=ATAN2(AIMAG(DATA(I)),REAL(DATA(I)))
    DATA(I)=CMPLX(XREAL,XIMAG)
33  CONTINUE
C
C   OUTPUT TO FNAME2
C   STRUCTURE OF FNAME2:
C   DATA(I):FREE COMPLEX FORMAT(*)
C
35  OPEN(UNIT=8,NAME=FNAME2,TYPE='NEW')
    DO 40 I=1,NSTEP
        WRITE(8,*) DATA(I)
40  CONTINUE
    CLOSE(UNIT=8,DISP='SAVE')
    GO TO 9999
8888 WRITE(6,*) 'ERROR:NOT ENOUGH SPACE SPECIFIED IN THE PROGRAM'
9999 STOP
    END

```

```

C
C
C      SUBROUTINE:      JPLOT
C
C      THIS SUBROUTINE WILL DO RECTANGULAR PLOT ON A COMPLEX ARRAY: 'DATA'
C      FOR REAL AND IMAGINARY PLOT OR MAGNITUDE (LINEAR) AND PHASE (RADIAN)
C      PLOT.
C          DATA      :ARRAY NAME
C          NPOINT     :THE ARRAY SIZE
C          FMIN       :SMALLEST ELEMENT OF THE ABSCISSOR
C          FINCR      :THE INCRMENT SIZE
C          NSTART     :THE START PLOTTING INDEX
C          NLAST      :THE LAST PLOTTING INDEX
C      IF (NLAST.GT.NPOINT) THE LAST POINT PLOTTED IS NPOINT
C
C      THIS REQUIRES THE SUPPORT OF 'PLOTLIB.'
C
C      SUBROUTINE JPLOT(DATA,NPOINT,FMIN,FINCR,NSTART,NLAST)
C      CHARACTER COM
C      COMPLEX DATA(NPOINT)
C      DIMENSION YAXIS1(9000),YAXIS2(9000),XAXIS(9000)
C      PI=3.14159265
C      MSIZE=9000
C
C      C
C      C      INITIALIZATION
C      C
C      DO 3 I=1,MSIZE
C          YAXIS1(I)=0.
C          YAXIS2(I)=0.
C          XAXIS(I)=0.
C
C      3      CONTINUE
C      5      WRITE(6,*) 'DO YOU WANT REAL AND IMAGINARY PLOT?Y/N'
C      ACCEPT 6, COM
C      6      FORMAT(A1)
C      IF (NLAST.GT.NPOINT) NLAST=NPOINT
C      NP=NLAST-NSTART+1
C      IF (COM.EQ.'N') GO TO 15
C      IF (COM.EQ.'Y') GO TO 5
C
C      C
C      C      REAL AND IMAGINARY PREPARATION
C      C
C      DO 10 I=1,NP
C          YAXIS1(I)=REAL(DATA(I+NSTART))
C          YAXIS2(I)=AIMAG(DATA(I+NSTART))
C          XAXIS(I)=(I-1+NSTART)*FINCR + FMIN
C
C      10     CONTINUE
C      GO TO 25
C
C      C
C      C      GENERATE AMPLITUDE AND PHASE
C      C
C      15     DO 20 I=1,NP
C          XAXIS(I)=(I+NSTART-1)*FINCR +FMIN

```

```
YAXIS1 (I)=CABS(DATA (I+NSTART))
IF (REAL (DATA (I+NSTART)).EQ.0.) GO TO 18
YAXIS2 (I)=ATAN2 (AIMAG (DATA (I+NSTART)),REAL (DATA (I+NSTART)))
GO TO 20
18 IF (AIMAG (DATA (I+NSTART)).EQ.0.) YAXIS2 (I)=0.
IF (AIMAG (DATA (I+NSTART)).LT.0.) YAXIS2 (I)=-PI/2
IF (AIMAG (DATA (I+NSTART)).GT.0.) YAXIS2 (I)=PI/2
20 CONTINUE
25 CALL PLTPKG (XAXIS,YAXIS1,9000,NP,1.0.1)
CALL PLTPKG (XAXIS,YAXIS2,9000,NP,1.0.1)
RETURN
END
```



```
C
C
C      FUNCTION:      SINC
C
C      THIS SUBROUTINE WILL CALCULATE SIN(X)/X
C      WHERE X IS ASSUMED TO BE IN RADIANS
C
C      FUNCTION SINC(X)
C      IF (X.EQ.0) GO TO 5
C      SINC=(SIN(X))/X
C      GO TO 10
5      SINC=1.
10     RETURN
      END
```

```

C
C PROGRAM :          FTGRID
C
C THIS PROGRAM WILL GENERATE ALL THE ANGLES AND FREQUENCIES
C FOR THE GRID IN THE FREQUENCY DOMAIN.  THE DATA ARE
C ARRANGED IN ORDER FROM SMALLEST ANGLE TO THE LARGEST ANGLE.
C (0 TO 2*PI) THE SMALLEST FREQUENCY
C RADIUS IS STORED.  SO AT THE TIME OF MEASUREMENT, ONLY
C MULTIPLICATION OF THE RADIUS IS NECESSARY.
C
C THE GRID POINTS ARE WRITE INTO FILE: 'OUT.DAT'
C THE DATA FORMAT OF 'OUT.DAT':
C FMIN.FMAX          :FREQUENCY RANGE SPECIFIED(2E15.8)
C FDELTA            :SAMPLING FREQUENCY(E15.8)
C NPOINT            :NUMBER OF POINTS IN THE FILE(18)
C ISO,RADIUS        :ISO=N, NON-ISOROPIC SAMPLING IS USED(A2)
C                   :ISO=T, ISOTROPIC SAMPLING IS USED
C                   :      RADIUS:RADIUS OF THE ISOTROPIC CELL IN MM(E15.8)
C V1.V2             :VECTORS USED TO DEFINE THE SAMPLING LATTICE(4E15.8)
C U1.U2             :VECTORS USED TO DEFINE THE PERIODIC LATTICE(4E15.8)
C DATA(*,1),DATA(*,2): DATA(4E15.8)
C DATA(*,1) IS THE MEASUREMENT ANGLE AND FREQUENCY ARRAY
C DATA(*,2) IS THE INDEX SPECIFYING HOW MANY UNITS OF
C V1.V2 ARE USED
C
C WARNING: SIZE OF DATA IS (10000,2)
C
C LINK FTGRID,GEN1,GEN2,SEARCH,INSERT,FUSH,NORMAL,'SSP
C
C COMPLEX V1.V2.V3.V4,U1,U2,DATA(10000,2)
C DIMENSION WORK1(2),WORK2(2)
C REAL MAG1,MAG2,MAX1,MARGIN,MATRIX(4)
C CHARACTER ISO
C MSIZE=10000
C PI=3.14159265
C
C START WORKING
C
C WRITE (6,*) ' LOWEST AND HIGHEST OPERATING FREQUENCY IN HERTZ '
C ACCEPT *, FMIN,FMAX
C IF (FMIN.GE.FMAX) GO TO 2
C WRITE (6,*) ' DO YOU WANT TO DO ISOTROPIC SAMPLING ? T/F '
C ACCEPT 4,ISO
C FORMAT (A1)
C IF (ISO.EQ.'F') GO TO 5
C IF (ISO.NE.'T') GO TO 3
C WRITE (6,*) ' DIAMETER OF NORMALIZATION IN MM?'
C ACCEPT *,RADIUS
C
C DEFINITION OF ISOTROPIC VECTORS
C
C

```

```

X1=(SORT(3.))/2.
Y1=-0.5
X2=0.
Y2=1.
GO TO 6

C
C
C
5
WRITE (6,*) 'THE OBJECT IS ASSUMED TO BE CONFINED TO A PARALLELOGRAM!'
WRITE (6,*) ' NORMALIZATION FACTOR IN MM'
ACCEPT *.RADIUS
WRITE (6,*) ' VECTOR1 IN X,Y :'
ACCEPT *, X1,Y1
WRITE (6,*) ' VECTOR2 IN X,Y :'
ACCEPT *, X2,Y2
6
WRITE (6,*) ' SAFETY MARGIN FACTOR ON THE TIME WAVEFORM'
ACCEPT *,MARGIN
U1=CMPLX(X1-Y1)
U2=CMPLX(X2-Y2)
MATRIX(1)=(X1)
MATRIX(2)=(Y1)
MATRIX(3)=(X2)
MATRIX(4)=(Y2)

C
C
C
MINV WILL DO MATRIX INVERSION. THIS SUBROUTINE IS IN SSP

CALL MINV(MATRIX,2,D,WORK1,WORK2)

C
C
C
NOTE THAT V1 AND V2 IS TAKEN FROM THE TRANSPOSE
OF THE INVERSE OF MATRIX. THIS IS TO BE CONSISTENCE WITH
DOT PRODUCT OF U(I) AND V(J) = DELTA(IJ)

C
C
C
U IS IN SPATIAL DOMAIN
V IS IN FREQUENCY DOMAIN
ALSO V1=(X-COMPONENT,Y-COMPONENT)

C
C
C
V1=CMPLX(MATRIX(1),MATRIX(3))
V2=CMPLX(MATRIX(2),MATRIX(4))
MAG1=CABS(V1)
PHASE1=ATAN2(AIMAG(V1),REAL(V1))
MAG2=CABS(V2)
PHASE2=ATAN2(AIMAG(V2),REAL(V2))
THETA=ABS(PHASE1-PHASE2)

C
C
C
PHASES ARE NORMALIZED TO THE RANGE 0:2*PI

CALL NORMAL(PHASE1)
CALL NORMAL(PHASE2)

C
C
C
SFACOR: FREQUENCY SAMPLING FACTOR

```

```

SFACTOR=(3.E11)/(RADIUS*MARGIN)
IF ((SFACTOR.LE.FMIN).OR.(FMIN.EQ.0.)) FDELTA=SFACTOR
IF ((SFACTOR.GT.FMIN).AND.(FMIN.NE.0.)) FDELTA=FMIN
RADIUS=1/(FDELTA*2.)
MAX1=(FMAX/FDELTA)

C
C STORE THE FIRST TWO VECTORS INTO THE ARRAY 'DATA'
C
IF (PHASE2.LT.PHASE1) GO TO 11
DATA(1.1)=CMPLX(PHASE1,MAG1)
DATA(1.2)=CMPLX(1.0)
DATA(2.1)=CMPLX(PHASE2,MAG2)
DATA(2.2)=CMPLX(0.1)
GO TO 12
11 DATA(1.1)=CMPLX(PHASE2,MAG2)
DATA(1.2)=CMPLX(0.1)
DATA(2.1)=CMPLX(PHASE1,MAG1)
DATA(2.2)=CMPLX(1.0)
12 NFOINT=2
C
C TO GENERATE THE FIRST QUADRANT POINTS
C POINTS ARE GENERATED AND STORED IN SUBROUTINE GEN1 AND GEN2
C
IF (THETA.LE.PI/2.)
& CALL GEN1(V1,V2,MAX1,MAX1,DATA,MSIZE,NFOINT,1,1)
IF (THETA.GT.PI/2.)
& CALL GEN2(V1,V2,MAX1,MAX1,DATA,MSIZE,NFOINT,1,1)
IF (NFOINT.GT.MSIZE) GO TO 888
V3=-V1
PHASE3 = ATAN2(AIMAG(V3),REAL(V3))
CALL NORMAL(PHASE3)
V3=CMPLX(PHASE3,CABS(V3))

C
C SEARCH FOR LOCATION :LOC TO PLACE THE POINT
C
LOC=SEARCH(V3,DATA,MSIZE,NFOINT)

C
C INSERT THE POINT INTO THE PROPER LOCATION
C
CALL INSERT(LOC,NFOINT,DATA,MSIZE,V3,-1.,0.)

C
C TO GENERATE THE 2ND QUADRANT POINTS
C
IF (THETA.LE.PI/2.)
& CALL GEN2(V1,V2,MAX1,MAX1,DATA,MSIZE,NFOINT,-1,1)
IF (THETA.GT.PI/2.)
& CALL GEN1(V1,V2,MAX1,MAX1,DATA,MSIZE,NFOINT,-1,1)
IF (NFOINT.GT.MSIZE) GO TO 888
V4=-V2
PHASE4 = ATAN2(AIMAG(V4),REAL(V4))
CALL NORMAL(PHASE4)

```

```

V4=CMPLX(PHASE4.CABS(V4))
LOC=SEARCH(V4,DATA,MSIZE,NFOINT)
CALL INSERT(LOC,NFOINT,DATA,MSIZE,V4.0.,-1.)
C
C
C   NOW TO GENERATE THE OTHER TWO QUADRANTS
      IF (THETA.LE.PI/2.)
&         CALL GEN2(V1.V2.MAX1,MAX1,DATA,MSIZE,NFOINT,1,-1)
      IF (THETA.GT.PI/2.)
&         CALL GEN1(V1.V2.MAX1,MAX1,DATA,MSIZE,NFOINT,1,-1)
      IF (NFOINT.GT.MSIZE) GO TO 888
      IF (THETA.LE.PI/2.)
&         CALL GEN1(V1.V2.MAX1,MAX1,DATA,MSIZE,NFOINT,-1,-1)
      IF (THETA.GT.PI/2.)
&         CALL GEN2(V1.V2.MAX1,MAX1,DATA,MSIZE,NFOINT,-1,-1)
      IF (NFOINT.GT.MSIZE) GO TO 888
C
C   OUTPUT GRID POINTS INTO FILE: 'OUT.DAT'
C
      OPEN(UNIT=8,NAME='OUT',TYPE='NEW')
      WRITE(8,301) FMIN,FMAX
301  FORMAT(2E15.8)
      WRITE(8,305) FDELTA
305  FORMAT(E15.8)
      WRITE(8,310) NFOINT
310  FORMAT(I8)
      WRITE(8,315), ISO,RADIUS
315  FORMAT(A2,E15.8)
      WRITE(8,320) V1,V2
320  FORMAT(2E15.8,2E15.8)
      WRITE(8,320) U1,U2
      DO 20 J=1,NFOINT
          WRITE(8,320) DATA(J,1),DATA(J,2)
20   CONTINUE
      CLOSE(UNIT=8,DISP='SAVE')
      GO TO 999
888  WRITE(6,*) 'ERROR:SPECIFIED ARRAY SIZE TOO SMALL!'
999  STOP
      END

```



```
10  & CONTINUE
5   CONTINUE
   RETURN
   END
```

```
CALL INSERT (LOC, M, DFILE, MSIZE, VECTOR, RJ, RI)
```



```

VECTOR=J*V1*N1SIGN +I*V2*N2SIGN
MAG=CABS(VECTOR)
C
C MAKE SURE THAT CHECK IS INCREMENTED PROPERLY
C
      IF ((NOT SAME).AND.((REAL(VECTOR)*AIMAG(VECTOR)).GT.0))
&          CHECK=CHECK + 1.
      IF ((SAME).AND.((REAL(VECTOR)*AIMAG(VECTOR)).LT.0))
&          CHECK=CHECK + 1
C
C MAKE SURE THE POINT GENERATED IS INSIDE THE CIRCLE
C
      IF (MAG.GT.AMAX) GO TO 5
C
C MAKE SURE THAT CHECK IS DECREMENTED PROPERLY
C
      IF ((NOT SAME).AND.((REAL(VECTOR)*AIMAG(VECTOR)).GT.0))
&          CHECK=CHECK - 1.
      IF ((SAME).AND.((REAL(VECTOR)*AIMAG(VECTOR)).LT.0))
&          CHECK=CHECK - 1.
      PHASE=ATAN2(AIMAG(VECTOR),REAL(VECTOR))
      CALL NORMAL(PHASE)
      VECTOR=CMPLX(PHASE,MAG)
      LOC=SEARCH(VECTOR,DFILE,MSIZE,M)
      RJ=FLOAT(J)
      RI=FLOAT(I)
      IF ((N1SIGN.LT.0).AND.(N2SIGN.LT.0))
&          CALL INSERT(LOC,M,DFILE,MSIZE,VECTOR,-RJ,-RI)
      IF ((N1SIGN.LT.0).AND.(N2SIGN.GT.0))
&          CALL INSERT(LOC,M,DFILE,MSIZE,VECTOR,-RJ,RI)
      IF ((N1SIGN.GT.0).AND.(N2SIGN.LT.0))
&          CALL INSERT(LOC,M,DFILE,MSIZE,VECTOR,RJ,-RI)
      IF ((N1SIGN.GT.0).AND.(N2SIGN.GT.0))
&          CALL INSERT(LOC,M,DFILE,MSIZE,VECTOR,RJ,RI)
10      CONTINUE
5      CONTINUE
50     I1=J-2
      DO 15 I=I2.N2
          DO 20 J=I1.N1
              VECTOR=J*V1*N1SIGN +I*V2*N2SIGN
              MAG=CABS(VECTOR)
              IF (MAG.GT.AMAX) GO TO 15
              PHASE=ATAN2(AIMAG(VECTOR),REAL(VECTOR))
              CALL NORMAL(PHASE)
              VECTOR=CMPLX(PHASE,MAG)
              LOC=SEARCH(VECTOR,DFILE,MSIZE,M)
              RJ=FLOAT(J)
              RI=FLOAT(I)
              IF ((N1SIGN.LT.0).AND.(N2SIGN.LT.0))
&                  CALL INSERT(LOC,M,DFILE,MSIZE,VECTOR,-RJ,-RI)
              IF ((N1SIGN.LT.0).AND.(N2SIGN.GT.0))

```

```

&          CALL INSERT (LOC, M, DFILE, MSIZE, VECTOR, -RJ, RI)
&          IF ((NLSIGN.GT.0).AND.(NZSIGN.LT.0))
&          CALL INSERT (LOC, M, DFILE, MSIZE, VECTOR, RJ, -RI)
&          IF ((NLSIGN.GT.0).AND.(NZSIGN.GT.0))
&          CALL INSERT (LOC, M, DFILE, MSIZE, VECTOR, RJ, RI)
20          CONTINUE
15          CONTINUE
555         RETURN
          END

```



```

C
C
C
C
C
C
C
SUBROUTINE:   PUSH
THIS SUBROUTINE WILL PUSH ALL THE DATA IN 'DFILE' BY 1 POSITION
THE OPERATION IS SPECIFIED BY NSTART1 -THE BEGINNING OF PUSH
                                LAST1  -THE LAST LOCATION OF DFILE

SUBROUTINE PUSH(NSTART1, LAST1, DFILE, MSIZE)
COMPLEX DFILE(MSIZE, 2), TEMP1, TEMP2
N=LAST1- NSTART1 +1
DO 5 I=1, N
    TEMP1=DFILE(LAST1+1-I, 1)
    TEMP2=DFILE(LAST1+1-I, 2)
    DFILE(LAST1+2-I, 1)=TEMP1
    DFILE(LAST1+2-I, 2)=TEMP2
5  CONTINUE
LAST1 = LAST1 +1
RETURN
END

```

C
C
C
C
C
C
C
C

SUBROUTINE: NORMAL

THIS SUBROUTINE WILL NORMALIZE A PHASE RANGE OF (-PI TO PI)
TO A RANGE OF (0 TO 2*PI).

ALPHA: ANGLE IN RADIAN TO BE NORMALIZED

SUBROUTINE NORMAL (ALPHA)

PI=3.14159265

IF (ALPHA.LT.0) ALPHA=ALPHA + 2.*PI

RETURN

END

```

C
C PROGRAM: INTERPOL
C
C THIS PROGRAM WILL INTERPOLATE FOR 3 OPTIONS.
C FILE FNAME STORED THE GRID POINT INFORMATION GENERATED PREVIOUSLY.
C THIS PROGRAM WILL REPEAT ITSELF, EXIT ONLY BY CONTROL C
C THIS PROGRAM LINKS WITH 'PLOT.LIB'
C
C THIS PROGRAM REQUIRES AN INPUT OF A MEASUREMENT FILE :FNAME
C THE STRUCTURE OF FNAME:
C FMIN.FMAX -MAXIMUM AND MINIMUM FREQUENCY USED IN HZ (2E15.8)
C FDELTA -NORMALIZATION FACTOR IN FREQUENCY (1E15.8)
C NPOINT -NUMBER OF POINTS IN THIS FILE (I8)
C ISO,RADIUS-ISO='T' IF ISOTROPIC SAMPLING WAS DONE (A2)
C -ISO='F' IF ISOTROPIC SAMPLING WAS NOT DONE
C -RADIUS IS THE ISOTROPIC CIRCLE RADIUS USED IN SECOND (E15.8)
C V1,V2 -VECTOR1 AND VECTOR2 IN FREQUENCY DOMAIN (4E15.8)
C U1,U2 -VECTOR1 AND VECTOR2 IN TIME/SPACE DOMAIN (4E15.8)
C *,*,*,-REAL AND IMAG MEASUREMENT;N1,N2 FOR THE MEASUREMENT (4E15.8)
C (MAKE SURE ALL THE ABOVE ARGUMENTS ARE SEPARATED BY COMMAS IN FNAME!)
C
C N1*V1.N2*V2 SPECIFIES THE SAMPLING LATTICE
C
C LINK INTERPOL,WFILE,SUM,CONST1,CONST2,FUNCI,FUNC2,FUNC3,SINC,-
C RPL0T,ELIM,'PLOT.LIB'
C
C COMPLEX SUM,DATA(360),V1.V2.U1.U2.FREQD,COEFF(10000.2),TEMP1
C CHARACTER ISO
C CHARACTER*10 FNAME
C MSIZE=10000
C
C NDATA :SPECIFIES THE NUMBER OF ANGULAR POINTS
C NUM :SPECIFIES THE NUMBER OF FREQUENCY POINTS
C
C NDATA=360
C NUM=201
C PI=3.14159265
C WRITE(6,*) ' FILE WHICH HAS GRID POINT MEASUREMENT?'
C ACCEPT 50, FNAME
C 50 FORMAT (A10)
C OPEN(UNIT=9,NAME=FNAME,TYPE='OLD')
C
C READ IN NECESSARY DATA
C
C READ(9,550) FMIN.FMAX
C 550 FORMAT (2E15.8)
C READ(9,551) FDELTA
C 551 FORMAT (E15.8)
C READ(9,552) NPOINT
C 552 FORMAT (I8)
C IF (NPOINT.GT.MSIZE) GO TO 8888

```

```

553 READ(9,553) ISO,RADIUS
    FORMAT(A2,E15.8)
554 READ(9,554) V1,V2
    FORMAT(2E15.8,2E15.8)
    READ(9,554) U1,U2
    V1=2.*PI*FDELTA*V1
    V2=2.*PI*FDELTA*V2
    U1=U1/(FDELTA)
    U2=U2/(FDELTA)

C
C OPTIONS TO GUARD AGAINST MEASUREMENT DATA IN FORMAT
C OTHER THAN REAL AND IMAGINARY
C
570 WRITE(6,*) 'DATA IN WHICH FORMAT:1) REAL AND IMAG'
    WRITE(6,*) '          2) AMP(LINEAR) AND PHASE(RADIAN)'
    WRITE(6,*) '          3) AMP(DB) AND PHASE(RADIAN)'
    WRITE(6,*) '          4) AMP(DB) AND PHASE(DEGREE)'
    ACCEPT *,NCOM1
    IF ((NCOM1.GT.4).OR.(NCOM1.LT.1)) GO TO 570
    DO 560 I=1,NPOINT
        READ(9,554) XREAL,XIMAG,COEFF(I,2)
        IF(NCOM1.EQ.1) GO TO 580
        AMP=XREAL
        PHASE=XIMAG
        IF((NCOM1.EQ.3).OR.(NCOM1.EQ.4)) AMP=10**(AMP/20)
        IF(NCOM1.EQ.4) PHASE=PHASE*PI/180.
        XREAL=AMP*COS(PHASE)
        XIMAG=AMP*SIN(PHASE)
580 COEFF(I,1)=CMPLX(XREAL,XIMAG)
560 CONTINUE
    CLOSE(UNIT=9,DISP='SAVE')

C
C ASK FOR THE TYPE OF INTERPOLATION
C
5 WRITE(6,*) ' 3 CHOICES :1) INTERPOLATE FOR 1 ASPECT ANGLE AND OUTPUT'
    WRITE(6,*) '          201 FREQUENCY POINTS.'
    WRITE(6,*) '          2) INTERPOLATE FOR 1 FREQUENCY AND OUTPUT '
    WRITE(6,*) '          360 DEGREE POINTS.'
    WRITE(6,*) '          3) INTERPOLATE INTO 2-D SQUARE GRID'
    ACCEPT *, NCOM

C
C THE BRANCHING OF DECISION
C
    IF (NCOM.EQ.2) GO TO 200
    IF (NCOM.EQ.3) GO TO 300
    IF (NCOM.NE.1) GO TO 5

C
C TO INTERPOLATE FOR 1 ASPECT ANGLE BUT 201 FREQUENCY POINTS
C
10 WRITE(6,*) 'FREQUENCY RANGE? LOW TO HIGH IN HZ'
    ACCEPT *, FMIN,FMAXS

```

```

IF (FMINS.GE.FMAXS) GO TO 10
WRITE(6,*) ' WHICH ASPECT ANGLE?(degree) '
ACCEPT *, ANGLE
ANGLE=ANGLE*PI/180.
FINCR=(FMAXS-FMINS)/(NUM-1)
DO 15 I=1,NUM
  WRITE(6,*) 'WORKING ON: ',I,' LAST ONE: ',NUM
  AFREQ=FMINS + FINCR*(I-1)
  IF (AFREQ.EQ.0.) GO TO 13
C
C
C
C
  MAKE SURE THE INTERPOLATION IS DONE BETWEEN THE MEASURED FREQUENCY
  RANGE
  IF (((AFREQ).GT.FMAX).OR.((AFREQ).LT.FMIN)) GO TO 13
  FREQ=OMPLX(AFREQ*COS(ANGLE),AFREQ*SIN(ANGLE))
  DATA(I)= SUM(FREQ,COEFF,MSIZE,V1,V2,U1,U2.ISO,NFOINT,RADIUS)
  GO TO 15
13  DATA(I)=(0.,0.)
15  CONTINUE
C
C
C
C
  PLOT AND WRITE FILE
  CALL PLOT(DATA,NUM,FMINS,FINCR)
  CALL WFILE(DATA,NDATA,NUM)
  GO TO 5
C
C
C
C
  SECOND SECTION OF THE PROGRAM
  TO INTERPOLATE FOR 1 FREQUENCY, BUT 360 DEGREE POINTS
200 WRITE(6,*) 'WHICH FREQUENCY?(HZ) '
  ACCEPT *, AFREQ
  DO 205 I=1,NDATA
    WRITE(6,*) 'WORKING ON: ',I,' LAST ONE: ',NDATA
    ANGLE=(I-1)*PI/180.
    IF (AFREQ.EQ.0.) GO TO 203
C
C
C
C
    MAKE SURE THE INTERPOLATION IS DONE BETWEEN THE MEASURED FREQUENCY
    RANGE
    IF (((AFREQ).GT.FMAX).OR.((AFREQ).LT.FMIN)) GO TO 203
    FREQ=OMPLX(AFREQ*COS(ANGLE),AFREQ*SIN(ANGLE))
    DATA(I)= SUM(FREQ,COEFF,MSIZE,V1,V2,U1,U2.ISO,NFOINT,RADIUS)
    GO TO 205
203  DATA(I)=(0.,0.)
205  CONTINUE
C
C
C
C
  PLOT AND WRITE THE FILE
  POLARP :A SUBROUTINE IN 'PLOTLIB
C
  CALL POLARP(DATA,3.5.3.1,NDATA,1,1)
  CALL WFILE(DATA,NDATA,NDATA)

```

```
GO TO 5
C
C   THIRD PART OF THE PROGRAM
C   TO INTERPOLATE INTO A 2-D SQUARE GRID
C   (DUE TO TIME CONSUMPTION, THIS IS NOT IMPLEMENTED.  BUT IT CAN
C   BE DONE SIMILARLY AS PART 1 AND 2)
C
300 WRITE(6,*) 'NOT READY YET!'
GO TO 5
8888 WRITE(6,*) 'ERROR:THE SIZE OF INPUT FILE IS LARGER THAN SPECIFIED!'
GO TO 5
END
```



```
          AB(J,1)=((AB(J,2))**2.)
800  CONTINUE
      CALL ELIM(AB,3,4,3)
      CONST1=(FUNC3(AB(1,4),AB(2,4),AB(3,4),W2*R))
      GO TO 1000
888  CONST1=FUNC2(R,W2)
      GO TO 1000
999  CONST1=FUNC1(R,W1,W2)
1000 RETURN
      END
```

C
C
C
C
C

FUNCTION: FUNC1

THIS IS THE RECONSTRUCTION FUNCTION WHEN THE DENOMINATOR IS
NOT ZERO.

```
FUNCTION FUNC1 (R,W1,W2)
C=SQRT(3.)
D1=(W1-C*W2)*R
D2=(W1+C*W2)*R
X1=(COS(R*W1/C))*COS(R*W2)
X2=-COS(2.*R*W1/C)
X3=(W2*R)*(SINC(R*W1/C))*(SIN(R*W2))
FUNC1=2.*(X1+X2+X3)/(D1*D2)
RETURN
END
```

C
C
C
C
C

FUNCTION: FUNC2

THIS IS THE RECONSTRUCTION FUNCTION WHEN $w_1^{**2} - 3*w_2^{**2} = 0$

FUNCTION FUNC2 (R, W2)
C1=(2./3.)*SINC(2.*R*W2)
C2=(1./3.)*(SINC(R*W2))**2.
FUNC2=C1+C2
RETURN
END

```
C
C   FUNCTION:      FUNC3
C
C   THIS FUNCTION WILL PRODUCE THE LINEAR INTERPOLATION PORTION
C   OF THE RECONSTRUCTION FUNCTION
C   WHEN THE UNDERFLOW PROBLEM OCCURS
C
C   FUNCTION FUNC3 (A, B, C, W2)
C   X1=A*(W2**2)
C   X2=B*W2
C   FUNC3=X1+X2+C
C   RETURN
C   END
```



```

C
C SUBROUTINE :ELIM
C
C THIS SUBROUTINE IS COURTESY OF MR. BING KWAN[16]
C
C SUBROUTINE ELIM(AB,N,NP,NDIM)
C DIMENSION AB(NDIM,NP)
C THIS SUBROUTINE SOLVES A SET OF LINEAR EQUATIONS.
C THE GAUSS ELIMINATION METHOD IS USED, WITH PARTIAL PIVOTING.
C MULTIPLE RIGHT HAND SIDES ARE PERMITTED, THEY SHOULD BE SUPPLIED
C AS COLUMNS THAT AUGMENT THE COEFFICIENT MATRIX.
C PARAMETERS ARE:
C AB COEFFICIENT MATRIX AUGMENTED WITH R.H.S. VECTORS.
C N NO. OF EQUATIONS
C NP TOTAL NO. OF COLUMNS IN AB
C NDIM NO. OF ROWS IN AB
C
C BEGINS THE REDUCTION
C NM1=N-1
C DO 35 I=1,NM1
C FIND THE ROW NUMBER OF THE PIVOT ROW. WE WILL THEN
C INTERCHANGE ROWS TO THE PIVOT ELEMENT ON THE DIAGONAL.
C IPVT=I
C IP1=I+1
C DO 10 J=IP1,N
C IF(ABS(AB(IPVT,I)).LT.ABS(AB(J,I))) IPVT=J
10 CONTINUE
C CHECK TO BE SURE THE PIVOT ELEMENT IS NOT TOO SMALL, IF SO
C PRINT A MESSAGE AND RETURN.
C IF(ABS(AB(IPVT,I)).LT.1.E-5) GO TO 99
C NOW INTERCHANGE , EXCEPT IF THE PIVOT ELEMENT IS ALREADY ON
C THE DIAGONAL, DO NOT NEED TO.
C IF(IPVT.EQ.I) GO TO 25
C DO 20 JCOL=I,NP
C SAVE=AB(I,JCOL)
C AB(I,JCOL)=AB(IPVT,JCOL)
C AB(IPVT,JCOL)=SAVE
20 CONTINUE
C NOW REDUCE ALL ELEMENTS BELOW THE DIAGONAL IN THE I-TH ROW.
C CHECK FIRST TO SEE IF ZERO ALREADY PRESENT. IF SO
C CAN SKIP REDUCTION FOR THAT ROW.
25 DO 32 JROW=IP1,N
C IF(AB(JROW,I).EQ.0.0) GO TO 32
C RATIO=AB(JROW,I)/AB(I,I)
C DO 30 KCOL=IP1,NP
C AB(JROW,KCOL)=AB(JROW,KCOL)-RATIO*AB(I,KCOL)
30 CONTINUE
32 CONTINUE
35 CONTINUE
C WE STILL NEED TO CHECK A(N,N) FOR SIZE.
C IF(ABS(AB(N,N)).LT.1.E-5) GO TO 99

```

```

C NOW WE BACK SUBSTITUTE.
  NP1=N+1
  DO 50 KCOL=NP1,NP
    AB(N,KCOL)=AB(N,KCOL)/AB(N,N)
    DO 45 J=2,N
      NVBL=NP1-J
      L=NVBL+1
      VALUE=AB(NVBL,KCOL)
      DO 40 K=L,N
        VALUE=VALUE-AB(NVBL,K)*AB(K,KCOL)
40      CONTINUE
      AB(NVBL,KCOL)=VALUE/AB(NVBL,NVBL)
45      CONTINUE
50      CONTINUE
      RETURN
C MESSAGE FOR A NEAR SINGULAR MATRIX.
99  WRITE(66,100)
100 FORMAT(/,'SOLUTION NOT POSSIBLE. A NEAR 0 PIVOT ENCOUNTERED.')
```

```

C
C   SUBROUTINE:   WFILE
C
C   THIS SUBROUTINE WILL WRITE A COMPLEX 'DATA' ARRAY OF SIZE
C   'MSIZE' INTO A FILE 'FNAME1'. THE NUMBER OF NON ZERO
C   ELEMENT IS SPECIFIED BY 'NUM'.
C
SUBROUTINE WFILE(DATA,MSIZE,NUM)
COMPLEX DATA(MSIZE)
CHARACTER*10 FNAME1
CHARACTER WRI
10  WRITE (6,*) 'DO YOU WANT TO WRITE INTO A FILE?Y/N'
ACCEPT 9010, WRI
IF (WRI.EQ.'N') GO TO 9999
IF (WRI.NE.'Y') GO TO 10
WRITE(6,*) 'STORAGE FILE NAME:'
ACCEPT 9020,FNAME1
OPEN(UNIT=8,NAME=FNAME1,TYPE='NEW')
DO 30 I=1,NUM
WRITE(8,*) DATA(I)
30  CONTINUE
CLOSE(UNIT=8,DISP='SAVE')
9010 FORMAT(A1)
9020 FORMAT(A10)
9999 RETURN
END

```



```

IF (MSIZE.GT.NP1) GO TO 998
IF (MSIZE.GT.NPL) GO TO 110
120 WRITE(6,*) 'IS THIS ONE QUADRANT DATA?Y/N'
ACCEPT 9020,ONE
IF (ONE.EQ.'N') GO TO 110
IF (ONE.NE.'Y') GO TO 120
130 WRITE(6,*) 'COMPLEX CONJUGATE IN 2ND AND 3RD QUADRANTS?Y/N'
ACCEPT 9020,ODD
IF ((ODD.NE.'Y').AND.(ODD.NE.'N')) GO TO 130
C
C TO GUARD AGAINST POSSIBILITY OF MEASUREMENT IN OTHER FORMAT
C
110 WRITE(6,*) 'FORMAT OF DATA: 1)REAL AND IMAGINARY'
WRITE(6,*) ' 2)AMP(LINEAR) AND PHASE(RADIAN) '
WRITE(6,*) ' 3)AMP(LINEAR) AND PHASE(DEGREE) '
WRITE(6,*) ' 4)AMP(DB) AND PHASE(RADIAN) '
WRITE(6,*) ' 5)AMP(DB) AND PHASE(DEGREE) '
ACCEPT *,NFORM
IF((NFORM.GT.5).OR.(NFORM.LT.1)) GO TO 110
WRITE(6,*) 'STORAGE FILE NAME:'
ACCEPT 9000,FNAME2
WRITE(6,*) 'NAME OF THE RECTANGULAR TO POLAR FILE:'
ACCEPT 9000,FNAME3
C
C INITIALIZATION
C
DO 10 I=1,NP1
DATA1(I)=(0.,0.)
10 CONTINUE
C
C READ IN MEASUREMENT DATA
C
OPEN(UNIT=8,NAME=FNAME1,TYPE='OLD')
DO 60 I=1,MSIZE
READ(8,9030) DUMMY
CALL APTORI(DUMMY,NFORM)
DATA1(I)=DUMMY
60 CONTINUE
CLOSE(UNIT=8,DISP='SAVE')
C
C EXPAND TO FILL THE HALF OF THE SPAN OF THE FFT REPETITIVE UNIT
C
IF (MSIZE.LE.NPL)CALL EXPAND(DATA1,DATA2,NP1,MSIZE,NPL)
IF (MSIZE.GT.NPL)CALL EXPAND(DATA1,DATA2,NP1,MSIZE,NP1)
IF (MSIZE.GT.NPL) GO TO 170
C
C CASE OF FULL PLANE DATA INFUT
C
IF (ONE.EQ.'N') CALL EXPAND(DATA1,DATA2,NP1,NPL,NP1)
IF (ONE.EQ.'N') GO TO 170
C

```

```

C   FILL IN THE OTHER HALF OF THE SPAN BY COMPLEX CONJUGATE OR
C   THE SAME
C
MSIZE=NPL
DO 160 I=1,MSIZE-2
    IF (ODD.EQ.'N') DATAL(I+MSIZE)=DATAL(MSIZE-I)
    IF (ODD.EQ.'Y') DATAL(I+MSIZE)=CONJG(DATAL(MSIZE-I))
160 CONTINUE
MSIZE=2*MSIZE-2
DO 165 I=1,MSIZE
    IF (ODD.EQ.'N') DATAL(I+MSIZE)=DATAL(I)
    IF (ODD.EQ.'Y') DATAL(I+MSIZE)=CONJG(DATAL(I))
165 CONTINUE
MSIZE=MSIZE*2
IF (MSIZE.GT.NPL) GO TO 998
170 MSIZE=NPL
C
C   DELTA   :SIZE OF EACH ANGLE INCREMENT
C
DELTA=2.*PI/MSIZE
OPEN(UNIT=8,NAME=FNAME3,TYPE='OLD')
READ(8,*) NPOINT
IF (NPOINT.GT.NPOLAR) GO TO 998
C
C   READ THE RECTANGULAR TO POLAR COORDINATE CONVERSION FILE
C
DO 100 I=1,NPOINT
    READ(8,9005) POLAR(I),RECT(I)
100 CONTINUE
CLOSE(UNIT=8,DISP='SAVE')
CALL FORT(DATAL,M,S,I,IFERR)
C
C   THE VALUE OF AMP1 =-1 IS ONLY A DUMMY TO START THE ROUTINE
C
AMP1=-1.
DO 200 J=1,NPOINT
    WRITE(6,*) 'WORKING ON:'.J,' LAST ONE:'.NPOINT
    IF (REAL(POLAR(J)).EQ.AMP1) GO TO 50
    AMP1=POLAR(J)
    DO 17 I=1,NPL
        DATA2(I)=(0.,0.)
17    CONTINUE
    DO 20 I=1,MSIZE
        THETA=(I-1)*DELTA
        PHI=2.*PI*(REAL(POLAR(J)))*TIME*FREQ*COS(THETA)
C
C   FUNC1: EXP(JWT)
C   THEREFORE, XREAL=COS(PHI)
C   YIMAG=SIN(PHI)
C
XREAL=COS(PHI)

```

```

                YIMAG=SIN(PHI)
                DATA2(I)=CMPLX(XREAL, YIMAG)
20          CONTINUE
C
C          GO TO FREQUENCY DOMAIN
C
C          CALL FORT(DATA2.M,S,2.IFERR)
C
C          CONVOLUTION IN TIME <=> MULTIPLICATION IN FREQUENCY
C
C          DO 25 I=1,NP1
                DATA2(I)=DATA1(I)*DATA2(I)
25          CONTINUE
C
C          GO BACK TO TIME DOMAIN
C
C          CALL FORT(DATA2.M,S,-2.IFERR)
C
C          NOW POLAR(J) IS THE INTEGRAL VALUE OF 2D FOURIER TRANSFORM
C          WITH IMPULSIVE RADIUS VALUE (MENSEA'S INTEGRAL)
C
50          ANGLE=AIMAG(POLAR(J))
                POLAR(J)=PICK(DATA2.NP1,0.,DELTA,ANGLE)
                POLAR(J)=(POLAR(J)/FLOAT(MSIZE))*FREQ*XNOR
200         CONTINUE
C
C          WRITE OUT THE FILE
C          FILE FORMAT:
C          NPOINT:NUMBER OF POINTS(I10)
C          REAL,IMAGINARY,X-COORDINATE,Y-COORDINATE (4E15.8)
C
                OPEN(UNIT=9,NAME=FNAME2.TYPE='NEW')
                WRITE(9,9010) NPOINT
                DO 300 I=1,NPOINT
                    WRITE(9,9005) POLAR(I),RECT(I)
300         CONTINUE
                CLOSE(UNIT=9,DISP='SAVE')
                GO TO 999
998         WRITE(6,*) 'ERROR: SIZE OF FILE TOO LARGE!'
C
C          FORMAT STATEMENTS
C
9000        FORMAT(A10)
9005        FORMAT(4E15.8)
9010        FORMAT(I10)
9020        FORMAT(A1)
9030        FORMAT(2E15.8)
C
999         STOP
                END

```

```

C
C
C
C
C
C
C
C
C
C
SUBROUTINE:    EXPAND
THIS SUBROUTINE WILL EXPAND AN ARRAY DATA(MSIZE) CONTAINING 'NFILL'
DATA ELEMENTS INTO 'NEXP' DATA ELEMENT USING LINEAR INTERPOLATION
2<NFILL<NEXP
WORK: A DUMMY ARRAY FOR TEMPORARY STORAGE
SUBROUTINE EXPAND(DATA,WORK,MSIZE,NFILL,NEXP)
COMPLEX DATA(MSIZE),WORK(MSIZE),DIFF
ERROR=1E-6
DELTA1=1./FLOAT(NFILL-1)
DELTA2=1./FLOAT(NEXP-1)
DO 10 I=1,NFILL
    WORK(I)=DATA(I)
10 CONTINUE
DATA(1)=WORK(1)
DATA(NEXP)=WORK(NFILL)
DO 20 I=1,NEXP-2
    X=(I)*DELTA2
    N=INT(X/DELTA1)+1
    REMAIN=AMOD(X,DELTA1)
    RATIO=(X-DELTA1*FLOAT(N-1))/DELTA1
    DIFF=(WORK(N+1)-WORK(N))*RATIO
    DATA(I+1)=WORK(N)+DIFF
20 CONTINUE
RETURN
END

```


C
C
C
C
C
C
C
C
C
C

SUBROUTINE: APTORI

THIS SUBROUTINE WILL CONVERT AMPLITUDE AND PHASE (VALUE) INTO
REAL AND IMAGINARY (VALUE).

BY SPECIFYING N

N=1:VALUE IS ALREADY IN REAL AND IMAGINARY FORM

N=2:AMPLITUDE (LINEAR), PHASE (RADIAN)

N=3:AMPLITUDE (LINEAR), PHASE (DEGREE)

N=4:AMPLITUDE (DB), PHASE (RADIAN)

N=5:AMPLITUDE (DB), PHASE (DEGREE)

SUBROUTINE APTORI (VALUE,N)

COMPLEX VALUE

IF (N.EQ.1) GO TO 999

PI=3.14159265

AMP=REAL (VALUE)

PHASE=AIMAG (VALUE)

IF ((N.EQ.4).OR.(N.EQ.5)) AMP=10.0**(AMP/20.)

IF ((N.EQ.3).OR.(N.EQ.5)) PHASE=PHASE*PI/180.

VALUE=CMPLX (AMP*COS (PHASE),AMP*SIN (PHASE))

999 RETURN

END

```

C
C PROGRAM : RECTPOLAR
C
C THIS PROGRAM WILL CHANGE RECTANGULAR COORDINATES TO
C POLAR COORDINATES. THE FILE 'FNAME' OUTPUTS IN THE
C FOLLOWING FORMAT:
C RADIUS, PHI (RADIAN), X, Y (4E15.8)
C THE FILE WILL ALSO BE ORGANIZED FROM SMALLEST RADIUS
C TO THE LARGEST RADIUS.
C NOTE THE MAXIMUM X COORDINATE VALUE: 'MAX' WILL GIVE
C (MAX*2)**2 +2*2*MAX +1 DATA POINTS
C THEREFORE A GRID OF 256X256 CAN ACCOMMODATE MAX=127
C
C LINK RECTPOLAR, GEN. SEARCH1, INSERT1, PUSH, NORMAL
C
C COMPLEX DATA(65536.2)
C CHARACTER*10 FNAME
C WRITE(6,*) 'FILE NAME FOR STORAGE OF RESULTS:'
C ACCEPT 5,FNAME
5 FORMAT(A10)
C WRITE(6,*) 'MAXIMUM X COORDINATE VALUES:'
C ACCEPT *,MAX
C MSIZE=65536
C PI=3.14159265
C M=0
C M=M+1
C DATA(M,1)=CMPLX(0.,0.)
C DATA(M,2)=CMPLX(0.,0.)
C
C THIS DO LOOP GENERATES ALL THE AXIS POINTS
C
C DO 10 J=1,MAX
C X1=FLOAT(J)
C M=M+1
C DATA(M,1)=CMPLX(X1,0.)
C DATA(M,2)=CMPLX(X1,0.)
C M=M+1
C DATA(M,1)=CMPLX(X1,PI/2)
C DATA(M,2)=CMPLX(0.,X1)
C M=M+1
C DATA(M,1)=CMPLX(X1,PI)
C DATA(M,2)=CMPLX(-X1,0.)
C M=M+1
C DATA(M,1)=CMPLX(X1,3.*PI/2.)
C DATA(M,2)=CMPLX(0.,-X1)
10 CONTINUE
C WRITE(6,*) 'CALCULATING FIRST QUADRANT POINTS!'
C CALL GEN(MAX,DATA,MSIZE,M,1,1)
C WRITE(6,*) 'CALCULATING SECOND QUADRANT POINTS!'
C CALL GEN(MAX,DATA,MSIZE,M,-1,1)
C WRITE(6,*) 'CALCULATING THIRD QUADRANT POINTS!'

```

```
CALL GEN(MAX,DATA,MSIZE,M,-1,-1)
WRITE(6,*) 'CALCULATING FOURTH QUADRANT POINTS!'
CALL GEN(MAX,DATA,MSIZE,M,1,-1)
OPEN (UNIT=8,NAME=FNAME,TYPE='NEW')
WRITE(8,*) M
DO 20 I=1,M
    WRITE(8,1000) DATA(I,1),DATA(I,2)
20  CONTINUE
1000 FORMAT(4E15.8)
STOP
END
```



```

C
C PROGRAM:          SUM3D
C
C THIS PROGRAM CAN DO THE FOLLOWING:
C   1) READ A DATA FILE
C   2) SUMMING OF DATA FILES
C   3) PLOT A DATA FILE IN A) 3-D PICTURE PLOT
C                                     B) CONTOUR PLOT
C   4) 2-D FOURIER TRANSFORM
C   5) MODIFIES FREQUENCY DATA BY A) 1/JW
C                                     B) -1/W**2
C   6) COSINE TAPERING LOW PASS THE FREQUENCY DATA
C   7) HIGH PASS THE FREQUENCY DATA
C   8) WRITE OUT THE FILE
C
C THE INPUT (OR OUTPUT) FILE FORMAT:
C   NPOINT:NUMBER OF POINTS IN THE FILE(I10)
C   DATA,X-COORDINATE,Y-COORDINATE(4E15.8)
C
C THE CONTOUR PLOT LINKS WITH NCAR PLOTTING PACKAGES
C THE LINKING REQUIRED IS:
C $CASSIGN DRA2:[NCAR2.NCARPLOT.PLOTLIB] NCAR_PLOT_LIB
C $ASSIGN DRA2:[NCAR2.NCARLIB] NCAR_LIB
C $ASSIGN DRA2:[NCAR2.NCARPLOT] NCAR_PLOT
C $ASSIGN DRA2:[NCAR2.NCARPLOT.CHROME] NCAR_PLOT_CHROME
C $ASSIGN DRA2:[NCAR2.NCARPLOT.TEST] NCAR_PLOT_TEST
C $ASSIGN DRA2:[NCAR2.NCARPLOT.DOC] NCAR_PLOT_DOC
C $ASSIGN DRA2:[NCAR2.NCARPLOT.TRANS] NCAR_PLOT_TRANS
C $LINK SSUM3D,DPL0T,TRAN2D,WEIGHT,PLOT3D,APTORI,'SSP','PLOTLIB,-
C DRA2:[NCAR2.NCARPLOT.PLOTLIB]NCARCONRE/LIB,NCARDASHC/LIB,-
C NCARGRAPP/LIB,NCARGRAPH/LIB,[NCAR2.NCARLIB]UTILITY/LIB
C
C COMPLEX DATA(31,31),DUMMY,APTORI,CJ
C DIMENSION ARRAY1(31,31),ARRAY2(31,31),ARRAYP(31,31)
C CHARACTER*10 FNAME1,FNAME2
C CHARACTER ADD.OMEGA,SPACE,LP,HP
C N1=5
C MSIZE=2*N1-1
C PI=3.14159265
C CJ=OMPLX(0.1)
C K=MSIZE/2+1
C
C INITIALIZATION
C
C DO 5 I=1,MSIZE
C   DO 6 J=1,MSIZE
C     DATA(I,J)=(0.,0.)
C   CONTINUE
C CONTINUE
C WRITE(6,*) 'DATA FILE NAME:'
C ACCEPT 9000,FNAME1

```

```

110 WRITE(6,*) 'WHAT IS THE DATA FORMAT:  1) REAL AND IMAG'
    WRITE(6,*) '                               2) AMP(LINEAR) AND PHASE(RADIAN)'
    WRITE(6,*) '                               3) AMP(LINEAR) AND PHASE(DEGREE)'
    WRITE(6,*) '                               4) AMP(DB)      AND PHASE(RADIAN)'
    WRITE(6,*) '                               5) AMP(DB)      AND PHASE(DEGREE)'
    ACCEPT *,NCOM
    IF ((NCOM.GT.5).OR.(NCOM.LT.1)) GO TO 110

C
C   READ IN THE DATA
C
    OPEN(UNIT=10,NAME=FNAME1,TYPE='OLD')
    READ(10,9010) NPOINT
    DO 10 I=1,NPOINT
        READ(10,9020) DUMMY,X1,Y1
        CALL APTORI(DUMMY,NCOM)
        M=INT(X1) +K
        N=INT(Y1) +K
        DATA(M,N) = DATA(M,N) +DUMMY
10   CONTINUE
    CLOSE(UNIT=10,DISP='SAVE')

C
C   PLOT
C
    CALL DPLOT(DATA,MSIZE,ARRAY1,ARRAY2,ARRAYP)

C
C   ADD ANOTHER FILE
C
20   WRITE(6,*) ' ADD ANOTHER FILE?  Y/N'
    ACCEPT 9030, ADD
    IF (ADD.EQ.'Y') GO TO 8
    IF (ADD.NE.'N') GO TO 20

C
C   WRITE INVID A FILE
C
25   WRITE(6,*) ' WRITE YOUR DATA INVID A FILE?  Y/N'
    ACCEPT 9030,KEEP
    IF (KEEP.EQ.'N') GO TO 30
    IF (KEEP.NE.'Y') GO TO 25
    WRITE(6,*) 'FILE NAME:'
    ACCEPT 9000,FNAME2
    OPEN(UNIT=8,NAME=FNAME2,TYPE='NEW')
    WRITE(8,9010) MSIZE**2
    DO 27 I=1,MSIZE
        WRITE(8,9020), (DATA(I,J),FLOAT(I-K),FLOAT(J-K),J=1,MSIZE)
27   CONTINUE
    CLOSE(UNIT=8,DISP='SAVE')

C
C   FOURIER TRANSFORM
C
30   WRITE(6,*) ' GO TO FREQUENCY DOMAIN?  Y/N'
    ACCEPT 9030,OMEGA

```

```

IF (OMEGA.EQ.'N') GO TO 50
IF (OMEGA.NE.'Y') GO TO 30
CALL TRAN2D(DATA,MSIZE,-1)
CALL DPLOT(DATA,MSIZE,ARRAY1,ARRAY2,ARRAYP)
GO TO 25

C
C INVERSE FOURIER TRANSFORM
C
50 WRITE(6,*) ' GO TO TIME DOMAIN? Y/N'
ACCEPT 9030,TIME
IF (TIME.EQ.'N') GO TO 60
IF (TIME.NE.'Y') GO TO 50

C
C MODIFY TO PREPARE FOR STEP OR RAMP RESPONSE
C
120 WRITE(6,*) ' WANT TO MODIFY DATA? BY 1)1'
WRITE(6,*) ' 2)1/JW'
WRITE(6,*) ' 3)-1/W**2'
ACCEPT *,MOD
IF ((MOD.GT.3).OR.(MOD.LT.1)) GO TO 120
IF (MOD.EQ.1) GO TO 95
IF (MOD.EQ.3) GO TO 130

C
C MODIFY BY 1/JW
C
DO 125 I=1,MSIZE
DO 127 J=1,MSIZE
W=2.*PI*SORT(FLOAT((I-MSIZE/2-1)**2+(J-MSIZE/2-1)**2))
IF (W.NE.0.) DATA(I,J)=DATA(I,J)/(CJ*W)
IF (W.EQ.0.) DATA(I,J)=(0.,0.)
127 CONTINUE
125 CONTINUE
GO TO 145

C
C MODIFY BY -1/W**2
C
130 DO 135 I=1,MSIZE
DO 140 J=1,MSIZE
W=2.*PI*SORT(FLOAT((I-MSIZE/2-1)**2+(J-MSIZE/2-1)**2))
IF (W.NE.0.) DATA(I,J)=-DATA(I,J)/(W**2)
IF (W.EQ.0.) DATA(I,J)=(0.,0.)
140 CONTINUE
135 CONTINUE
145 CALL DPLOT(DATA,MSIZE,ARRAY1,ARRAY2,ARRAYP)

C
C COSINE TAPERING LOW PASS
C THIS IS BY SPECIFYING THE NUMBER OF HARMONICS
C
95 WRITE(6,*) 'WANT TO DO COSINE LOW-PASS?Y/N'
ACCEPT 9030,LP
IF (LP.EQ.'N') GO TO 100

```

AD-A162 553

SPACE-FREQUENCY SAMPLING CRITERIA FOR ELECTROMAGNETIC
SCATTERING OF A FINITE OBJECT(U) OHIO STATE UNIV
COLUMBUS ELECTROSCIENCE LAB F Y FOK AUG 85

3/3

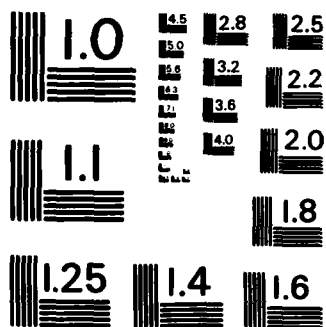
UNCLASSIFIED

ESL-714190-11 N00014-82-K-0037

F/G 20/14

NL





MICROCOPY RESOLUTION TEST CHART
NATIONAL BUREAU OF STANDARDS-1963-A

```

IF (LP.NE.'Y') GO TO 95
WRITE(6,*) 'CUT-OFF ELEMENT NUMBER:'
ACCEPT *,NCUT
DO 200 I=1.MSIZE
  DO 300 J=1.MSIZE
    DATA(I,J)=DATA(I,J)*WEIGHT(NCUT,I,J,MSIZE)
300   CONTINUE
200   CONTINUE
    CALL DPLOT(DATA,MSIZE,ARRAY1,ARRAY2,ARRAYP)
C
C   HIGH PASS FILTERING
C   AGAIN BY SPECIFYING THE NUMBER OF HARMONICS
C
100  WRITE(6,*) 'HIGH PASS FILTERING?Y/N'
    ACCEPT 9030,HP
    IF(HP.EQ.'N') GO TO 400
    IF(HP.NE.'Y') GO TO 100
    WRITE(6,*) 'CUT-OFF ELEMENT NUMBER:'
    ACCEPT *,NCUT
    DO 500 I=1.MSIZE
      DO 600 J=1.MSIZE
        RRFREQ=SQRT((FLOAT(I-MSIZE/2-1))**2 + (FLOAT(J-MSIZE/2-1))**2)
        IF (RRFREQ.LE.FLOAT(NCUT)) DATA(I,J)=(0.,0.)
600   CONTINUE
500   CONTINUE
    CALL DPLOT(DATA,MSIZE,ARRAY1,ARRAY2,ARRAYP)
C
C   DO FOURIER TRANSFORM NOW
C
400  CALL TRAN2D(DATA,MSIZE,1)
    WRITE(6,*) 'THE DATA ARE IN TIME DOMAIN NOW!'
    CALL DPLOT(DATA,MSIZE,ARRAY1,ARRAY2,ARRAYP)
    GO TO 25
9000 FORMAT(A10)
9010 FORMAT(I10)
9020 FORMAT(4E15.8)
9030 FORMAT(A1)
60   STOP
    END

```

```

C
C      SUBROUTINE:      DPLOT
C
C      THIS SUBROUTINE WILL PLOT 3-D FOR A COMPLEX ARRAY DATA
C      EITHER IN A 3-D PICTURE OR A CONTOUR PLOT
C      THE CONTOUR PLOT LINKS WITH NCAR PLOTTING PACKAGE
C
C      DATA      :2-D COMPLEX ARRAY TO BE PLOTTED
C      MSIZE      :SIZE OF DATA
C      ARRAY1,ARRAY2,ARRAYP:DUMMY ARRAYS WITH SAME DIMENSIONS AS DATA
C
C      SUBROUTINE DPLOT(DATA,MSIZE,ARRAY1,ARRAY2,ARRAYP)
C      COMPLEX DATA(MSIZE,MSIZE)
C      DIMENSION ARRAY1(MSIZE,MSIZE),ARRAY2(MSIZE,MSIZE),ARRAYP(MSIZE,MSIZE)
C      CHARACTER ACT,FLO,COM,COM2,COM3,COM4,COM5,LINE,PICK
10  WRITE(6,*) 'DO YOU WANT TO PLOT?Y/N'
    ACCEPT 9030,COM
    IF (COM.EQ.'N') GO TO 9999
    IF (COM.NE.'Y') GO TO 10
C
C      NORMALIZE THE WHOLE DATA FILE BY SOME FACTOR
C
500 WRITE(6,*) 'DO YOU WANT TO NORMALIZE WITH A FACTOR?Y/N'
    ACCEPT 9030,COM5
    IF (COM5.EQ.'N') GO TO 510
    IF (COM5.NE.'Y') GO TO 500
    WRITE(6,*) 'FACTOR:'
    ACCEPT *,FACTOR
    GO TO 20
510 FACTOR=1.
20  WRITE(6,*) ' PLOT REAL AND IMAGINARY? Y/N'
    ACCEPT 9030,ACT
    IF (ACT.EQ.'N') GO TO 50
    IF (ACT.NE.'Y') GO TO 20
    DO 40 I=1,MSIZE
        DO 30 J=1,MSIZE
            ARRAY1(I,J)=FACTOR*REAL(DATA(I,J))
            ARRAY2(I,J)=FACTOR*AIMAG(DATA(I,J))
30      CONTINUE
40  CONTINUE
    GO TO 100
C
C      CONVERSION INTO LINEAR AMPLITUDE AND PHASE(RADIAN)
C
50  DO 70 I=1,MSIZE
        DO 60 J=1,MSIZE
            ARRAY1(I,J)=FACTOR*CABS(DATA(I,J))
            IF ((REAL(DATA(I,J)).EQ.0.) .AND.
                (AIMAG(DATA(I,J)).EQ.0.)) GO TO 55
            ARRAY2(I,J)=ATAN2(REAL(DATA(I,J)),AIMAG(DATA(I,J)))
            GO TO 60

```

```

55             ARRAY2(I,J)=0.
60             CONTINUE
70             CONTINUE
C
C*****
C
100          WRITE(6,*) '1) 3D PICTURE, 2) CONTOUR PLOT'
              ACCEPT 9030, PICK
              IF ((PICK.NE.'2').AND.(PICK.NE.'1')) GO TO 100
101          WRITE(6,*) 'PLOT AMPLITUDE/REAL?Y/N'
              ACCEPT 9030, COM4
              IF (COM4.EQ.'N') GO TO 150
              IF (COM4.NE.'Y') GO TO 101
              IF (PICK.EQ.'1') GO TO 102

C
C           CONTOUR PLOT
C
              IF (PICK.EQ.'2') CALL EZCNTR (ARRAY1.MSIZE,MSIZE)
              GO TO 150

C
C           PLOT 3 D PICTURE
C
102          CALL VPLOTS(0.0,0)
120          WRITE(6,*) 'PLOT X-LINE, Y-LINE, OR BOTH?X, Y, B'
              ACCEPT 9030, LINE
              IF ((LINE.NE.'X').AND.(LINE.NE.'Y').AND.(LINE.NE.'B')) GO TO 120
              CALL SET_LINES 3D(LINE)
              CALL SET_ROTATION 3D(0)
              XMAX=ARRAY1(1,1)
              XMIN=ARRAY1(1,1)
              DO 300 I=1,MSIZE
                  DO 310 J=1,MSIZE
                      XMAX=AMAX1 (ARRAY1(I,J),XMAX)
                      XMIN=AMIN1 (ARRAY1(I,J),XMIN)
                      ARRAYP(I,J)=ARRAY1(I,J)
310          CONTINUE
300          CONTINUE
              WRITE(6,*) 'SCALE OF AMPLITUDE/REAL PLOT:'
              WRITE(6,*) '(MAX=',XMAX,' MIN=',XMIN
              WRITE(6,*) ' RECOMMEND SCALE:'.0.5/(XMAX-XMIN),')'
              ACCEPT *,SCALE
              WRITE(6,*) 'WHAT IS THE VIEW ANGLE W.R.T. X-Y PLANE?'
              WRITE(6,*) '(RECOMMENDING:45)'
              ACCEPT *,VIEW
              CALL PLOT_3D_SURFACE (ARRAYP,MSIZE,MSIZE,VIEW,0.,0.,SCALE)
4001         WRITE(6,*) 'IS THIS THE LAST PLOT?Y/N'
              ACCEPT 9030, FLO
              IF ((FLO.NE.'Y').AND.(FLO.NE.'N')) GO TO 4001
              IF (FLO.EQ.'N') NSIGN=-1
              IF (FLO.EQ.'Y') NSIGN=1
              CALL PLOT(0.,0.,NSIGN*999)

```

```

C*****
C
C   PLOT IMAGINARY OR PHASE
C
150  WRITE(6,*) 'PLOT THE PHASE/IMAGINARY?Y/N'
      ACCEPT 9030,COM3
      IF (COM3.EQ.'N') GO TO 5000
      IF (COM3.NE.'Y') GO TO 150
      IF (PICK.EQ.'1') GO TO 157

C
C   CONTOUR PLOT
C
      CALL EZCVR (ARRAY2,MSIZE,MSIZE)
      GO TO 5000

C
C   3 D PICTURE PLOT
C
157  CALL VPLOTS(0.0.0)
220  WRITE(6,*) 'PLOT X-LINE,Y-LINE,OR BOTH?X,Y,B'
      ACCEPT 9030,LINE
      IF ((LINE.NE.'X').AND.(LINE.NE.'Y').AND.(LINE.NE.'B')) GO TO 220
      CALL SET_LINES 3D(LINE)
      CALL SET_ROTATION 3D(0)

C
C   FIND THE MINIMUM AND MAXIMUM IN THE PLOTTING SET
C
      XMAX=ARRAY2(1,1)
      XMIN=ARRAY2(1,1)
      DO 400 I=1,MSIZE
        DO 410 J=1,MSIZE
          XMAX=AMAX1 (ARRAY2(I,J),XMAX)
          XMIN=AMIN1 (ARRAY2(I,J),XMIN)
          ARRAYP(I,J)=ARRAY2(I,J)
410   CONTINUE
400   CONTINUE
      WRITE(6,*) 'SCALE OF PHASE/IMAGINARY PLOT:'
      WRITE(6,*) '(MAX='XMAX,' MIN='XMIN
      WRITE(6,*) ' RECOMMEND SCALE:'0.5/(XMAX-XMIN),')'
      ACCEPT *,SCALE
      WRITE(6,*) 'WHAT IS THE VIEW ANGLE W.R.T. X-Y PLANE?'
      WRITE(6,*) '(RECOMMENDING:45)'
      ACCEPT *,VIEW
      CALL PLOT_3D SURFACE (ARRAYP,MSIZE,MSIZE,VIEW,0.,0.,SCALE)
4000 WRITE(6,*) 'IS THIS THE LAST PLOT?Y/N'
      ACCEPT 9030, FLO
      IF ((FLO.NE.'Y').AND.(FLO.NE.'N')) GO TO 4000
      IF (FLO.EQ.'N') NSIGN=-1
      IF (FLO.EQ.'Y') NSIGN=1
      CALL PLOT(0.,0.,NSIGN*999)
5000 WRITE(6,*) 'PLOT AGAIN?Y/N'
      ACCEPT 9030, COM2

```

```
IF (COM2.EQ.'Y') GO TO 100
IF (COM2.NE.'N') GO TO 5000
9030 FORMAT (A1)
9999 RETURN
END
```



```

C
C   PUT THE FOUR CORNERS BACK TO THE CENTRE
C
DO 120 I=1,N
    DO 115 J=1,N
        DATA(N+I-1,N+J-1)=WORK1(I,J)
115     CONTINUE
120     CONTINUE
DO 130 I=1,N-1
    DO 125 J=1,N-1
        DATA(I,J)=WORK1(MSIZE1-N+I+1,MSIZE1-N+J+1)
125     CONTINUE
130     CONTINUE
DO 140 I=1,N
    DO 135 J=1,N-1
        DATA(J,I+N-1)=WORK1(MSIZE1-N+J+1,I)
        DATA(I+N-1,J)=WORK1(I,J+MSIZE1-N+1)
135     CONTINUE
140     CONTINUE
RETURN
END

```

C
C
C
C
C
C
C
C
C
C
C

FUNCTION: WEIGHT

THIS FUNCTION WILL CALCULATED THE COSINE LOW PASS WEIGHTING
WITH THE ASSUMPTION THAT THE FREQUENCY RESPONSE DATA IS LOCATED
IN THE MIDDLE OF THE PLOT

NCUT- CUT-OFF NUMBER FOR THE LOW PASS FROM THE CENTER
NX - X-COORDINATE IN THE MSIZE X MSIZE
NY - Y-COORDINATE IN THE MSIZE X MSIZE
MSIZE- SIZE OF THE ARRAY

FUNCTION WEIGHT(NCUT,NX,NY,MSIZE)
CHARACTER LP
PI=3.14159265
X=ABS(FLOAT(NX-MSIZE/2-1))
Y=ABS(FLOAT(NY-MSIZE/2-1))
RADIUS=SQRT(X**2+Y**2)
IF (RADIUS.LE.FLOAT(NCUT)) WEIGHT=0.5*(1.+COS(PI*RADIUS/FLOAT(NCUT)))
IF (RADIUS.GT.FLOAT(NCUT)) WEIGHT=0.
RETURN
END

REFERENCES

- [1] Shannon, C. E.: 'Communication in the presence of noise' IRE Proceedings, January 1949.
- [2] Papoulis, A.: Fourier Integral and Its Applications McGraw-Hill, New York, 1962.
- [3] Kennaugh and Cosgriff: 'The use of impulse response in electromagnetic scattering problems.' 1958 IRE National Convention Record Part 1, pp 72-77.
- [4] Kennaugh and Moffatt: 'Transient and impulse response approximation.' IEEE Proceedings, August 1965, pp 893-901.
- [5] Lewis, R. M.: 'Physical optics inverse diffraction.' IEEE Transactions on Antenna and Propagation, Vol. AP-17, No. 3, May 1969, pp 308-314.
- [6] Bojarski, N. N.: 'A survey of the physical optics inverse scattering identity.' IEEE Transactions on Antenna and Propagation, Vol. AP-30 No. 5, September 1982, pp 980-988.
- [7] Petersen and Middleton: 'Sampling and reconstruction of wave-number limited functions in N-dimensional Euclidean Spaces.' Information and Control 5, 1962, pp 279-323.
- [8] Mensa, Halevy and Wade: 'Coherent doppler tomography for microwave imaging.' IEEE Proceedings Vol. 71, No. 2, February 1983, pp 254-261.
- [9] Coxeter, H. S. M.: 'Extreme forms.' Canadian Journal of Mathematics 3, 1951, pp 391-441.
- [10] Harris, F. J.: 'On the use of window for harmonic analysis with the discrete Fourier transform.' IEEE Proceedings Vol. 66, No. 1, January 1978, pp 51-83.
- [11] Dominek, A. K.: Personal communication.
- [12] Walton, E. K.: Personal communication.

- [13] Goodman, J. W.: Introduction to Fourier Optics
McGraw Hill, New York, 1968.
- [14] Marhefka, R. J.: Personal communication.
- [15] Peters, Leon: Personal communication.
- [16] Kwan, B. W.: Personal communication.

END

FILMED

1-86

DTIC